Design and MEMS Microfabrication of an Optrode for Combined Optogenetics and Electrophysiology Studies

Chengyu Huang

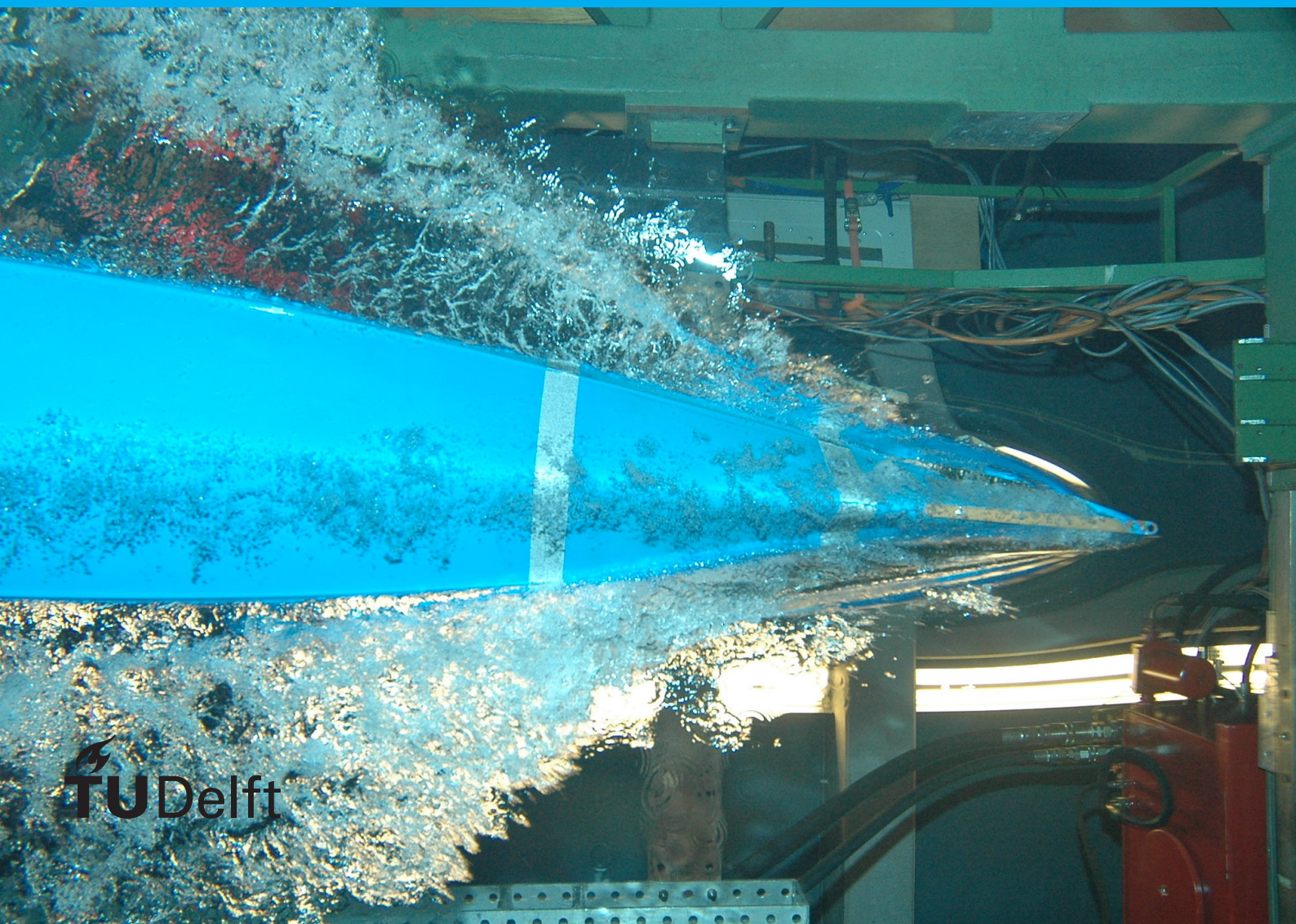

TU Delft

Design and MEMS Microfabrication of an Optrode for Combined Optogenetics and Electrophysiology Studies

by

Chengyu Huang

to obtain the degree of Master of Science
at the Delft University of Technology,
to be defended publicly on Nov. 29th, 2018 at 14:00 PM.

Student number: 4502132
Project duration: June 1, 2017 – November 29, 2018
Thesis committee:

Prof. dr. ir. Wouter A. Serdijn,	TU Delft, supervisor
Prof. dr. P. J. French,	TU Delft
dr. V. Giagka,	TU Delft
MSc. Ronaldo Martins da Ponte,	Daily Supervisor

TU Delft

Preface

First of all, I would like to thank my supervisor Prof. Wouter A. Serdijn for giving me the chance to do my master thesis project in Bioelectronics group. During the whole project, he gave me lots of support and guidance on scientific thinking and setting goals and arranging contents of the project as well. I would also like to thank people from the Department of Human Genetics in Leiden University Medical Center for giving me the opportunity to do the internship there and inspiring me the idea to start this project.

I'm especially grateful to my daily supervisor Ronaldo Martins da Ponte for all his help and efforts. He not only helped me with the design and experiment of the optrode, but also enlightened me with many interesting and innovative ideas. And a lot thanks to him for revising my thesis report.

I did most of my experiments and fabrication processes in the Else Kooi Lab and this is my first time getting in touch with the micro-fabrication processes. I would like to thank Jia Wei, who mentored me on the mask design layouts and my process flowchart, and gave me a lot of help during the fabrication process. Also I would like to thank all the engineers in EKL for their kind help in the clean room. Thanks to Yue Zhang for helping me with the wire bonding process in the MEMS lab.

During the experiments in the clean room, I not only made some new friends, but also met Boyao Zhang, who is now my girl friend. In the lab, she introduced me the basic knowledge in chemical processes and helped me with the wire bonding experiment. In our daily life, she took care of me when I was sick and gave me much mental support when I was stressed with the project.

Last but foremost, I should say thanks to my parents for supporting me in the past three years. Due to various reasons, I spent an extra year on my master program. But they always give me lots of patience and care, which encourages me to continue with the master program.

Chengyu Huang
Delft, November 2018

Abstract

Optogenetics is a biological technique that uses light to control cells in living tissues, typically neurons, that have been genetically modified to express light-sensitive ion channels. Using this technique, neuroscientists can investigate the neural circuits underlying neurological diseases with a higher spatio-temporal resolution when compared to other known neuromodulation methods.

As employed today, optogenetics requires methods for guiding sufficiently strong and precisely timed light to specific brain regions, while the experimental subject carries out behaviors of interest. For this role, miniaturized devices (namely optrodes) shall be properly engineered to hold the required components (e.g. light source, recording electrodes, etc) whilst complying with some surgical and biocompatibility issues.

In this work, an optrode was designed and fabricated using an in-house MEMS microfabrication technology. The custom-made device featured (a) low impedance level with TiN-coated microelectrodes, (b) sufficient optical power delivery through on-chip-μLEDs, and (c) miniaturized dimensions with tolerable tissue damage during long-term animal experiments. In addition, different optrodes were fabricated to allow different experiment conditions (i.e. chronic or acute implantation, multi-site or multi-layer studies). A MEMS cavity for the on-chip-μLED was engineered on the optrode's shaft in order to further minimize the induced tissue damage during the surgical implantation. Last but not least, this customized optrode is also compatible with our in-house CMOS technology and can be further upgraded with additional electronic functionalities, as well as with the deposition of novel materials.

After the microfabrication and system integration, in-vitro experiments on three different designs were performed to characterize electrically the electrode impedance, the control of μLED's light intensity and pulse frequency.

Contents

1 Introduction

The thesis project started from an internship experience in the Department of Human Genetics in Leiden University Medical Center (LUMC). In this chapter, a research background during the internship phase is firstly introduced. Then the underlying problems of the current experiment setups are stated and the primary objectives for the thesis project are set.

1.1. Research Background in LUMC

The neuroscientists in the Department of Human Genetics, Leiden University Medical Center (LUMC) used implanted microwires to measure and record the brain activities in freely behaving animals (with or without genetic changes found in human beings). These microwires were placed into mouse's brain cortex and measure the electrical signals from the nearby neurons. Besides the neural recording, scientists also tried to manipulate part of the animal's brain function by means of "Optogenetics", which was carried out in the lab by using an externally controlled laser beam.

Cortical spreading depression (CSD) is one of their research topics. The CSD is basically a slow cortical wave of electrophysiological hyperactivity caused by neuronal and glial depolarization and followed by a wave of temporary inhibition of neuronal activity, which could be measured and recorded by the microelectrode array. Neuroscientists stimulated the mouse cortical layer with a beam of laser light to induce cortical spreading depression and studied its intracortical DC-potentials, multi-unit activity and laser Doppler flowmetry [1].

Both the neural recording and the optical stimulation were done in a faraday cage to reduce the powerline noise and the effects from external electrical field. The neural signals were transmitted through long wires to the signal processing system including signal amplification, filtering and analog-to-digital converter. The lab used Spike2 to control part of the experimental equipment and present the recorded neural signals.

Table 1.1 lists the specifications of the microwires electrodes and Table 1.2 lists the frequency range of recorded neural signals.

Table 1.1: Specifications of microwires

Number of wires	7
Core Material	Pt-10%Ir
Insulation	PTFE
Diameter	125μm (core: 75μm)

Table 1.2: Neural signals of interest

DC-EEG	DC-500Hz
Local Field Potential	0.05-500Hz
Neuronal Activity	500-5500Hz

1.2. Problem Statement and Primary Objectives

The electrical recording units were made of microwires and the optical stimulation units used the laser beam. With the current setup, there existed some problems:

1. Electrical recording units
    - Fabrication of microwire electrodes: Seven microwires were manually inserted into a cylindrical head-stage to serve as the microelectrodes, which was time consuming and difficult to handle.
    - Dimension of the recording microwire: The core diameter of microwires is 75 μm, which is much larger than the body of a single neuron and makes the spike sorting difficult to reach.
    - Limitations on the number of recording sites: Among the seven implanted microwires, only five performed recording functions. The other two were the ground and reference electrodes. The microwires limit the number of recording units within a certain volume.
2. Optical stimulation units
    - The laser system too bulky
    - The laser head can't be inserted to stimulate deeper brain regions.

Hence, the two primary objectives are:
(1) To design and fabricate a microelectrode array that allows multi-site and multi-layer recordings with improved signal-to-noise ratio (SNR);
(2) To integrate the light source in the implanted probe so that a localized optical stimulation in deeper brain regions is realized.
And the device interfaces need to be biocompatible to allow safe implantation and experiments.
Chapter 2 and 3 elaborate more on the two objectives.

1.3. Thesis Outline

The thesis outline is planned as follows:

- Chapter 1: Introduction;
- Chapter 2: Literature review;
- Chapter 3: Design specifications and design layouts;
- Chapter 4: MEMS microfabrication processes;
- Chapter 5: System integration;
- Chapter 6: Experiments and results;
- Chapter 7: Conclusions and Recommendations.

2

Background and Literature Review

The goal of this project is to build an optrode - a single device that combines both optical stimulation and electrical recording elements, which is mainly used in physiological studies. In this chapter, we first give an introduction of optogenetic techniques, including its basic principles and a comparison of different light delivery methods within this technology. Then we introduce the principles of microelectrodes and their in-vivo experimental requirements, including a list of some promising material candidates for the recording electrodes. A review of recently developed optrode prototypes and a performance comparison of these devices are carried out afterwards. In the last part of this chapter, we briefly introduce different fabrication methods and give a statement of problems that we might encounter in the future design and process.

2.1. Optical Stimulation

The mammalian brain is the most complex organ in the living system, comprising billions of neurons being interconnected into neural circuits by trillions of synapses. To improve the understanding of this complexity and the correlated neurological disorders, it's important to identify underlying neural circuits and ascertain the relationship between their function and the neuronal structures. Specific and precise experimental manipulations and interventions are prerequisites to achieve these goals. Electrical stimulation is one commonly used method that stimulates the neurons in a given volume with temporal precision. However, such technique is not spatially precise, lacking cell type specificity, and could lead to unwanted physiological changes on surrounding cells. On the other hand, the pharmacological and the genetic manipulations provide a good cell specificity and spatial resolution, but lack temporal resolution at the scale of neural signaling [2, 3, 4, 5]. A new set of biological tools called 'Optogenetics' was developed early this century and can be used to manipulate cells with both high spatial and temporal precision by the use of microbial opsins in a surgical mean and followed by an illumination to those modified cells. In this section, we briefly introduce the mechanism of the optogenetics approach and their use in neural circuits.

2.1.1. Basic principles in optogenetics

The optogenetics approach combines both genetic and optical methods to control the activity of proteins and cellular functions, inducing excitatory or inhibitory events in specific cell types of living tissue and behaving animals. Such technique consists of three major components: (1) microbial opsins (encode 7 transmembrane and light-sensitive proteins that cause structural rearrangements in response of light and lead to electrical current across the cellular membranes), (2) sufficient and specific opsin gene expression in the living tissue (e.g. neurons, cardiac myocytes), and (3) precisely controlled light guide, modulation and delivery to target cells/tissue.

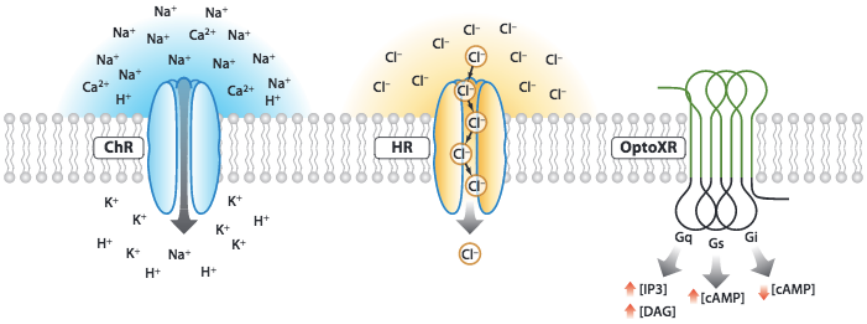

Figure 2.1: Optogenetic Tool Families [2]

Figure 2.1 describes three mainly used optogenetic constructs in experiments. The channelrhodopsin family light gate cation channel (i.e. ChR2), as shown in the left side in the picture above, fluxes $H^+/Na^+/K^+$ across the membrane along the electrochemical gradient when exposed to blue light (at a wavelength of 400-500 nm), inducing action potentials. In contrast, the halorhodopsins family light gated chloride pumps (i.e. NpHR) pump Cl^- into the cytoplasm and lead to cellular hyperpolarization and inhibition of neural activity when illuminated with yellow light (at a wavelength of 550-620 nm). The third type of optogenetic constructs is the OptoXR that controls the intracellular signaling transduction. This G protein-coupled rhodopsin activates the G proteins in response to light at 500 nm and causes a decrease of intracellular level of cAMP. The latter procedure could have a direct effect on ion channels in the plasma membrane and influence the neural activity. [3]

Those optogenetic constructs could be applied in different experiments and research studies based on their own characteristics. For example, the channelrhodopsins could be used in the study of auditory dysfuntions for cochlear excitation and the halorhodopsins could be applied in epilepsy for seizure suppression. Since optogenetics is still a relatively new technology, there exist opportunities for further optogenetic applications and a demand for engineers to develop more advanced tools in this field.

2.1.2. Light propagation and light delivery methods

The light delivery technology is the fundamental part of optogenetics technique, which includes both in-vitro and in-vivo modulations. In order to trigger a certain cell activity, the illumination intensity should reach a threshold. The light intensity threshold for ChR2 is less than 1 mW/mm^2 and for NpHR is less than 7 mW/mm^2, which is relatively a low dose in optical modulation, thanks to the recent advance in optogenetics [6]. The in-vitro optogenetic tools typically include mercury arc lamps, lasers, light-emitting diodes (LEDs). While the in-vivo stimulation of behaving animals is done mostly with laser light via optical fiber and fiber-coupled high power LEDs. Chronic implantation of LEDs is a new direction in recent years of research. In this subsection, we illustrate the light transmission efficiency in living tissue and give a comparison of the laser and LED light sources.

Light propagation in tissue

Since the brain tissue is not transparent to visible light, the in-vivo optogenetic experiments have limitations during light propagation and stimulation of deeper brain regions. The Beer-Lambert equation is used to make an estimation of light attenuation in the tissue due to light scattering and absorption [7] :

$$I(z) = I_0 e^{-\mu_t(\lambda)z} \tag{2.1}$$

$$\mu_t(\lambda) = \mu_a(\lambda) + \mu_s^{'}(\lambda) \tag{2.2}$$

$$\mu_s^{'} = \mu_s(1-g) \tag{2.3}$$

In Eq. (2.1), I(z) represents the light intensity after traveling a distance z in the tissue and I_0 represents the initial light intensity. The extinction coefficient μ_t in brain tissue is calculated through Eq. (2.2), where μ_a is the absorption coefficient and μ_s is the scattering coefficient in biological tissue. Those coefficients are all wavelength (λ) dependent. In Eq. (2.3), g is the anisotropic factor, which is due to the fact that light scattering is anisotropic in tissue. Table 2.1 listed the aforementioned coefficients and anisotropic factor for brain tissue at a wavelength of 500 nm.

Table 2.1: Extinction coefficients and anisotropic factor for brain tissue (λ =500 nm) [7]

Parameters	Tissue Type	Values
g	White matter	0.8
	Gray matter	0.88
μ_s	White matter	420 cm^{-1}
	Gray matter	110 cm^{-1}
μ_a	White matter	1 to 2 cm^{-1}
	Gray matter	0.17 to 20 cm^{-1}

As mentioned before, the light intensity threshold for generating action potential is approximately 1 mW/mm^2 for ChR2. In some articles, it's mentioned that a power density of 1 mW/mm^2 could approximately trigger 50% of cells at target sites and a power density of 1 to 10 mW/mm^2 is typically needed for the experiment [8]. There is nearly no stimulation at an intensity level of 0.1 mW/mm^2. The stimulation duration and its repetition rate should be both taken into consideration when deciding the right light intensity threshold.

The Boyden Lab [9] performed simulations of how blue (460 nm) and yellow (590 nm) light emitted by LEDs travel through the brain. The LEDs were modeled as 300 μm × 300 μm and were placed on the surface of a 4 mm^2 cube of brain gray matter. The μ_s is 100 $cm^{-}1$ for blue light and 90 $cm^{-}1$ for yellow light, and the μ_a is 0.7 $cm^{-}1$ for blue and 0.27 $cm^{-}1$ for yellow light. The anisotropic factor g is 0.88 for blue light and 0.89 for yellow light [9]. As depicted in Figure 2.2, the light intensity decreases to 10%, 1%, and 0.1% of the light intensity within a certain range around the LED surfaces.

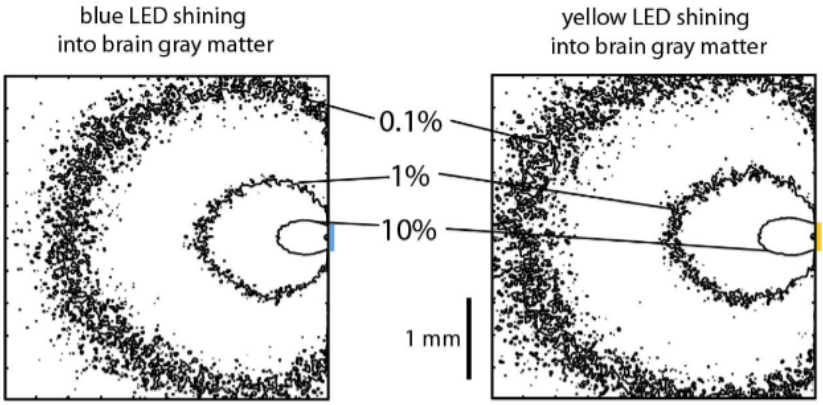

Figure 2.2: Monte Carlo simulations of blue and yellow LED light travel through brain [9].

Light sources: Laser vs. LED

The commonly used light sources in in-vivo experiments are fiber-coupled laser/LEDs and implanted μLEDs. The word laser stands for Light Amplification by the Stimulated Emission of Radiation. As a frequently used light source, laser has several good points. Laser is

monochromatic since it emits all photons with the same energy level, thus providing light with the same wavelength in an ideal case. The light emitted by laser also has advantages of coherence and low divergence, which means that all parts of light are in phase and travel in one direction. The most commonly used laser in optogenetics is the diode-pumped solid state (DPSS) laser [10]. However, the laser system is usually too bulky, of high price, and difficult to handle.

LEDs, different from laser, have nearly linear relationship between electrical current and optical output power, so would be a good light source for studies that require highly precise temporal patterns of stimulation. LEDs could provide a more stable light delivery, which is an important issue for the implanted devices. Other features of LEDs include low price, small space occupation, low power consumption, and the possibility to do experiments on freely behaving animals, when compared to lasers. For the fiber coupling LEDs, it's difficult to focus the light in a fiber as LEDs emit light in many directions. The normal fiber-coupled LED source have coupling efficiency below 10%. This problem could be avoided by using a direct μLED on optrode approach.

A comparison between LED and Laser as light sources is listed below in Table 2.2.

Table 2.2: Comparison between LEDs and Laser

	LED/μLED	Laser
Light delivery stability	+	-
Light intensity control & temporal control	+	-
Power consumption	+	-
System overall size	+	-
Experiment in freely behaving animals	+	-
Focused radiation (coherent, low divergence)	-	+
Fiber-coupling efficiency	-	+

2.2. Electrophysiological Recording

After an explanation of the optogenetics basics, we consider another essential part of this project: the recording electrodes. The microelectrodes record the neural signals in a given volume after the activation of neurons. There are a few requirements on the material selection at the recording sites, including biocompatibility, as little tissue damage as possible, and relatively low impedance at the electrode-electrolyte interface. Different materials are addressed in this section and we list the materials that might be used in the future development at the conclusion.

2.2.1. Classification of recording electrodes

The recording microelectrodes can be classified into the following categories: (1) Microwire electrodes; (2) Utah microelectrode array; (3) Michigan array; (4) Flexible array.

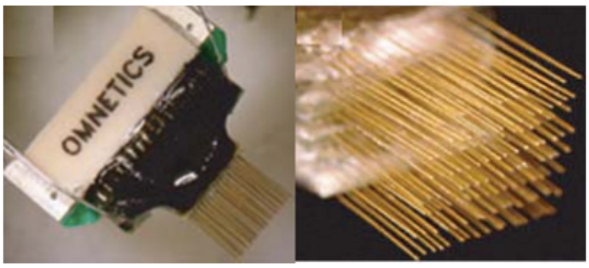

Figure 2.3: Microwire electrodes [11]

The microwire array, in Figure 2.3, is made of a number of microwires with the advantages of low price, good mechanical strength, and biocompatibility. But it's difficult and time consuming to produce such devices. Moreover, the size of the microwires and the interspace between each wire usually limit the number of recording units. And it's not feasible to detect multi-layer neural signals via a microwire array.

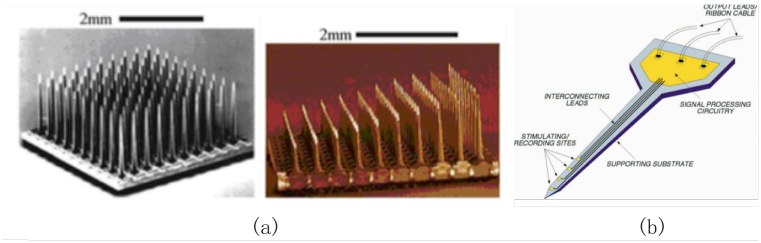

Figure 2.4: Micromachined MEA. (a) Utah arrays. (b) Michigan array. [11]

Examples of micromachined silicon-based array are presented in Figure 2.4. The micromachined MEA has advantages including batch production, high density of recording sites and good biocompatibility, but might be costly during the development of new designs. The Utah arrays consist of 100 conductive, sharpened silicon needles with tip diameter of 80 μm and maximum shaft length of 1.5 mm. The michigan array is a 2-D structure with multiple recording sites distributed along the shaft.

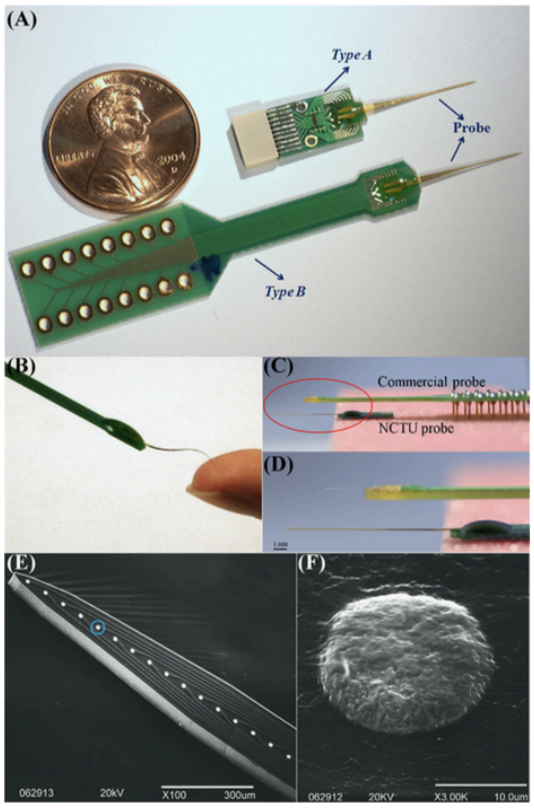

Figure 2.5: Polyimide-based microelectrode array. (a) NCTU probe bonded onto two PCBs; (b) Flexible NCTU probe; (c) & (d) Comparison between NCTU probe and commercial probe; (e) & (f) SEM images of the NCTU probe. [12]

The microwire and micromachined MEAs are made of rigid materials or substrates, thus tissue damage during the implantation is unavoidable. The flexible arrays, for example, constructed on polyimide (Figure 2.5 [12]) or parylene, allow the array to fit on the surface of

the brain and chronic neural recording is achieved in a less invasive way [11].

Some frequently used materials as recording sites in microwire, Utah array and Michigan array are listed in the Table 2.3 [11], giving an insight to the material candidates.

Table 2.3: Frequently used material in MEAs

MEAs	Substrate material	Material at recording sites
Microwires	-	Pt, Pt-Ir alloy, Stainless steel, Tungsten
Utah array	Boron doped silicon	Pt, IrOx
Michigan array	Silicon/Silicon dioxide/Parylene	Gold, PEDOT, Ir, CNTs
Flexible array	Polyimide/Parylene/PDMS	Gold, PEDOT

2.2.2. Impedance at the electrode-electrolyte interface

The impedance at the electrode-electrolyte interface is another key factor that need to be considered when determining the optimal material. A high impedance at the interface could lead to high thermal noise (lowering the SNR) and cause a mismatch between the electrode and the amplification system as well. However, it is challenging to achieve a low impedance at a micrometer scale of the plain electrodes. We explain the interface impedance first and then discuss several feasible ways to reduce the impedance.

The impedance is dependent on the selection of material, the composition of the electrolyte, the surface area of the recording sites, and the temperature [13]. In Figure 2.6 below, a simplified equivalent circuit that illustrates this interface is shown (Warburg impedance not included). The impedance Z_{CPA} represents the interface capacitance with a constant phase angle and R_{ct} represents the charge transfer resistance, in series with the solution resistance R_s. This model follows the formula below, and Table 2.4 lists the parameters of three materials measured by Wendy Franks et al. in 2005 [14]:

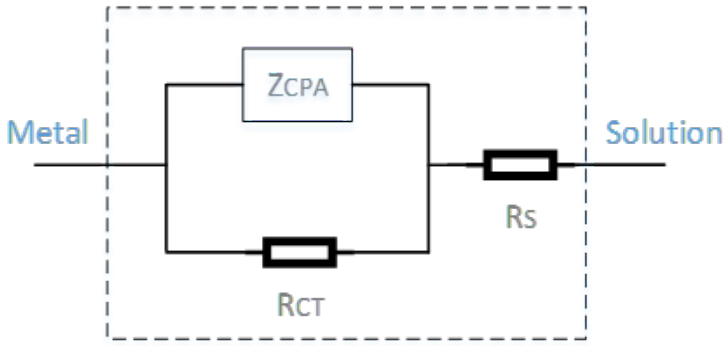

Figure 2.6: Equivalent circuit of the electrode-electrolyte interface [14]

$$Z_{CPA}(\omega) = \frac{1}{(j\omega Q)^n} \tag{2.4}$$

$$J = \frac{J_0 F \eta}{RT} \tag{2.5}$$

$$R_s = \frac{\rho}{4r} \tag{2.6}$$

Q: measure of the magnitude of Z_{CPA}
n: 0≤n≤1, inhomogeneties at the surface
J_0: equilibrium current density
F: Farady's constant
η: applied over-potential

R, T: gas constant, temperature
ρ: the solution resistivity
r: the radius of round electrode

In this simplified model, Z_{CPA} represents the non-faradaic impedance arising from the interface capacitance and is purely capacitive when n=1. As for the faradaic process, the oxidation and reduction currents flow across the electrode-electrolyte interface with current density J_0 at equilibrium state. Equation (2.5) is the Butler-Volmer equation applied in low field and is used to determine the current exchange and charge transfer resistance R_{ct}. The solution resistance R_s only depends on the the geometric area of the electrode interacted with the electrolyte.

From the experimental results in Table 2.4, we could get an estimation of the electrode-electrolyte interface impedance of Pt, Pt black and TiN with surface area 1 cm^2 at certain frequency. The impedance value at 1 kHz is a standard measure to evaluate the electrode and range from several tens of $k\Omega$ to 1 $M\Omega$. A frequently used way to reduce the electrode impedance is by surface modification and thus produce rough structure on plain electrodes to increase the effective interfacial area between electrode and electrolyte. Pt black has a lower impedance compared to Pt because of its porous and rough structure. TiN also has a relatively low impedance due to the formation of rough surface during the micro-fabrication process.

Table 2.4: Parameter results of three materials, measured area: 1 cm^2

	$Q(s\Omega^{-1/n})$	n	$R_s(\Omega)$	$R_{ct}(\Omega)$
Pt	2.72×10^{-5}	0.92	28.0	4.48×10^5
Pt black	2.08×10^{-3}	0.91	30.7	5.51×10^4
TiN	2.03×10^{-3}	0.91	42.3	3.00×10^5

2.2.3. List of materials

The material for implanted electrodes shall be biocompatible, such as Pt, PtIr, IrOx, TiN and gold, which perform with appropriate host responses. The tissue response caused by the implantation and experiment is one important issue. The tissue response consists of the inflammatory reaction and the process that tissue fluids dissolve the implants [13]. Soon after these tissue responses, encapsulation of fibrous tissue around the electrode is formed, separating recording sites from neural signals. Dymond et al. (1970) studied a few implanted metal materials in cat brains after 2 months research periods and ranked them in the following order: gold, platinum-10%iridium, platinum, stainless steel, titanium, and tungsten (only a part of the materials is mentioned). For a good microelectrode, a thin capsule surrounding the implant is desirable.

Pt, Pt alloys, TiN can be used as chronic stimulation and recording materials, whereas intrinsically conductive polymers and carbon nanotubes have emerged as alternatives recently [13, 15, 16].

(1) Gold. Au is a commonly used material used in recording electrodes. But the interface impedance of plain gold electrode is much higher than electrodes made of platinum black, titanium nitride and PEDOT and could induce higher thermal noise and reduce the SNR. A recent study by Anil Koklu et al. (2016) developed a rough gold electrode with low interface impedance through electrochemical deposition of gold and sintering of gold nanoparticles [15], stating a possibility of making gold recording electrodes with low impedance.

(2) Titanium nitride. TiN is a biocompatible ceramic material with rough surface, thus having a lower impedance compared with the current setups in LUMC (Pt-Ir alloy microwire electrode). The fabrication of TiN film is done by reactive DC magnetron sputtering method to deposit Titanium in a mixture of gas Argon (97%) and Nitrogen (3%) atmosphere under certain pressure.

(3) Poly (3,4 – ethylene dioxytiophene). Apart from the conventional metal and alloy elec-

trode, conductive polymers such as PEDOT has caught much attention because of its porous structure. PEDOT coated electrodes have 2 to 3 orders lower magnitude of impedance when compared to bare PtIr alloy electrodes according to the experiment by S. Venkatraman et al. [16]. PEDOT is deposited through electrochemical process onto the metal part of the electrode.

2.3. Literature Review of Optrode Designs

In this section, several optogenetic implants are reviewed, including their developments and limitations. These optogenetic implants are classified into two categories: wave-guided structure and μLED-on-optrode approach, based on the way of light delivery. The optical waveguide contains an optical fiber that is used for light coupling. The μLED-on-optrode approach uses μLED as direct light source with μLED bonded on the microelectrode implant and being inserted into brain tissue [17].

2.3.1. Wave-guiding structure

One of the earliest application for optical stimulation and electrical recording invented in 2012 is shown in Figure 2.7. This glass fiber-coupled optical probe is laser coupled. The optrode tip has a hollow core and is shaped to 10 μm diameter, thus could record single cell activity during light emission. The small probe tip minimises the tissue damage to the brain during implantation. However, this device only enables single site stimulation and recording, and is unable to study brain area with multi-site and multi-layer manipulation. The entire system dimension is not ideal for freely behaving animal experiments [18].

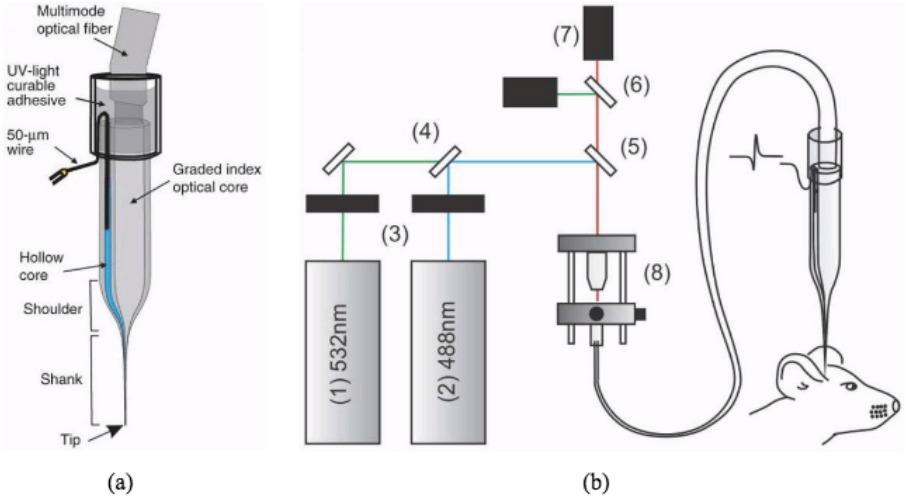

Figure 2.7: Optical and electrical microprobes. (a) Probe schematics for single recording. (b) Experimental setups [18]

Another wave-guided optrode-microelectrode array is presented in Figure 2.8. The design is based mainly on a 6×6 Utah microelectrode array (MEA) with one site being replaced by a fiber-coupled optical probe. The space between electrodes is 400 μm and the electrode shank length is 1 mm. The cannulated tube is used to guide both the optrode and the injection needle as described in Figure 2.8 (c). The power at the optrode tip is 1.8 mW and the light intensity is estimated to be 5 mW/mm^2 at the site 400 μm lateral to the stimulus and is enough for activating the ChR2-expressed cells [19]. This design can realize single site optical stimulation and multi-site electrical recording at the same plane/layer. Further development to multi-layer control is not possible with such structure. Moreover, the fabrication of Utah MEA and subsequent implementation is very complex.

The first two examples are all laser-based systems. There exist limitations on system

dimensions, power efficiency, the stability of illumination and restrictions to animals' movement. The third design is a μLED-based wave-guiding structure made in 2012. The μLED has advantages of more stable light delivery and lower power consumption as explained in the previous parts. Each single optical probe is 50 mm in length and has 4 sections. The tip is around 60-70 μm diameter with a tip angle of 12°. The complete optical array is presented in the right part of Figure 2.9 consisting of 6 individual probes with 200 μm spacing. An in-vivo experiment is taken in the hippocampus of freely moving rats expressing ChR2 and the blue light intensity is reported to be 3-30 μW at the fiber tip and 0.1-1 mW/mm^2 at the shank center [20]. This fiber-coupled optical array realizes multi-site and multi-layer stimulations by duplicating single probes 6 times. But the light intensity might not be very sufficient for neuron activation and the whole system dimensions are relatively large.

The wave-guiding structure (laser-coupled and LED-coupled) presented above could meet the requirements of implantable optogenetic applications, but still having some problems. The difficulty of multi-site/multi-layer stimulations, the bulky dimensions of overall systems, and the low fiber coupling efficiency of μLEDs limit the experiment, especially on freely-behaving animals or clinical applications.

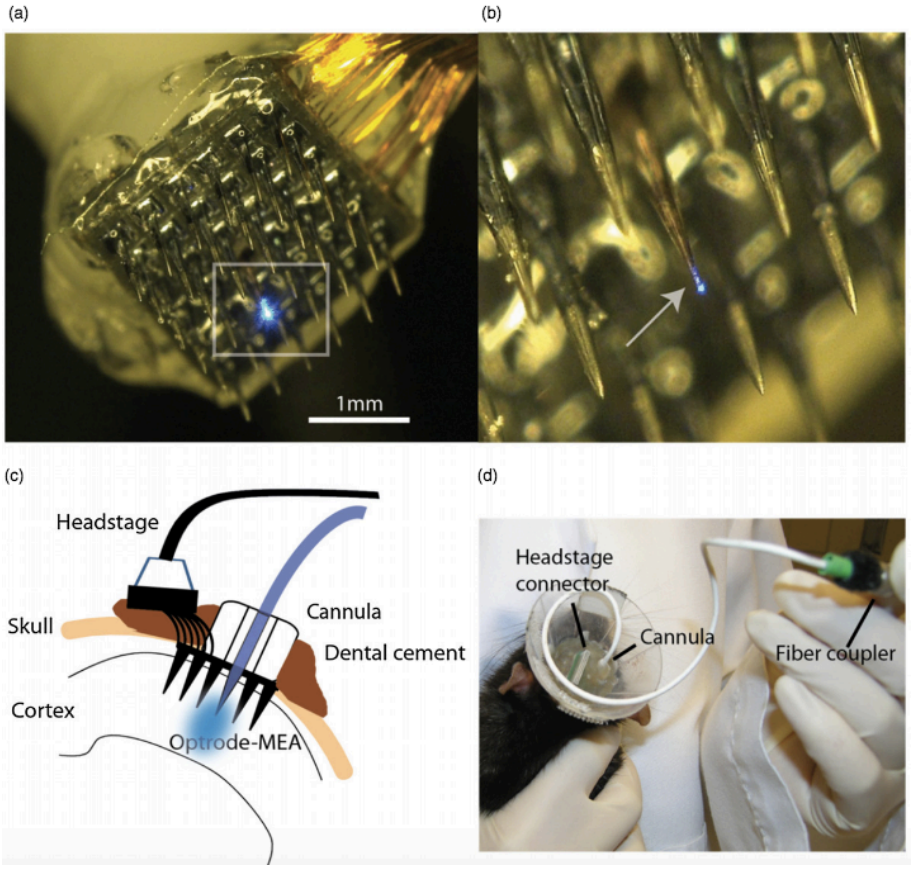

Figure 2.8: An overview of the optrode-microelectrode array [19]

2.3.2. Micro-LED on optrode

In this part, we discussed another type of optogenetic implants, which mounts the μLEDs directly on the optical probes and is inserted into the target area of the brain. The advantages of this design include higher light emission efficiency, multi-site and multi-layer stimulation, and can do free subjects experiments.

The first design example is a μLED optrode based on flexible polyimide, presented in Figure 2.10. The probe has 1 stimulation site (LED dimension: $1000 \times 200 \times 600\ \mu m^3$) and

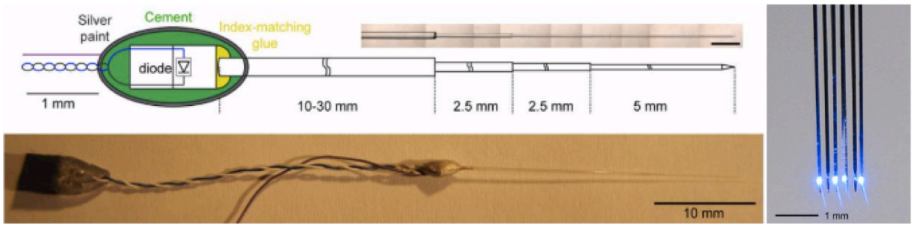

Figure 2.9: LED-coupled optical probe array [20]

three surrounding electrode recording sites. The shaft length is 12 mm and the width is 900 μm. This design realizes the simultaneous optical stimulation and neural recording. The drive voltage of the μLED is 2.9 V and the driven current is 5 mA. The light intensity is 0.7 mW/mm^2. [21] Despite of these features, this design has some drawbacks. Firstly, the device is too bulky for implantation and could cause more tissue damage. Secondly, the μLEDs' heating is not concerned in this design, which can induce overheating in brain tissue. The power required for 0.7 mW/mm^2 light intensity is reported to be 14.5 mW. Last but not least, such light intensity is difficult to activate the ChR2 properly.

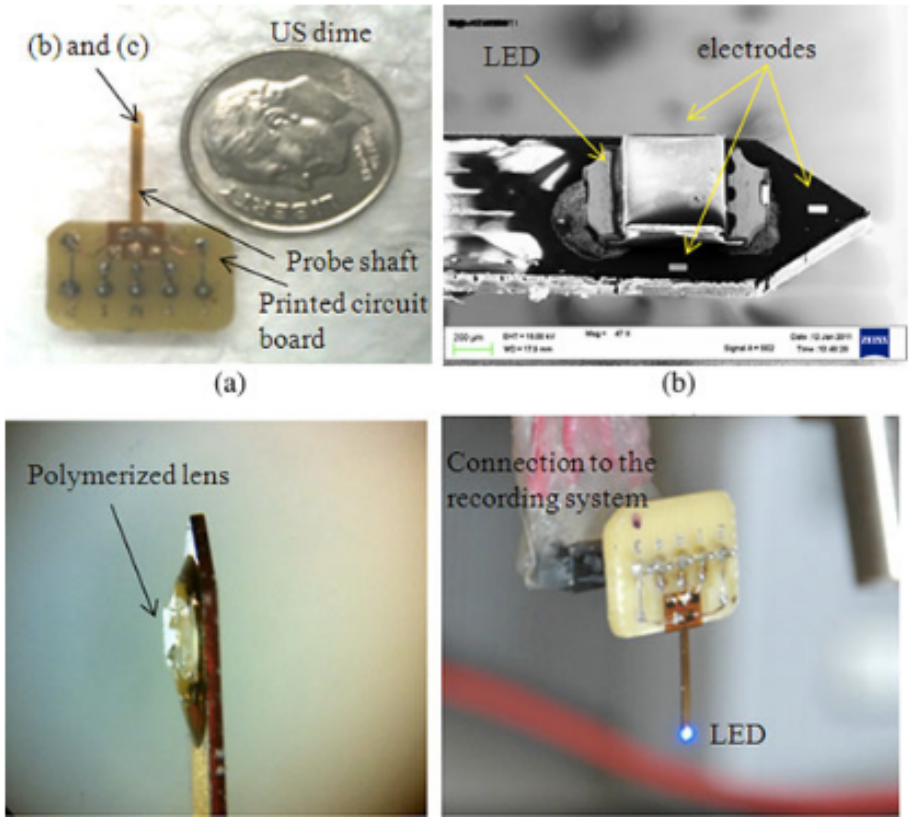

Figure 2.10: Optrode and the assembly [21]

A second example is a sapphire-based optical probe that integrate custom-designed GaN μLEDs, as shown in Figure 2.11. The shaft length is 1 mm long and the width of the shaft is 80 μm. Five 40 μm-diameter μLEDs are distributed along the shaft with spacing of 0.25 mm. Regarding to the LED bonding, five anode pads and one common cathode pads are constructed, and allows for individual control of each LED. The maximum illumination intensity is 600 mW/mm^2 with temperature increase of around 1.5°C. The highlights of this design include reasonable dimension of the probe, strong light intensity, and safe thermal effect to the surrounding tissue. But the biocompatibility and mechanical property of sapphire are

two concerns that might lead to tissue infection and damage [22]. In addition, this probe only provides the optical stimulation, and the recording units are nearly impossible to be integrated when considering the dimension of the optical shaft.

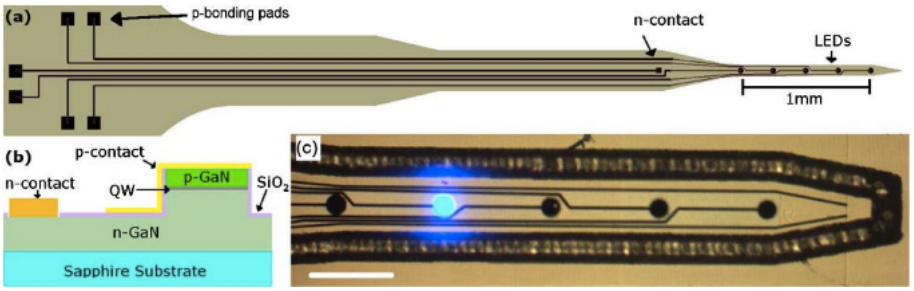

Figure 2.11: Sapphire based GaN μLED optrode [22]

In Figure 2.12 [10], a needle optrode designed in our lab is presented. Three μLEDs are places in a needle, with dimensions of 200 ×200 μm^2 and thickness of 95 μm. The output power of the selected Cree μLED (470 nm or 570 nm) is more than 6 mW/mm^2 with a 2.7 V forward voltage and 5 mA drive current, which is enough for optogenetics [10]. The optrode is controlled wirelessly through a properly programmed microcontroller unit.

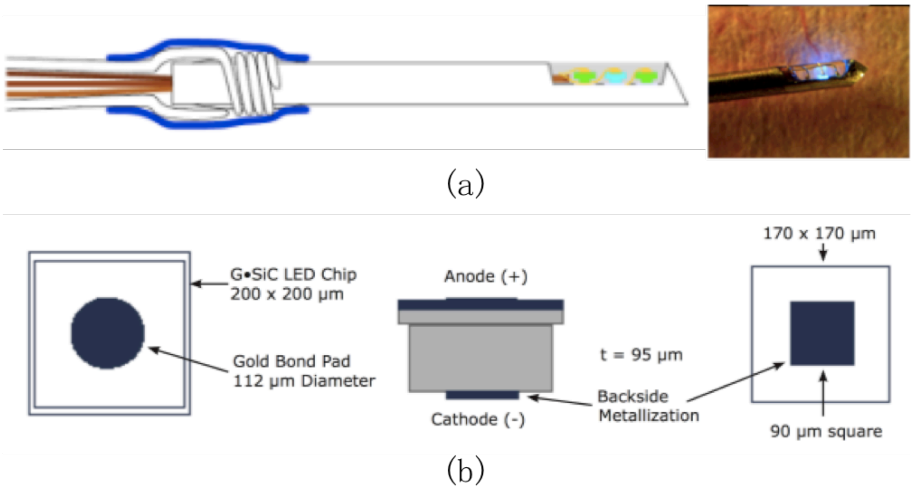

Figure 2.12: (a) Needle optrode and (b) Cree μLED [10]

A novel intelligent optrode design example is shown below in Figure 2.13. It can do well-controlled optical stimulation and local field potentials (LFPs) recording as a closed-loop optogenectic neural prosthetics. Other functions include onboard diagnostics, recording signal amplification, temperature sensing, and logic control. The optrode head size is $1mm$×$2mm$ and the shaft size is $300\mu m$×$4mm$. The μLED selected for experiment is from Panasonic Corporation with diameter of $200\mu m$. The typical forward current is $5mA$ and the forward voltage is $2.97V$. The luminance intensity is $14.18mW/mm^2$, which is strong enough to induce neural activation/inhibition. There are 6 stimulation sites and 4 recording sites along the probe shaft [17].

The development in both μLEDs and μLEDs-on-optrode devices makes the manipulation of deep brain tissues possible. Based on the above literature study of the optrode devices, we could see that there already exist some devices capable of optical stimulation and electrical recording. But there's still space for further improvement of the overall performance. The device miniaturization, sufficient illumination, good control over light intensity and frequency, thermal increment around the LEDs are all essential aspects that need to be concerned.

A summary of the performance of recently published optogenetic implants is given in Table 2.5.

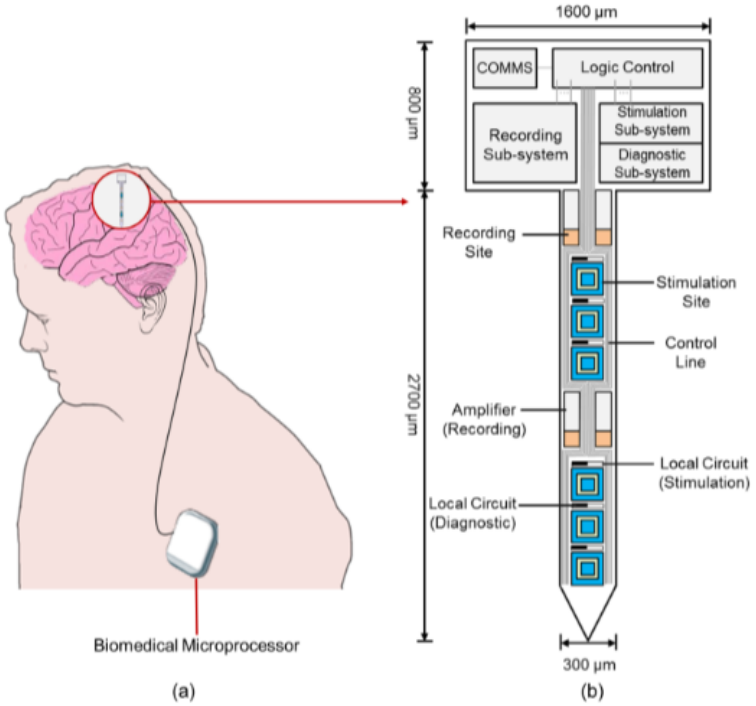

Figure 2.13: Intelligent implantable optrode [17]

2.4. Fabrication of Optrode Prototypes

The optrode combines electrical recording units and optical stimulation units in one tiny probe and functions in animal's brain. Such heterogeneously integrated micro-scale device can be fabricated by the Microelectromechanical systems (MEMS) technology with good quality control, high precision and batch production. The Microelectromechanical systems (MEMS) technique usually include the following procedures:

1. Deposition (evaporation, sputtering, CVD, etc.)
2. Photolithography
3. Etching (wet, dry, etc.), thin films
4. Wafer level bonding/packaging
5. Dicing, die attach, final packaging & testing

The deposition procedure is used for thin film growth, which could be applied in materials like dielectrics, silicon, metals, plastics and biomolecules. Metal (Al, Au, Pt, etc.) is frequently used as electrical interconnects and electrodes, being physically deposited or electroplated onto the substrate [23].

Photolithography process transfers the designed pattern from masks onto the wafer surface through coating, alignment and exposure, and development. Spin coating is an automatic process that covers the plain wafer with uniform light-sensitive photoresist. The uniformity and the thickness of coated photoresist are controlled by the wafer's rotation speed (rotations per minute, rpm). The patterns are transferred onto the wafer through aligning the mask with the processing wafer and expose the photoresist with UV light. The exposed parts of photoresist become more or less acidic (positive or negative) and can be removed by certain developers.

Etching could be divided into wet or dry etching, depending on whether via liquid chemicals or gas-phase chemistry. Isotropic etching and anisotropic (directional) etching could be used in either way, shown in figure 2.14 below.

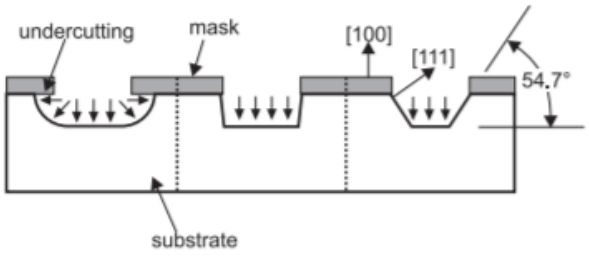

Figure 2.14: Isotropic (left) and anisotropic (middle, right) etching [23]

Other fabrication details are discussed in Chapter 3, 4, and 5 during the design and fabrication process.

2.5. Chapter Conclusion

In this chapter, we firstly introduced optogenetic techniques and how this could be used in the field of neuroscience. Two of the microbial opsin genes (ChR2 and NpHR) were listed as examples that perform the activation and inhibition of neurons respectively. Then, we discussed one of the essential parts of the optogenetics – the light delivery. After that, we discussed the recording electrodes and the favorable materials - Au, TiN and PEDOT. Then we reviewed previous optrode works and prototypes. Last but not least, we briefly introduced the microfabrication technique. Our goal is to design and make an optrode prototype that perform both optical stimulation and neural recording functions and is able to be chronically implanted into behaving mouse brains for research purposes. This optrode prototype should fulfill the following requirements:

1. For the neural signal recording part:
   (a) Biocompatible material for safe and chronic experiment;
   (b) Achieve relatively precise neural signal with low noise;
2. For the optical stimulation part,
   (a) Proper way of light delivery;
   (b) Precise and enough light emission;
   (c) Controllability over light intensity and frequency;
3. For optrode's physical properties,
   (a) Optimal size and geometry allowing safe implantation;
   (b) Capable of multi-site and multi-depth operations;
   (c) Enough mechanical strength.

Table 2.5: A summary of the performance of recently developed optrode prototype

Optical stimulation components				Electrical recording components				Other functions	Ref.
Light source	Dimensions (μm)	No. of channels	Max light intensity (mW/mm^2)	Dimensions (μm)	No. of channels	1kHz impedance	Substrate material		
Laser coupled fiber	Shaft tip diameter: 10	1	10	-	-	-	-	-	[18]
Laser coupled fiber	-	1	5	-	6×6	200kΩ-1MΩ	Silicon	-	[19]
Laser coupled fiber	Shaft diameter: 200	1	60-160 (473nm); 160-260 (561nm)	Diameter: 25	4	-	-	-	[24]
μLED coupled fiber	Shaft diameter: 60-70	6	40	-	-	-	-	-	[20]
μLED-on-optrode	Shaft width: 900	1	0.7	50×100	3	-	Polyimide	-	[21]
μLED-on-optrode	Shaft width: 80	5	600 (max.)	-	-	-	-	-	[22]
μLED-on-optrode	Shaft width: 1000	2	1.5	-	4	89.0, 20.6, 38.5, 54.8 kΩ	Polycrystalline Diamond	-	[25]
μLED-on-optrode	Shaft width: 400; Thickness: 20	4	40 (max.)	20×20	-	1 $M\Omega$	Silicon, polymer, platinum	Optical detection; Thermal sensing	[26]
μLED-on-optrode	-	3	2.7	-	-	-	-	-	[10]
μLED-on-optrode	Shaft width: 300	6	14.18	-	4	-	Silicon	Thermal sensing; Signal amplification; Logic control	[17]

3

Design Specifications and Design Layouts

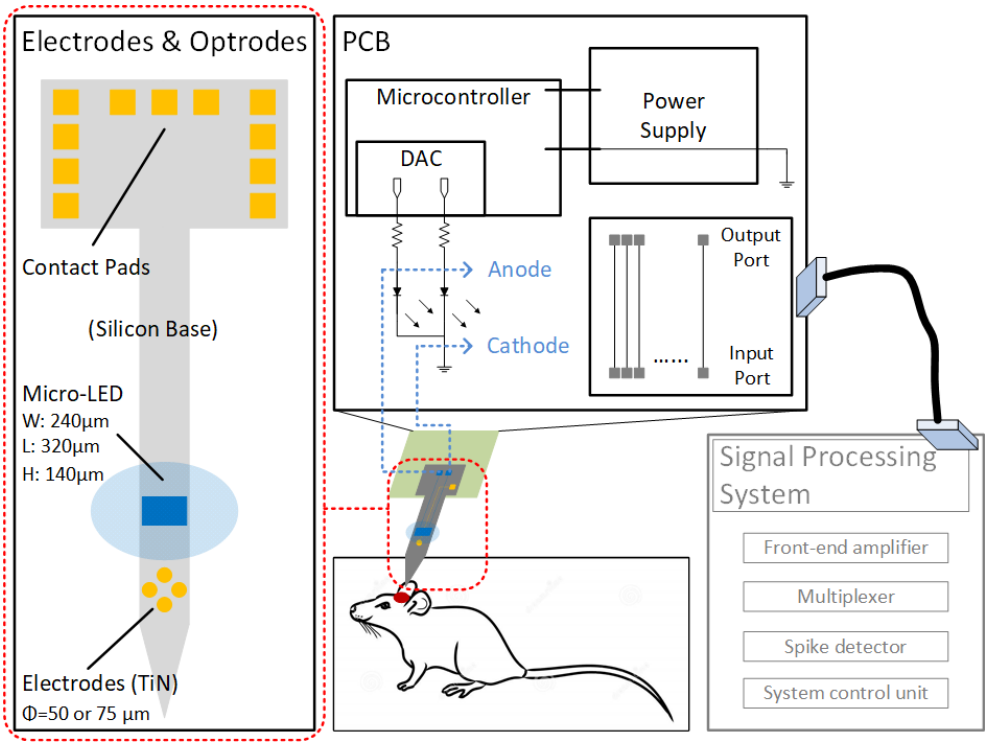

Figure 3.1: System Overview. Left: the optrode prototype; Right: the front PCB for signal transmission and powering the light source.

As mentioned in the previous chapter, the project goal is to design and fabricate an optrode prototype for simultaneous electrical recording and optical stimulation in the mouse brain. The system overview is depicted in Figure 3.1, comprising the design and fabrication of the optrode prototype and a PCB for transmitting neural signals and powering on-chip light sources. To achieve this goal, the following steps were taken, as shown in the diagram (Figure 3.2):

(1) Determine the proper light source we are going to integrate (which is the μLED), select a commercially available light source product, and present proper ways to control the light source;

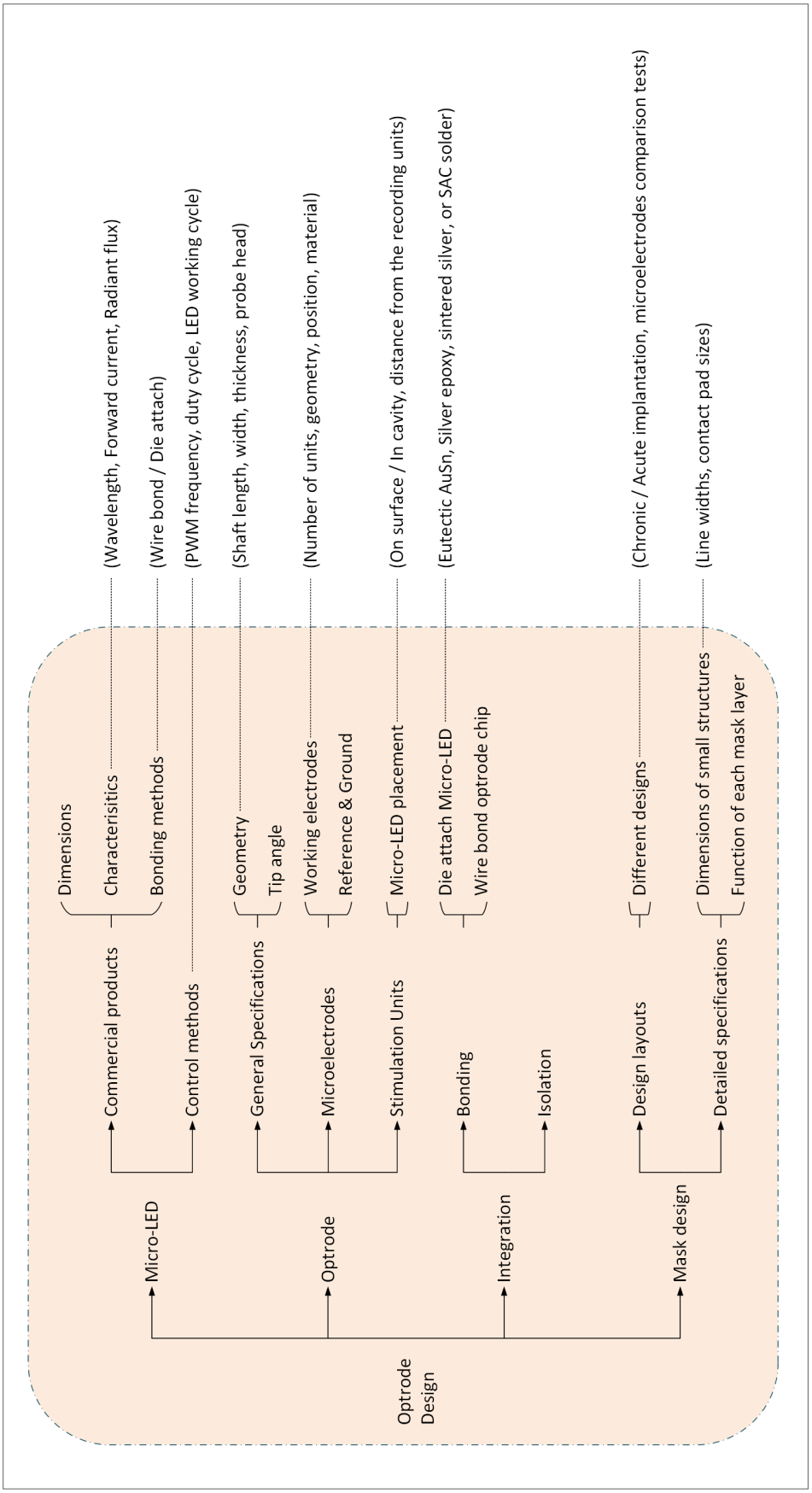

Figure 3.2: Diagram of Design Steps.

(2) Determine technical specifications of the micromachined optrode shaft, including the geometry and the tip angle of the probe shaft, the geometry, locations and materials of the recording electrodes, and the placement of light sources;

(3) Discuss the requirements for bonding and isolation of the device to ensure the signal transmission and the device's in-vivo safety, determine the die attach method for bonding the μLED;

(4) Determine detailed design specifications and produce mask layouts for the microfabrication process.

Correlations exist among the design steps. For example, the selection of the light source influences the geometry design of the optrode and integration steps. And the determination of some feature sizes during mask design is restricted by the microfabrication technologies.

In this chapter, the aforementioned design steps are discussed in details and a complete design specifications table and mask layouts are provided as a conclusion.

3.1. Light Source Determination

The first step in the actual optrode design is to choose a proper light source. In Chapter 2, we already compared different light sources - laser and on-chip-μLED, for application of optogenetics. We decided on the on-chip-μLED to be the light source because it has stable light delivery, good light intensity and frequency control, and possibility for freely behaving animal experiments when compared with the laser source. Moreover, μLED do not have light coupling efficiency issues when compared with LED-coupled optical fibers.

In this section, we provide some technical background on LEDs, followed with an investigation of multiple μLED products in the market, and different control methods of LEDs.

3.1.1. Fundamentals of LEDs

LED (Light-Emitting Diode) is a two-lead semiconductor device that converts the electrical current through its p-n junction into a light output. As depicted in Figure 3.3 [27], when an electric field is applied to the p-n junction (in the forward bias state), free electrons (in the conduction band with energy level, E_c) in the n-region pass across the junction and recombine with the holes in the p-region (in the valence band with energy level, E_v). Such recombination between electrons and holes of different energy levels lead to an energy dissipation, which is emitted in the form of thermal heat and light.

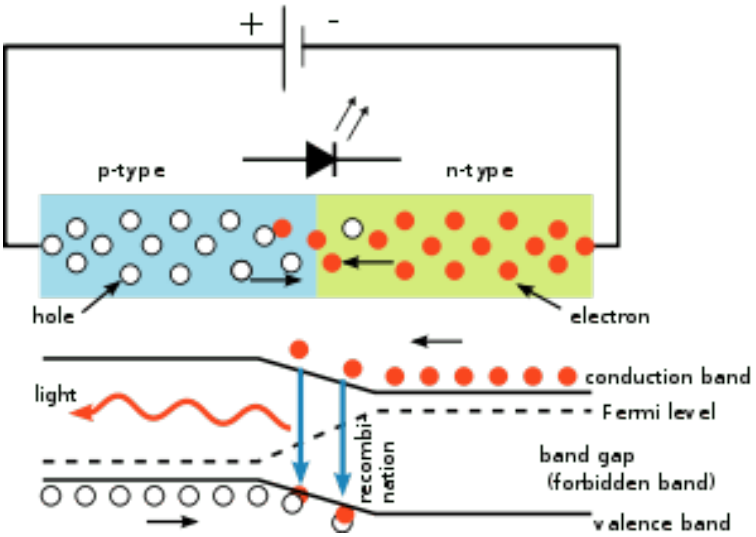

Figure 3.3: LED p-n junction in a forward-biased state [27].

The operation states of LEDs are presented in Figure 3.4 [27]. The forward bias state

is generated when the applied positive voltage level is higher than the intrinsic built-in p-n junction potential. The forward bias state is commonly used in LED applications to generate light emission. The other two states happen when a negative voltage difference is applied, which results in a negative leakage current passing through the LED. When this negative voltage is increased to V_{br}, a strong negative avalanche current is generated [17].

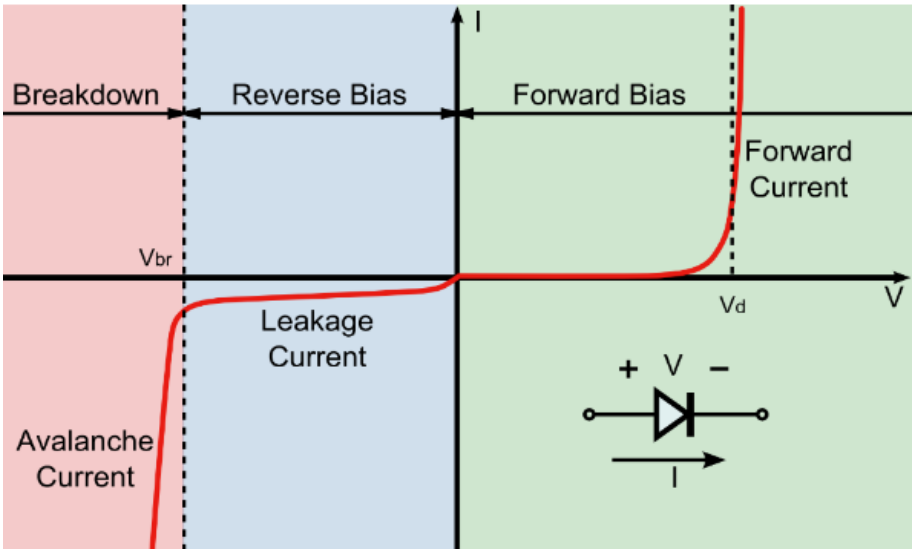

Figure 3.4: LED operation states [27].

3.1.2. Selection of the μLED

After deciding to integrate μLEDs on the optrode and understanding the basic operation states of the LED, investigations should be done on companies that could offer μLEDs suitable for the application. We chose to buy commercially available μLEDs because directly fabricating μLEDs is not feasible here.

The companies that offer μLEDs are: Cree, Lumileds, Tyndall, Panasonic, Samsung, Rohm. The proper μLED light sources are selected based on the emitted light wavelength, dimensions, bonding methods, forward current and power consumptions. Some of the requirements are listed in Table 3.1 below.

Table 3.1: Requirements for selecting commercial μLEDs.

	Requirements
Light color	Blue ($\sim$ 470 nm)
Dimensions	<300 μm
Bonding methods	Eutectic die attach

Blue μLED is selected to make our optrode prototype. And a maximum dimension below 300 μm is preferred when considering the in-vivo safety issue. Wire bond and die attach are two typically used methods to bond μLEDs onto substrates. Wire bonded μLEDs usually have a smaller dimension when compared to die attached μLEDs, such as Cree UT170 model with a dimension of 170×170×50 μm^3. However, the wire bonded μLEDs offer the risks of wire breakage and bonding failure when inserting the probe in the brain. Hence, a die-attach μLED was selected.

The thermal increment in the surrounding tissue by μLED heat dissipation is another important design concern to bound the search space of the μLED to be placed in the optrode. A temperature rise of less than 1 $^{\circ}C$ does not perturb brain functions, reported by Anderson *et al.* [28].

In Table 3.2, I list two μLED models from Cree Inc that meet our basic requirements - TR2227 and DA2432. Both μLEDs meet the requirements and can provide enough light intensity for optical stimulation.

Table 3.2: Main parameters of possible μLED choices from Cree Inc.

LED model	Cree TR2227	Cree DA2432
Wavelength (nm)	450&460	470
Dimensions (μm^3)	220×270×50	240×320×140
Radiant flux min. (mW)	21	30
Typical forward current (mA)	20	20
Typical forward voltage (V)	3.3	3.1
DC forward current max. (mA)	30	100
Bonding type	Epoxy die attach	Die attach

The μLED model DA2432 from Cree Inc has a higher radiant flux with a lower forward voltage when compared with model TR2227, and it allows eutectic die-attach bonding method with an improved thermal management. Hence, this model was selected as the optical stimulation source. The geometry parameters are presented in Figure 3.5. The chip bottom area is 240×320 μm^2 with overall thickness of 140 μm. The bond pad dimension for anode is 60×170 μm^2 and the dimension for cathode is 105×145 μm^2, with bond pad thickness of 3 μm.

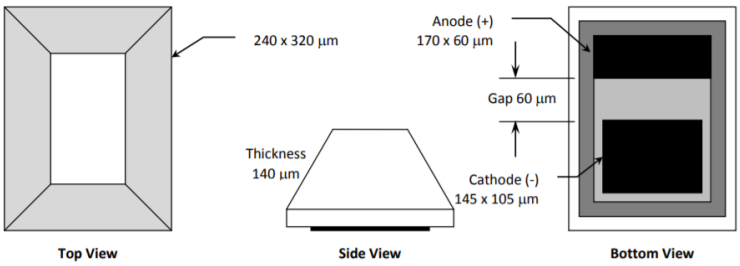

Figure 3.5: Chip diagram of the commercial μLED model: Cree DA2432.

The characteristic curves of the selected μLED are presented in Figure 3.6. The typical forward voltage is 3.1 V with a current flow of 20 mA. The minimum radiant flux [1] is 30 mW and the dominant wavelength is 470 nm. For blue light (wavelength of 470 nm), the radiation power will lose around 75% within a radius of 200 μm in brain tissue [10]. The μLED should be placed in a close proximity to the stimulation sites to ensure sufficient optical stimulation and avoid overheating in the surrounding tissue as well. The temperature change depends on both the optical power and the stimulation duty cycle. In Figure 3.7, an experimental result of the model Cree DA2432 LED is presented, proving that this product can supply enough optical power when working in a thermally safe condition [29].

3.1.3. μLEDs control

The next step taken was to decide how to control the intensity and the frequency of illumination. For that, there are two possible solutions: 1) via analog voltage control; 2) via digital voltage control. The LED current behaviours when dimming the LED with different methods are presented in Figure 3.8.

In the first solution, the LED is controlled through regulating the LED current input level by an external DC control voltage. Due to the direct changing of the DC current flow, color shift effect can appear during the LED dimming.

In the second solution, the LED is controlled through pulse-width-modulation (PWM) method. The PWM control method turns on and off the LED current for very short peri-

[1] The radiant energy emitted, reflected, transmitted or received, per unit time (J/s).

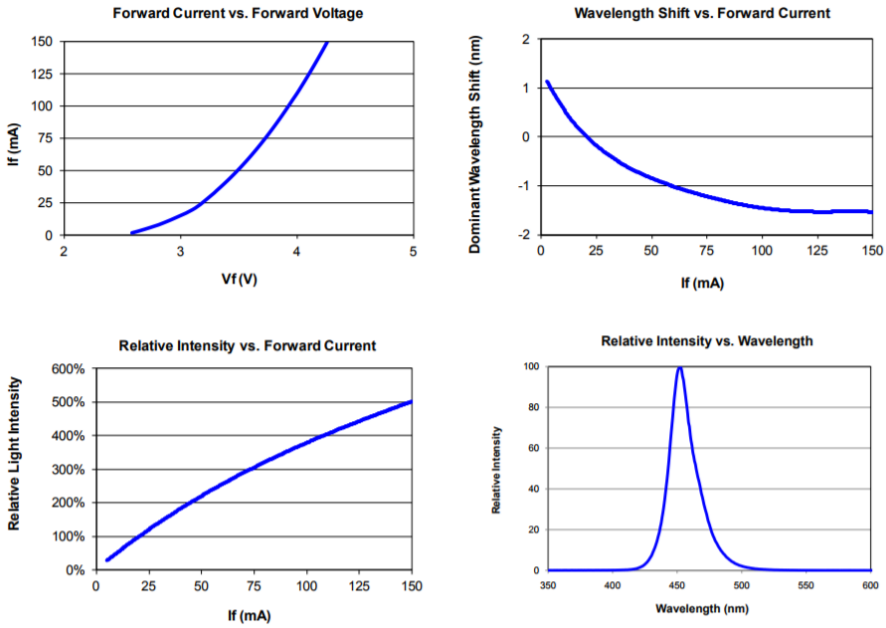

Figure 3.6: Characteristic curve of Cree DA2432 LED.

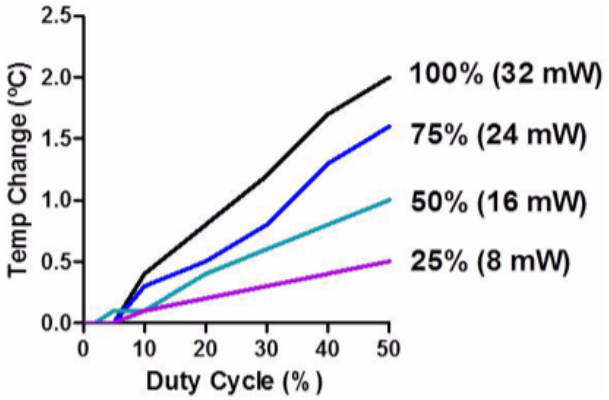

Figure 3.7: In vivo temperature change surrounding the μLED [29].

ods of time, with on/off frequency over 100Hz. The radiant flux is controlled by modulating the peak current with different duty cycles and there's no color shift effect due to the constant level of the output current.

The PWM control method is preferred here. The first reason is because of the simplicity of the control panel. For DC analog control, microprocessor, digital-to-analogue converter (DAC) and some associated components are usually required. However, the PWM control only needs a single MOSFET switch and a programmed microprocessor, which means less complexity, smaller size and less power consumption, and is possible for on-chip integration. In addition, full light intensity range can be achieved from 0% to 100% by adjusting PWM duty cycles. Fu-Yu Beverly Chen *et al.* indicated in 2017 that PWM with switching frequency of 10kHz is well beyond the physiological response rates of existing opsins [31]. Such PWM switching frequency can be achieved with the microprocessors and the neurons will not sense the flickering of μLEDs.

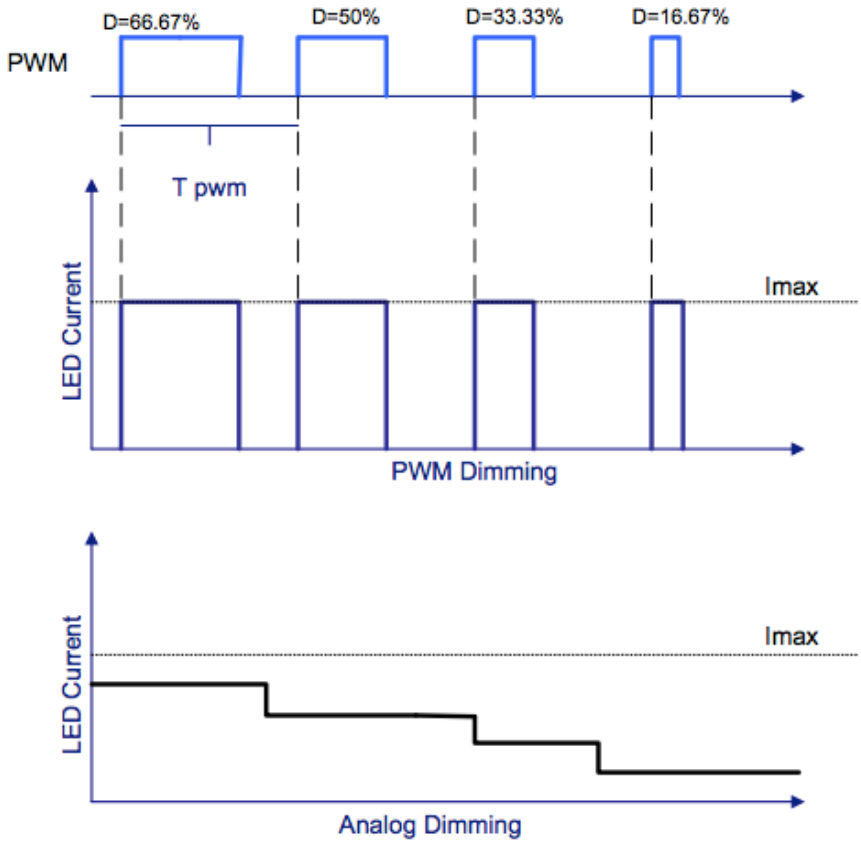

Figure 3.8: LED current behavior with different dimming options [30].

3.2. Conceptual Design of Optrode

As the optrode needs to be implanted in the mouse brain, several design aspects shall be considered to ensure both safe implantation and proper operation of the device. Therefore, in this section, we address several aspects of the optrode's design such as: size, dimensions, structures, geometry, functionalities, materials, and interconnections. We present these aspects in the following sequence:

(1) Schematics of the optrode: the design requirements provided by LUMC (locations of microelectrodes and light sources); restrictions on the shaft dimensions (width and thickness).

(2) Geometry of the optrode shaft: shaft length, width and thickness (contribute to the mechanical strength); tip angle (contribute to the surgical implantation).

(3) Technical aspects of microelectrodes: geometry (diameter); distributions (the number of recording sites and their locations); material (biocompatibility and low impedance level); reference and ground electrodes (locations and requirements).

(4) Other design specifications: placement of μLEDs; how to separate optrodes from the wafer.

3.2.1. Optrode schematics

The basic structure of this optrode prototype is similar to the Michigan array (Figure 2.4 (b)), in which the electrodes are distributed along the shaft, allowing multi-depth stimulation and recordings in the brain. Some requirements and restrictions have been given by the neuroscientists in LUMC and the initial probe schematics is presented in Figure 3.9.

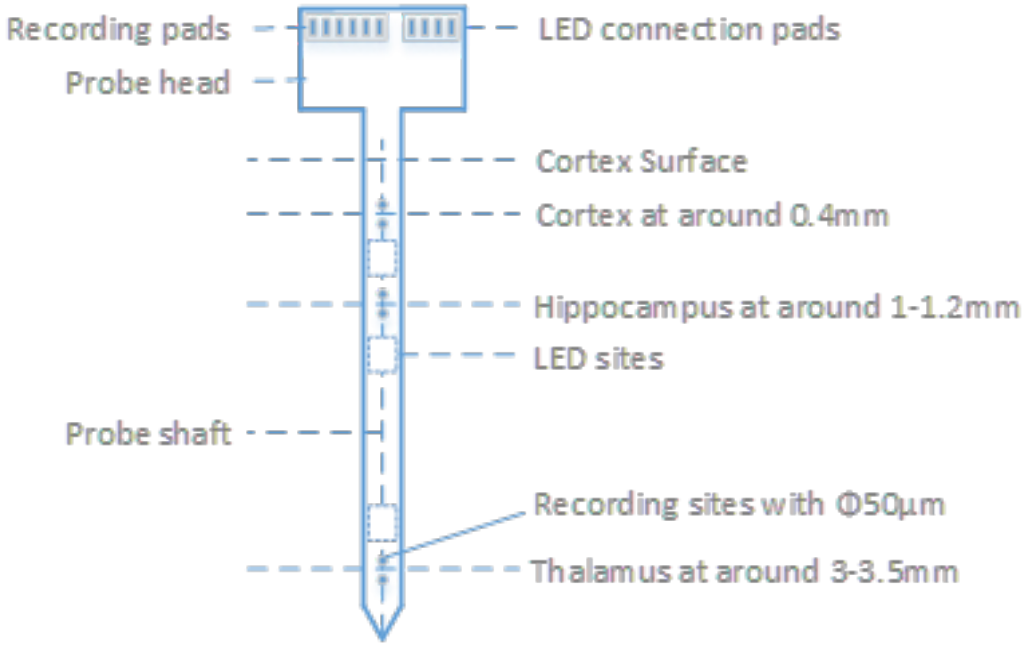

Figure 3.9: Conceptual design draft of the optrode probe.

For neural signal recording, there are three clusters of recording sites distributed along the probe shaft, aiming at different regions in the mouse brain. Each cluster has a pair of recording electrodes placed in a close distance with each other. The electrodes can be used individually to detect the local field potential (LFP) and close-contact DC signals, and can be used in pairs to measure the multi-unit activity by differentiating two signals. The first electrode pair is located in the layer of cerebral cortex at depth around 400 μm. The second pair is in the layer of hippocampus at depth around 1000-1200 μm. The last pair is located in thalamus at depth around 3000-3500 μm. For optical stimulation, three light sources are placed next to the electrode clusters to induce optical stimulation to the neurons in the corresponding region. The aforementioned parameters can indicate the total length of our optrode prototype, which consists of the length of the tip, the length of the shaft within the brain (from recording sites to the surface of the cortex) and the rest length above the cortex surface (meninges layers & in the air).

For the current setups in the Human Genetics lab in LUMC, the largest electrode they are using is a pair of parallel microwires (with a diameter of 125 μm) being placed closely and twisted. Such electrode structure wouldn't cause lethal tissue damage and could be left in the mouse brain for long term tests (1 to 3 months). This gives us restrictions when determining the shaft width and thickness of the probe.

As depicted in Figure 3.9, contact pads are placed at the head of the probe, allowing signal transmissions for both neural signals and powering the μLED light sources.

3.2.2. Geometry of the probe shaft

Microelectromechanical systems (MEMS) technology is the main fabrication method used for producing the micro- to millimeter scale optrode prototype with precision. In this part, we determine the geometry parameters of the shaft (probe length, width and thickness) and discuss if these parameters can provide enough mechanical strength during the implantation.

Mechanical strength

Silicon wafers are used as substrates because of their high compatibility with MEMS technology. Likewise, silicon wafers are also compatible with CMOS process, leading the

potential to integrate functional units such as temperature sensor for monitoring temperature change in surrounding tissues, pre-amplifiers for amplify neural signals, and MOSFET switch for PWM control. Because of the difference in Young modulus between the silicon substrate and the brain, tissue damage seems to be inevitable.

When the silicon probe presses against the tissue, the maximum load force on the probe shaft (Buckling load) is given by [32]:

$$P = \frac{EWt^3\pi^2}{6L^2} \tag{3.1}$$

E: silicon Young's modulus;
W: probe width;
t: probe thickness;
L: probe length;

The stress-strain relationship and the average strain on the probe shank are given by [32]:

$$\sigma = \epsilon E \tag{3.2}$$

$$\epsilon_{Avg} = \frac{3ty_A}{4L^2} \tag{3.3}$$

σ: stress on the probe;
ϵ: strain on the probe;
y_A: maximum deflection at the probe tip.

From the above formula, the buckling load P defines the substrate's stiffness when pressing against the tissue and the stress σ defines the strength of the substrate [32]. The thickness and the width of the substrate should be increased and the substrate length should be as small as possible for producing a stiff and strong probe.

According to K. Najafi and J.F. Hetke, a silicon probe with thickness of 15 μm, length of 2-3 mm, and width of 20-100 μm is strong enough for all experiments, including penetrating arachnoid and pia mater (layers that cover the cerebral cortex, with abundant blood vessels) [32]. Considering silicon wafers in EKL clean room have thickness of either 500 μm or 300 μm, the probe with a width of 350 μm and a length of 7 mm ensures enough stiffness and strength. For safety concerns during animal experiments, the width and the thickness of the probe shaft should be minimized, which could be realized by bulk etching the silicon wafer from the backside. However, the integration of μLEDs into the probe makes the mechanical strength of the whole shaft difficult to predict and calculate. The bulk etching of silicon wafer backside is thus bypassed.

Tip angle

The tip of the shaft shall be sharpened in order to facilitate the optrode implantation. According to David J. Edell *et al.*, a probe with tip angle larger than 40-50° is difficult to penetrate into the dura mater and the probe with tip angle less than 20° could slip into dura without causing dimples [33]. However, for the same shaft width, a decrease in tip angle will result in a longer tip length. Taking both factors into considerations, the tip angle is determined to be 20°, suitable for surgical implantation procedure and has a tip length of around 1 μm for a 350 μm width shaft.

Different design layouts

In the actual design, the initial idea presented by neuroscientists in LUMC to include multi-sites and multi-depth recordings within one single probe (targeting cortex, hippocampus and thalamus simultaneously) is difficult to reach since it's difficult to control the implantation depth with precision (to place three clusters of electrodes in three different brain regions of interests). Therefore we break the initial design draft down to two different design

layouts - one probe with a shaft length around 4 *mm* for long term experiment in cerebral cortex and one probe with a shaft length of 7 *mm* for acute experiment in hippocampus or thalamus. We also make design layouts with electrodes alone in order to compare the signal quality of different electrode sizes and make a comparison between the Pt/Ir electrodes in Human Genetics Lab in LUMC and our electrodes. The main differences between those design layouts are their shaft lengths, the arrangement of electrodes and the light sources and their own functions. The design layouts will be presented and illustrated later in section 3.4.

3.2.3. Microelectrodes

In this part, microelectrodes are discussed on their geometry, number of recording units and their distributions, material selection, and the requirements for the reference and ground electrodes.

Geometry

The diameters of published recording electrodes range from 5 to 50 μm, according to Kim et al. (2014) [34]. The small surface area contributes to a much higher electrode impedance and a surface modification process is suggested to lower the impedance level. While larger electrodes (diameter>50 μm) have lower impedance and reduced thermal noise but record signals from a larger population of neurons. The peak amplitude of the action potential is averaged since the smaller amplitude neuron signals from a certain distance are taken into account, which results in lower SNR [35]. Camunas-Mesa et al. (2013) studied the optimal size for electrode through several simulations (not considering the electrode thermal noise) and found out that the SNR reached a maximum value for electrode diameters range from 30 to 50 μm and 40 μm is the optimal size [36]. 50 μm was then selected to be the electrode size to allow good neural signal qualities with a lower impedance level. We also include 75 μm microelectrode sites to make a comparison with the existing microwire electrodes (75 μm Pt-10%Ir) in the Human Genetics lab in LUMC.

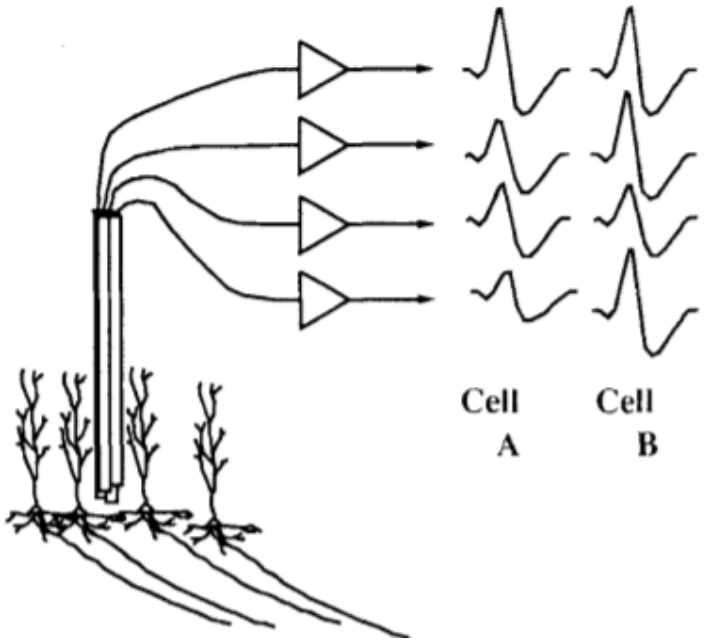

Figure 3.10: Schematic diagram of the four-channel tetrode [37].

Distributions of recording microelectrodes

The single electrode records the action potentials from a population of neurons nearby. However, it can not identify neuron's spatial information as the recorded signal contains spike amplitudes from different cells. The earliest tetrode (Recce and O'keefe, 1989; Wilson and McNaughton, 1993) is an electrode with four microwires insulated to the tips, and is used for multi-neuronal recordings [38]. A schematic diagram of the four-channel tetrode among four pyramidal cells is presented in Figure 3.10 [37]. Tetrode can be used to separate the spikes from different neurons based on the fact that spike amplitude decreases with the distance between the electrode site and the neuron. With the help of advanced spike-sorting algorithms and software, the tetrode structure is capable of recording a group of nearby neurons and providing reliable spike information from different neurons. Thus, we include 4 electrodes in one electrode cluster for the extracellular recordings, accompanied with one ground and one reference electrode on each probe shaft.

Reference and ground electrodes

The reference electrodes are the same size as the recording electrodes and the ground electrodes are determined to be 100 μm in diameter. Both reference and ground electrodes will be placed near the cortex surface (approximately the surface of cortex or in pia mater) to be electrophysiologically "silent" when compared to working electrodes. In practical, the impedance level of reference and ground electrode should be low when compared to working electrodes. This can be done with a material surface modification (i.e. electrochemical methods) to both reference and ground sites.

Electrodes material

Titanium nitride (TiN) was selected as the electrodes material because of its in-vivo biocompatibility, low impedance level due to the rough surface conditions and the easiness for fabrication. It was reported that the impedance of a flat and round TiN microelectrode with diameter larger than 30 μm is below 100 $k\Omega$ at 1 kHz and is approximately 250 to 400 $k\Omega$ for smaller diameters [39]. The actual impedance of TiN microelectrodes depends on both the fabrication environment (such as temperature, gas pressure) and applied recipes during microfabrication processes.

3.2.4. Other design specifications

In this part, other design considerations are introduced, including the etching of silicon wafer surface to create the cavity structure for placing the μLED and the breaking groove structure for detaching the optrode from the silicon wafer, and the optrode head dimension.

μLED-in-cavity

On account of the extra tissue damage caused by the thickness of the μLED (140 μm), a cavity on the optrode surface was designed to reduce its topography. Two cavity structures were created, as illustrated in Figure 3.11.

The etching process could either create a straight cavity wall or a sloped cavity wall with a slope angle of 54.7°. The straight wall is not feasible in this case since photolithography steps can not be applied to it to create the desired patterns. The <111> crystal plane sidewalls appear during the KOH anisotropic etching process due to the etch rate difference between the <111> and <100> crystal plane, and 54.7° is the angle between the two planes, as depicted in Figure 3.12.

Taking this slope angle into consideration, the area occupied on the probe surface is $240 + 2 \times h/tan(54.7°)$ μm by $320 + 2 \times h/tan(54.7°)$ (h is the depth of the cavity). For a depth of 140 μm, an area of 438.3 μm by 518.3 μm is required to place the μLED inside, which is too much for a 300 to 350 μm width probe shaft. So we consider removing cavity walls along the

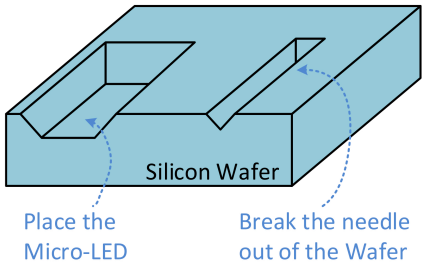

Figure 3.11: Two cavity structures for the LED placement and the optrode detachment from the wafer.

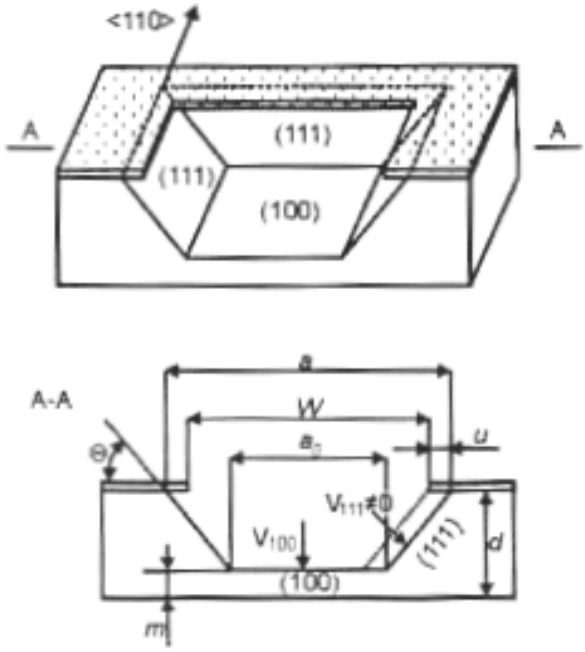

Figure 3.12: An anisotropic wet etch on a silicon wafer [40].

shaft side, as presented in Figure 3.13. And a width of 350 μm is enough for placing both the μLED and electrode wires. The cavity is placed near the electrodes (within a distance of 200 to 300 μm) to ensure sufficient light delivery to the stimulation region.

Breaking groove

For a standard fabrication process, the chips are detached from the processed wafer through wafer dicing. The dicing saw cuts the silicon wafer in straight lines automatically. The optrode consists of a narrow probe shaft and a wider rectangular probe head, which makes it impractical to separate the probe from the wafer with a dicing procedure. Hence, the optrode substrates are bend and detached from the wafer manually and a groove structure (Figure 3.11 & Figure 3.13) is created by the end of the probe head to adjust the mechanical stress and strain during detachment without causing unwanted damages.

Probe head

The dimensions requirements of the probe shaft have been discussed previously, as well as the distributions of the electrodes and μLEDs along the shaft. The probe head contains the contact pads for recording electrodes and cathodes and anodes of μLEDs. Its dimension depends on the size of the connection pads, the space between these pads, and the dimen-

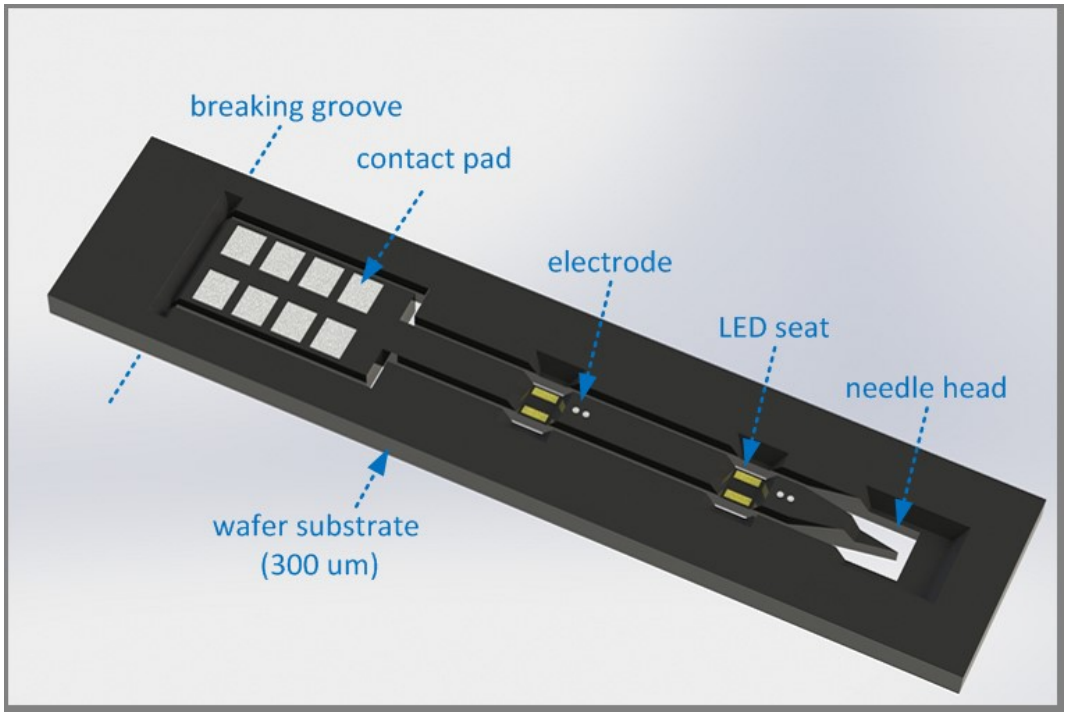

Figure 3.13: Artwork illustration of the optrode (created with SolidWorks). Optrode's structure, recording sites, bonding pads and cavities for placing the μLEDs are depicted.

sions of the corresponding connection sites on PCB board. The detailed dimension values are presented later in this chapter when designing mask layouts.

3.3. Bonding and Isolation

After the fabrication of the optrode body in the clean room, μLED was bonded onto the probe's shaft, and the optrode was bonded onto a PCB afterwards. Isolation material was added to cover all the active electronic components to prevent electrical leakage in vivo. In this section, different bonding and isolation methods are discussed.

3.3.1. Bonding methods

Die attach bonding

As explained before, wire bonding has the risks of wire breakage in the middle of the wire and at bonding sites. Moreover, it requires long interconnection lengths and has the disadvantage of degrading electrical performance. For these reasons, we choose die attach bonding methods for integrating the μLED. The anode and cathode of Cree DA2432 μLED are made of AuSn and can be bonded through eutectic die attach approach.

The die attach technology contains the following platforms: Gold-tin eutectic, Conductive adhesives, Sintered materials and Solder [41]. Eutectic Gold-tin (AuSn) is a standard die-attach material and is used because of its proven thermal conductivity (57 W/mK) and its high reliability. Conductive adhesives (mostly silver filled epoxies) are widely applied not only in the field of LED die attach but also for semiconductor packages [41]. Their thermal conductivity is typically up to 50 W/mK. Sintered materials (i.e. sintered silver) are materials that consist of micro/nano scale metal particles and can form nano-porous yet pure metal joint. It has higher thermal performance and mechanical reliability than AuSn. Solders are mostly SAC (Sn/Ag/Cu) based and has thermal conductivity around 50-60 W/mK. Compar-

isons of different die attach approaches are presented in Table 3.3. Eutectic die attach is the first option for bonding μLEDs and silver epoxy is an alternative.

Table 3.3: Comparisons of die attach material platforms [41].

	Au/AuSn	Silver Epoxy	Sintered Silver	SAC Solder
Secondary reflow possible	Yes	Yes	Yes	No
Thermal conductivity (W/mK)	$\sim$ 57	2-50	>100	$\sim$ 60
Cost	High	Medium	Medium to High	Low

Wire bonding

To convey the neural signals to the signal processing system and give power supply to the μLEDs, we need to bond the optrode onto a minimized PCB. The PCB is the part of the head-stage and is less sensitive to the wire damage. The wire bond method was selected in this case. This process is critical due to the dimension difference between the probe and the PCB, and also the micro-scale dimension of the contact pads and their inter-spaces. For wire bonding, gold, aluminum and copper are typically used. There are two categories of wire bonding - ball-wedge bond and wedge-wedge bond. Ball-wedge bonding is used in this case. And the loop height of wire bonding is typically 400 μm, as presented in Figure 3.14.

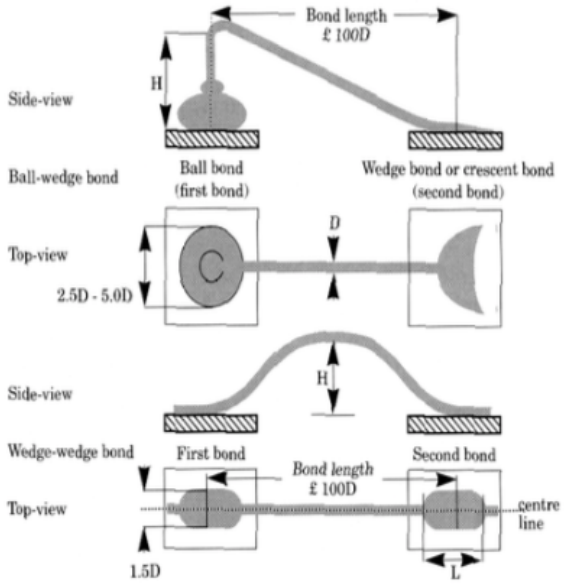

Figure 3.14: Typical dimensions for wire bonding.

Other bonding methods

For attachment between the optrode probe and printed circuit board, non-conductive epoxy or glue can be used. For example, H20S non-conductive epoxy from Epoxy Technology Inc can be dipped between two substrates and be cured in 150 °C for 1 hour.

3.3.2. Isolation

After the bonding procedure, the die-attached bare μLED dies need to be isolated from the tissue and in-vivo environment.

UV-Curing Optical Adhesives from Thorlabs can be coated onto the LEDs to form a protective layer. However, one concern is that the isolation procedure using optics glue might

have an coverage on the recording sites as well because of the small dimension of the optrode and the close proximity between the μLED and recording sites.

PDMS and parylene are two available materials in EKL that can be used to cover μLEDs because of their biocompatibility and their sufficient transparency to light. The isolation process can be supplemented to the microfabrication process after die attaching μLEDs to form a uniform isolation layer and provide the possibility for batch production in the future.

3.4. Masks Layouts

So far, the light source, the technical specifications of the optrode and the integration technique have been discussed and determined. The results are presented in Table 3.4.

Table 3.4: General Design Specifications.

Section 3.1 Light Source	
Light source	μLED
Commercial model	Cree DA2432
Wavelength (nm)	470
Dimensions (μm^3)	240×320×140
Radiant flux (mW)	30
Bond method	Die attach
Control method	PWM
Section 3.2 Optrode Conceptual Design	
Fabrication Technique	MEMS
Substrate material	Silicon
Material property	Rigid
Targeting brain layers	Cerebral cortex, hippocampus, thalamus
Shaft thickness (nm)	300
Shaft width (nm)	350
Shaft length	Varies with different designs
Tip angle	20 °
Microelectrodes geometry	Flat & round
Recording sites diameter (μm)	50 & 75
Electrodes distributions	Tetrodes
Electrodes material	TiN
Reference & Ground	Require surface modification
Section 3.3 Bond and Isolation	
μLED to optrode substrate	Die attach (AuSn or Silver epoxy)
Optrode to PCB	Wire bond
μLED isolation	PDMS

The next step was to generate masks to pattern the desired structures (i.e. microelectrodes, contact pads, μLED bond pads) onto the silicon wafer with the photolithography process. Tanner L-Edit IC Layout software was used to design and produce the mask layouts for the fabrication process.

3.4.1. Mask layouts of different designs

To fulfill the experimental requirements from LUMC, five probes were designed with different specifications and functions. Three of them were optrodes with both electrical recording and optical stimulation functions, and the rest two contained only microelectrodes. In this part, mask layouts of different designs are presented, accompanied with a brief summary of the function of each design.

Multi-depths recording and stimulation

The initial design (Figure 3.15) contains three electrical recording sites and two optical stimulation sites within close proximity, aiming at simultaneous recording and stimulation over different brain layers: cerebral cortex, hippocampus and thalamus.

However, this design is not practical during the electrophysiological experiments, as explained in section 3.2. We kept this design layout because it can be used to test the feasibility of fabricating multiple recording and μLED stimulation sites on one single shaft and test the induced neural signal artifacts by μLEDs.

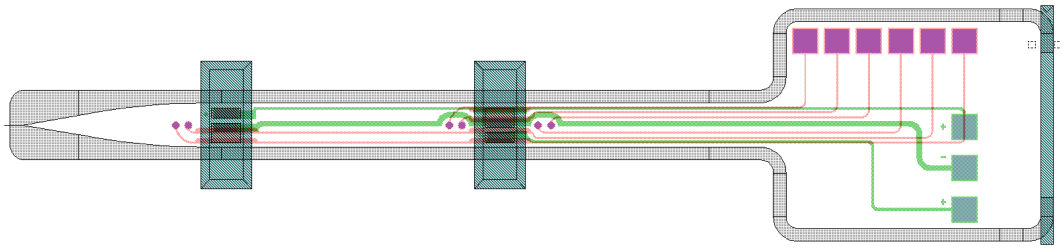

Figure 3.15: Mask Layout 1: Optrodes for multi-depth recording and stimulation

Chronic experiments in cerebral cortex

In practice, different designs are made to target different brain layers separately. The Mask Layout 2 (Figure 3.16) is designed for chronic electrophysiological experiments targeting the mouse cerebral cortex region (thickness of 1200 μm [42]) at around 400 μm depth. It has two shafts with a distance of 1000 μm. One tetrode and one μLED are integrated on each shaft, allowing for stimulating and recording at two different sites with the same depth simultaneously. With optical stimulation on one shaft and recording spread neuron signals from the other, the cortical spread depression (CSD) can be studied as well. The total length of the shaft is determined to be 4000 μm, containing an extra length of more than 2000 μm above the cerebral cortex surface.

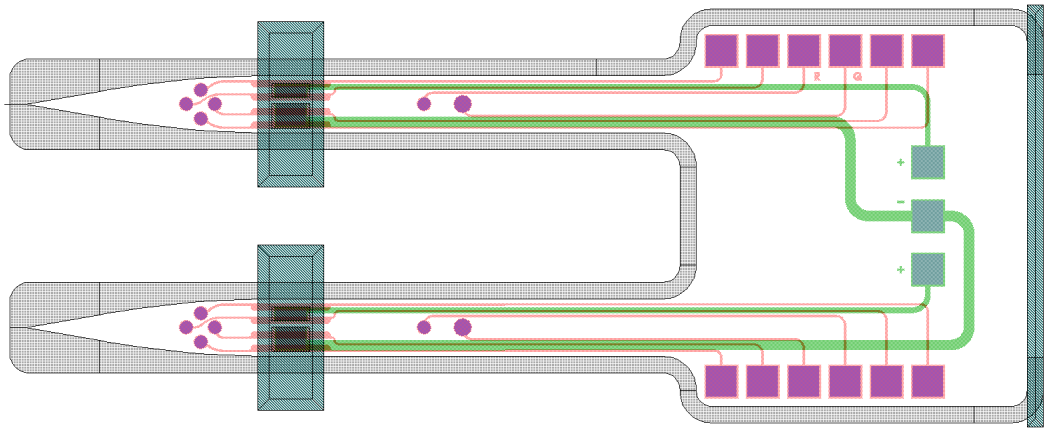

Figure 3.16: Mask Layout 2: Optrodes for chronic implant in the cerebral cortex

Acute experiments in deep brain regions

The third design (Figure 3.17) aims acute experiments for studying deeper sites in the brain such as hippocampus (1200 μm depth) and thalamus (3500 μm depth). Only one shaft is required with one tetrode and one μLED stimulation site built in. The total shaft length

is increased by 3000 μm compared with the second design for chronic experiments. As the probe's implanted length increases, more tissue damage and tissue response happen. The increased tissue damage limits the experimental time in animals to be an "acute" experiment.

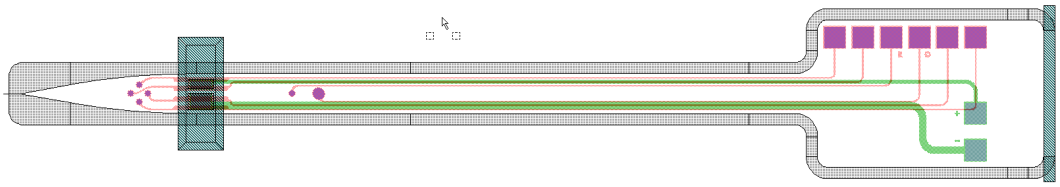

Figure 3.17: Mask Layout 3: Optrodes for acute implant in deep brain areas

Microelectrodes for control experiments

Different from the previous three design layouts, the fourth and fifth design only function as neural signal recording, which are used to verify the microelectrodes performance of different sizes and materials. The Mask Layout 4 (Figure 3.18 (a)) is designed along with the initial design (Figure 3.15) and contains two separately located microelectrode clusters. Mask Layout 5 (Figure 3.18 (b)) contains two closely placed tetrodes of different sizes (50 μm and 75 μm) and is used to compare the simultaneously recorded neural signals from different electrodes.

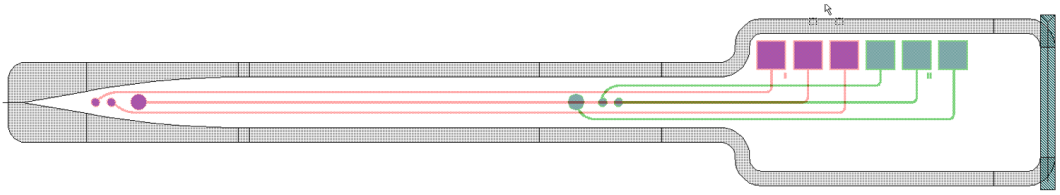

(a) Electrode pairs - Different Depths

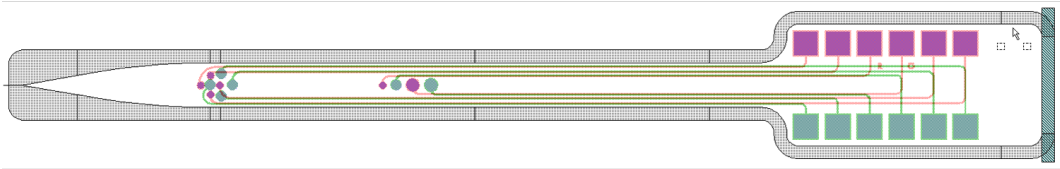

(b) Electrode clusters - Different Sizes

Figure 3.18: Mask layouts of microelectrodes 4 & 5

The overall mask layer layout is presented in Figure 3.19.

3.4.2. Other mask design considerations

Apart from the specifications explained in section 3.2 (i.e. shaft width, shaft length, tip angle, electrode size and distributions), there remain some important factors that we need to take into considerations during the mask design. In this part, we explain how the line width and dimensions of the contact pads are determined. And explain how we determine the number of total masks and the function of each mask layer.

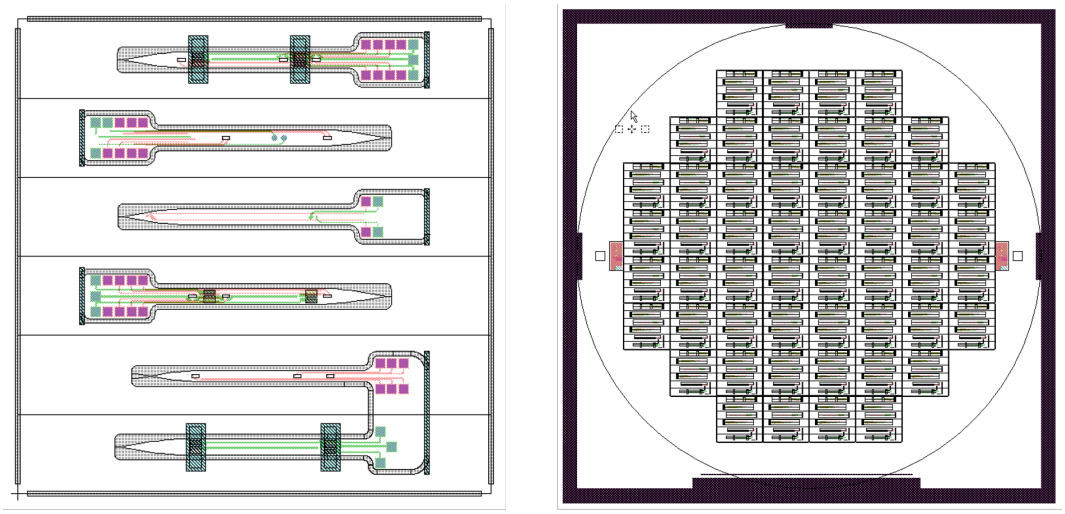

(a) Masks - One Block (b) Masks - Wafer Level

Figure 3.19: Masks overall layouts. (a) Mask layers in one block; (b) Mask layers in wafer level

Line width determination

We need to determine the line width of microelectrodes (both on wafer surface and in the MEMS cavity) and the line width of the cathode and anode of μLEDs. With regard to fabrication techniques, some restrictions of the line width and the line placement exist:

(1) The Contact aligner (Alignment and exposure machine) has a feature size above 2 μm and has limited overlay accuracy when compared to Waferstepper (feature size ~ 0.5 μm, overlay accuracy of 0.1 μm). Therefore the minimum line width on silicon wafer surface is preferable to be above 5 μm.

(2) MEMS cavities are created on the silicon wafer for placing μLEDs, and several tracks need to pass through these cavities. During the photolithography process, a gap exists between the aligned mask and the base level of the MEMS cavity, which reduces the exposure resolution at the cavity bottoms (details explained in section 4.1.2). The width of the metal lines passing both through the sloped wall and the base level of the MEMS cavity shall be as wide as possible. The microelectrode metal line width is set to be 10 μm on the wafer surface and 40 μm in the cavity. The inter spaces between lines in the cavity are also 40 μm. The distance between the probe edge and the outermost line is hence 35 μm.

(3) The wet etch steps during the microfabrication process can lead to under-etch at the edge of silicon probes. A space >10 μm between the probe edge and the outermost line is safe enough to stand through the wet etch process.

For the tetrode microelectrodes, four lines need to be placed starting from the probe tip to the probe head. The 350 μm width of optrode shaft is not enough for placing both the lines and the μLED bond pads. Therefore, microelectrodes and μLED bond pads are placed in different layers.

For metal lines that connect the μLED anode and cathode, 20 μm is wide enough for a current flow of several milliamps. Because the μLEDs have a common cathode, the line width of cathode is twice as the anode line width.

Dimensions of contact pads for wire bonding

The wire bond technique is used to connect the optrode to the front PCB. Typical wires are made of Au and Al. We designed the wire bond pads on the probe head to be 180 × 180 μm^2. Such dimension is enough for bonding Au or Al wire with a diameter around 30 to 40 μm.

Determination of masks

Gold (Au) was selected to be the μLED bond pad material in the first place because we'd like to use eutectic die attach method to bond μLEDs with Gold Tin (AuSn). However, with regard to the fabrication process, Au belongs to contaminated metals and is not compatible with the CR100 environment in EKL. Deposition of Au layer on our optrodes will increase the difficulty and the overall fabrication time. For this reason, the eutectic die attach bond method was replaced by silver epoxy die attach bond method for our optrode prototype. The bond pads shall be made of conducting materials. We then modified the second metal layer recipe to be TiN/Ti as well. An extra mask is designed for evaporating Au onto μLED bond pads in case the silver epoxy die-attach doesn't work well, as presented in Figure 3.20.

The modification of μLED bond pad material from Au to TiN and the modification of bonding methods from eutectic die attach to silver epoxy die attach simplify the fabrication process and save the fabrication time. However, such changes decrease the heat dissipation property at the bond sites due to a reduce in material's thermal conductivity, as stated before (AuSn: 57 W/mK; silver epoxy: 2-50 W/mK).

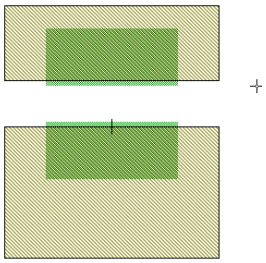

Figure 3.20: Cell of the Au deposition mask

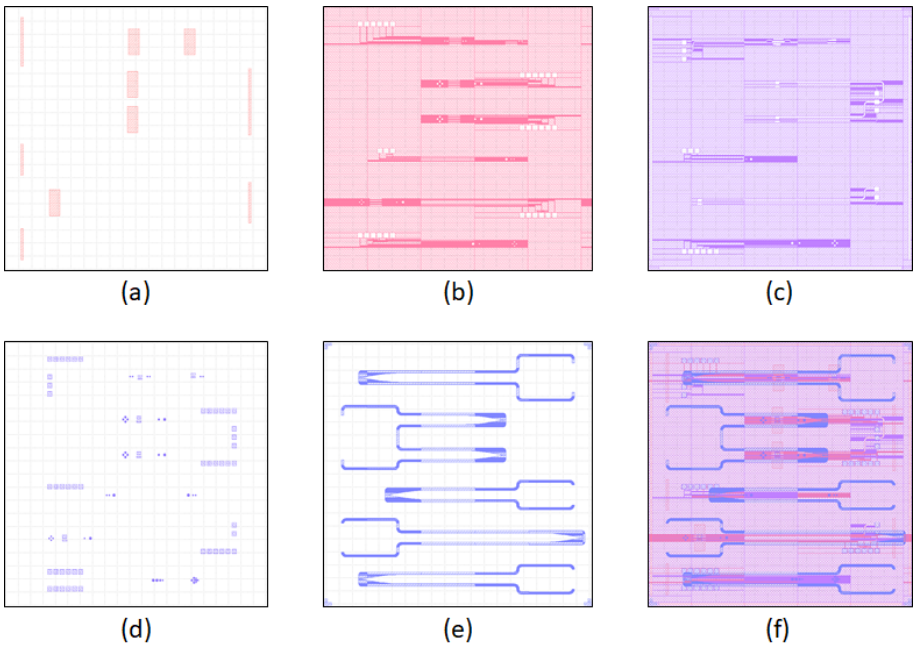

Figure 3.21: Oasis mask file by Photronics. (a) Mask "Cavity"; (b) Mask "Metal-1"; (c) Mask "Metal-2"; (d) Mask "Contact"; (e) Mask "DRIE"; (f) All 5 Masks.

To summarize the mask design layout, we have the following masks for our fabrication:

1. **Cavity**: for creation of cavities and breaking groove structures;
2. **Metal-1**: for patterning the microelectrodes layer;
3. **Metal-2**: for patterning μLED bond pads layer;
4. **Contact**: for opening the contact pads (microelectrode sites, μLED bond pads and wire bond pads);
5. **DRIE**: for creating optrode probe structure through silicon wafer backside DRIE process;
6. **Au (optional)**: for gold deposition on μLED bond pads.

Figure 3.21 shows the oasis mask files provided by Photronics Inc (only one block is presented).

3.5. Chapter Conclusion

Table 3.5: Detailed design specifications for 5 designs on 300 μm thick Si Wafer

	Design 1	Design 2	Design 3	Design 4	Design 5
Number of shafts	1	2	1	1	1
Distance between the shafts (μm)	/	1000	/	/	/
Number of μLEDs on one shaft	2	1	1	/	/
Number of wire bond sites (electrodes + LEDs)	6+3	12+3	6+2	6+0	12+0
Tip angle ($^{\circ}C$)	20	20	20	20	20
Tip length (μm)	1100	900	900	450	1300
Shaft Length (μm)	6000	4000	7000	5000	6000
Shaft width (μm)	350	350	350	350	350
Optrode head (μm^2)	2000×1600	2000×2300	2000×1300	2000×950	2000×950
Cavity for LED (μm^2)	400×1000	400×1000	400×1000	/	/
Breaking groove (μm^2)	100×1100	100×1700	100×1100	100×750	100×750
Working electrode (Φ: μm)	50	75	50	50	50 & 75
Reference electrode (Φ: μm)	/	75	50	50	50 & 75
Ground electrode (Φ: μm)	/	100	100	100	100
Electrodes wire width (μm)	10	10	10	10	10
μLED wire width Cathode & Anode (μm)	20 & 40	30 & 60	20 & 40	/	/
Contact pads (μm)	180×180	180×180	180×180	180×180	180×180
Electrode material	TiN/Ti	TiN/Ti	TiN/Ti	TiN/Ti	TiN/Ti
μLED bond sites material	TiN/Ti	TiN/Ti	TiN/Ti	TiN/Ti	TiN/Ti
Bond method	Silver epoxy	Silver epoxy	Silver epoxy	Silver epoxy	Silver epoxy

In this chapter, the design specifications were discussed in details and the mask layouts were generated. In Table 3.4 and Table 3.5, design specifications were concluded. The design highlights are listed here as a conclusion of this chapter:

1. Carefully designed geometrical specifications allowing for:

(a) Safe implantation with enough mechanical strength and tolerable tissue damage;
(b) Different designs for multiple experimental tasks (acute or long-term implantation, cortex or deeper regions in the brain, comparison between different size electrodes);
(c) Less tissue damage during probe implantation due to smoothing of all sharp angles, as

can be seen from Figure 3.15 to Figure 3.18.

2. Simultaneous function of recording electrodes and optical stimulation through:
(a) Tetrode working electrodes for recording LFP, DC potential, action potentials;
(b) Close proximity of working electrodes and μLED for studying localized neuronal activities;
(c) Appropriate isolation methods for μLED to prevent electrical leakage without covering electrode sites.

3. Special modifications on silicon wafer surface:
(a) μLED-in-cavity structure to reduce unwanted tissue damage and tissue response;
(b) Breaking grooves to reduce the risks of wafer damage when detaching the optrodes;
(c) Cavity structure provides space for applying isolation material on the μLED and reduce the chance to influence electrode areas.

4. Multiple design accessories (in Chapter 6):
(a) Minimized PCBs with gold finish, allowing connection between the optrodes and the signal processing system & supplying power and control over μLEDs;
(b) 3D printed head-stage for fixing the optrode probe on the mouse brain.

4

MEMS Microfabrication Processes

After determining the design specifications and producing the masks layouts, the fabrication process flow needs to be set based on the available fabrication techniques in EKL. In this chapter, the contents are arranged with the following sequence:

Section 4.1: the process flowchart is presented with a brief summary of the main fabrication steps.

Section 4.2: fabrication steps are explained in details, and the microscopic results are provided.

Section 4.3: a troubleshooting table is concluded to deliver a clear view of the problems I met during the fabrication, possible causes to these problems and solutions.

The microfabrication process flow for producing optrode substrates has been tested and verified in this chapter.

4.1. Process Flowchart

The process flow is presented in Figure 4.1 to give an overview of the optrode body's microfabrication process. The main steps include:

- KOH etching silicon wafer (Figure 4.1 (b), (c)): to create cavity structures for the μLED placement and for optrode detachments, as explained in section 3.2.4.
- Deposition of PECVD SiO_2 layers (Figure 4.1 (d), (e), (g)): isolating layers to protect metal lines from in-vivo environment. Three silicon oxide layers are deposited in total to enclose two metal layers.
- Deposition of two TiN/Ti layers (Figure 4.1 (d), (f)): for microelectrodes and for μLED bonding sites respectively. The TiN/Ti are patterned with photolithography and dry etching processes.
- Wet & dry etching of PECVD SiO_2 (Figure 4.1 (g), (i)): to open all contact pads.
- Deep reactive ion etching on the back of the silicon wafer (Figure 4.1 (h), (i)): to create the optrode substrate structure.

The fabrication was processed on wafers with high topography (a large number of KOH-etched cavities), which increased the fabrication difficulty. Therefore, the whole fabrication process was divided into two stages.

The first stage was to fabricate optrode chips on a plain silicon wafer. The purposes of this stage were to:

(1) get familiar with the MEMS fabrication technique in CR100 in EKL;

(2) calibrate the selected recipes (i.e. deposition of metals and SiO_2, opening of contact pads);

(3) prepare the optrode substrate backups in case the proposed design (with KOH-etched cavity structures) did not work well.

The total fabrication time was estimated to be within two weeks and all processes were done automatically.

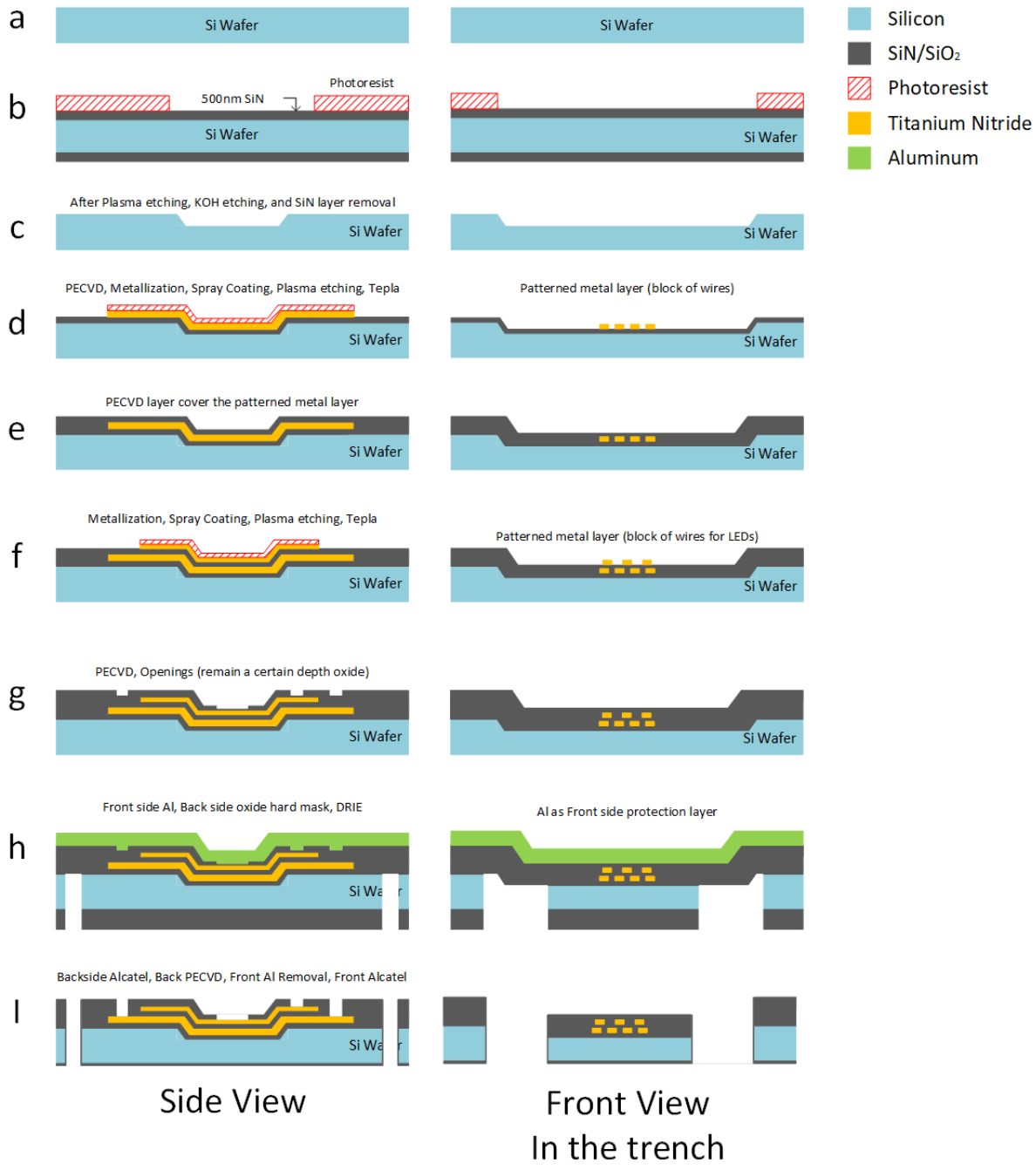

Figure 4.1: Process Flow. (a) Bare Si wafer with alignment marks (thickness: 300 μm); (b) Patterned SiN layer as the hard mask for Si wet etch; (c) KOH/TMAH wet etch of Si and removal of SiN layer afterwards; (d) Deposition of first SiO_2 layer, deposition and patterning of TiN/Ti; (e) Deposition of second SiO_2 layer; (f) Deposition and patterning of TiN/Ti; (g) Deposition of third SiO_2 layer and opening contact pads through wet etching process; (h) Deposition of thick Al layer on front side as the support layer during backside DRIE, Si wafer backside patterning, and backside DRIE process; (i) Removal of SiO_2, Al, and photoresist layers, fully opening of contact pads through dry etching process.

After fabricating all processes on plain wafers, the second stage was carried out to fabricate optrode substrates with KOH-etched cavities. The fabrication flowcharts for wafers without and with KOH-etched cavities are included in Appendix A and Appendix B respectively.

4.2. Fabrication Process and Microscopic Results

Specific fabrication methods (or recipes) were selected based on the design and fabrication criteria. In this section, the selected recipes and their corresponding microscopic results are presented and illustrated.

4.2.1. Zero-layer and alignment marks

The starting procedure was to prepare bare silicon wafers with zero-layers. The zero-layer contains alignment marks that can be used to align all subsequent masks and processing wafers with fixed positions during the photolithography process. An example is shown in Figure 4.2 (aligning the mask “Cavity” and the processing wafer with alignment mark “1N” in the EVG520 Contact Aligner system). In Appendix A and B, the zero-layer process starts from step 1 to step 6, including:

- Coat positive photoresist in EVG120 Coater/Developer;
- Alignment and exposure with Mask “COMURk” in PAS5500/80 waferstepper;
- Development in EVG120 Coater/Developer;
- Inspection of photoresist residues;
- Plasma etching Si in Trikon Ωmega 201 plasma etcher;
- Removal of photoresist and process standard Si wafer cleaning procedures.

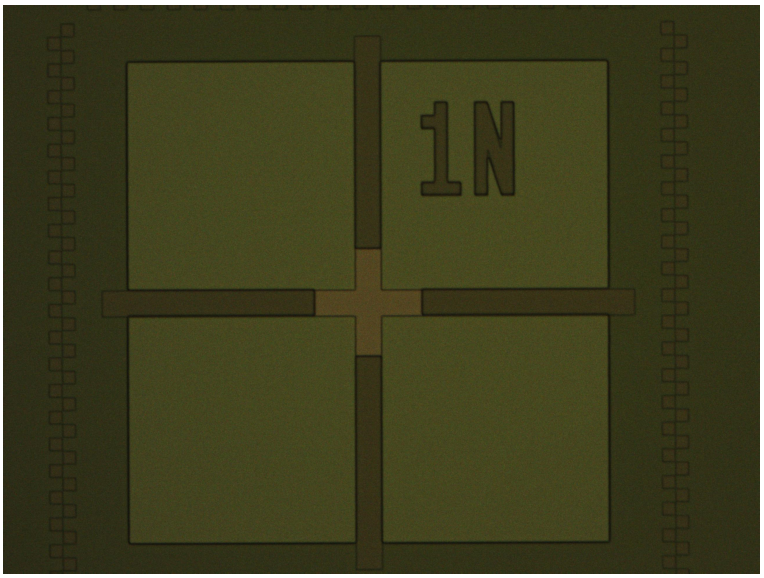

Figure 4.2: Alignment (alignment mark 1N) for exposure process.

4.2.2. Cavity creation by KOH wet etching

For wafers with KOH-etched cavities, the cavities need to be created from the start after the preparation of zero-layers. The corresponding procedure starts from step 7 to step 19 in Appendix B.

KOH and TMAH (TMAOH) are two commonly used etchants to etch silicon (preferentially on the <100> plane) and produce an anisotropic cavity structures with sidewalls of a 54.7 ° angle, as explained in section 3.2.4. To perform the KOH (or TMAH) wet etching process, a

hard mask needs to be firstly deposited on the wafer to define the etching area and protect the remaining silicon areas. Photoresist was not used as a soft mask here because the wet etching process takes a long time (> 1 hour) and the photoresist can be easily dissolved in the etchant.

The whole processes are listed here:

- Deposit 500 nm low-stress LPCVD SiN layer in Furnace E2;
- Measure SiN thickness on the test wafer in Leitz MPV-SP measurement system;
- Spin coat 3.1 μm positive photoresist in EVG120 Coater/Developer;
- Alignment and exposure (~12 s) with Mask "Cavity" in EVG420 Contact Aligner;
- Development in EVG120 Coater/Developer;
- Inspection of photoresist residues;
- Plasma etch SiN in Drytek Triode 384T;
- Removal of photoresist in Tepla and process standard Si cleaning procedures;
- Wet etch 100 μm Si in 33% KOH bath at 85 $^{\circ}C$ in the SAL lab;
- Process Si+ cleaning and standard Si cleaning;
- Wet etch SiN in 85% Phosphoric acid at 157 $^{\circ}C$.

500 nm Silicon nitride (SiN) layers were deposited on both sides of the silicon wafer through a low-pressure chemical vapor deposition (LPCVD) process, which results in a dense SiN layer with high quality and can last long in the KOH (or TMAH) etchant. The thickness of deposited SiN on the test wafer was measured in the Leitz MPV-SP measurement system with a value of $515.660 \pm 2.735\ nm$.

The front side SiN layer was then patterned through photolithography process with the mask "Cavity" and a dry etching process in the Drytek Triode 384T machine. The photoresist was then removed and a wafer cleaning procedure was done afterwards. The backside SiN was used to protect the backside silicon from the etchant.

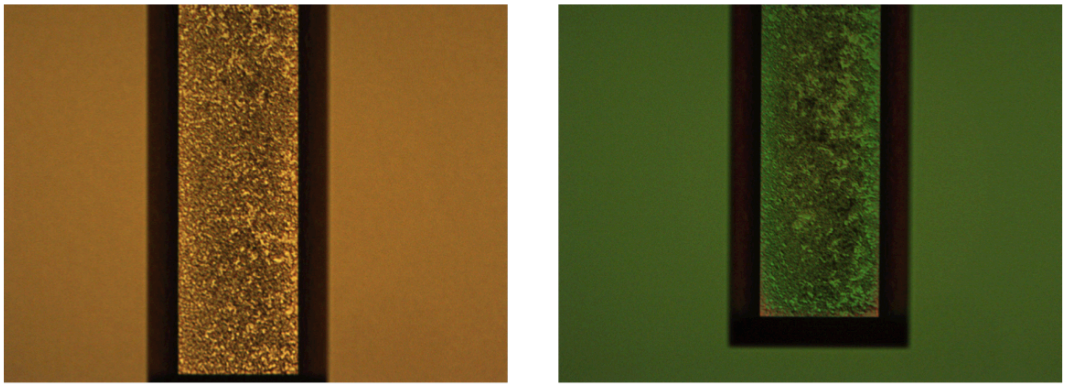

Figure 4.3: Cavities. (a) Before SiO_2 deposition; (b) After SiO_2 deposition

The KOH wet etching process was performed in the SAL lab in a 33 % KOH bath at 85 $^{\circ}C$. Here, a test wafer was etched for 65 min, which resulted in a depth of 86.4 μm. For processing wafers, the etch time was set at 70 min and resulted in a depth of 96.7 - 96.9 μm. The depth results were obtained in the Dektak profilometer after the removal of SiN layers in phosphoric acid bath at 157 $^{\circ}C$ for 4 hours (overetching of SiN to ensure no SiN residues exist on Si wafer surface). The microscopic views of KOH-etched cavities are presented in Figure 4.3, taken by the Axitron microscope in the litho-room.

Problem statement

After dry etching the SiN layer in the Drytek Triode 384T, some SiN residues were found in the wafer's central area, which resulted in incomplete etching of the cavity structures, as depicted in Figure 4.4. The possible reasons could be (a) the increase of helium flow when processing 300 μm wafers and (b) the dry etching profile instability of Drytek Triode 384T system.

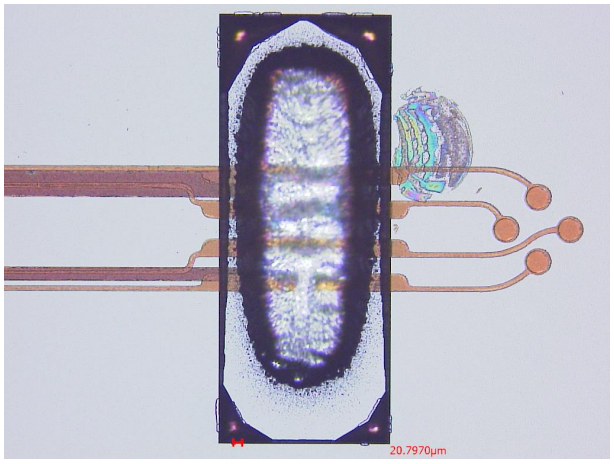

Figure 4.4: Incomplete etch of SiN and Si in the wafer center due to Drytek Triode machine instability

4.2.3. Isolation of metal lines by PECVD SiO_2

Both fabrication stages (Appendix A & B) shared some same processes. The first similarity was to deposit SiO_2 layers on wafer surface to (1) enclose and protect all metal lines from the in-vivo environment and (2) to serve as insulating layers between conductive layers.

Thin SiO_2 films can be grown by thermal oxidation (900-1200 $^\circ C$), or be deposited by LPCVD (600-660 $^\circ C$) or PECVD (200-400 $^\circ C$) method. The high temperature processes (thermal oxidation and LPCVD) can possibly lead to (1) oxidation of the metal surface; (2) diffusion of the metal particles in the furnace chamber; (3) machine inconsistency and cross contamination to other user's wafers. Therefore, the PECVD method was selected to deposit the SiO_2 layer.

The plasma-enhanced chemical vapor deposition (PECVD) SiO_2 deposition process steps referenced in Appendix A and Appendix B are listed in Table 4.1:

Table 4.1: Deposition of PECVD SiO_2 layers

PECVD SiO_2	First layer (1000 nm)	Second layer (1000 nm)	Third layer (2000 nm)
Appendix A	No. 7	No. 18	No. 29
Appendix B	No. 20	No. 31	No. 42

The first SiO_2 layer served as the insulating layer between the first metal layer (TiN/Ti) and the silicon wafer substrate and the layer thickness is 1000 nm.

The second SiO_2 layer separated the first and the second metal layer, which limits the influence of the μLED current flow (< 20 mA) on the recording layer. The SiO_2 thin film has a dielectric constant ranging from 3.9 to 4.5 [43] and a dielectric strength of 10^7 V/cm [44], makes it a good dielectric isolation layer. The second PECVD SiO_2 had a thickness of 1000 nm.

The third PECVD SiO_2 layer protected metal lines from the in-vivo environment. Considering the average dissolution rate of PECVD SiO_2 in vivo is around 3.5 nm/day (reported by

John M. Maloney *et al.* in 2005), the outer SiO_2 layer thickness was determined to be 2000 nm. Such thickness was enough for a long-term animal experiment.

The PECVD SiO_2 deposition process was followed by a thickness measurement to ensure the formation of a uniform layer with desired thickness, which was done in the Leitz MPV-SP measurement system.

4.2.4. Thin film sputtering of TiN/Ti layers

TiN/Ti was selected as the material for metal layers, as explained before. The TiN thin films were deposited by the DC magnetron sputtering method in the Ar and N_2 atmosphere [45]. It was reported that the roughness of TiN thin films RMS (root-mean-square) increased as the substrate temperature increased (200 °C, 300 °C, 500 °C) [45]. For the TRIKON Sigma Sputtering system in CR100, the maximum TiN sputtering temperature of existed recipes was set at 350 °C. The first recipe we used was depositing 200 nm Ti and 50 nm TiN with 350 °C processing temperature in one run. However, later we modified the recipe to be 50 nm Ti and 350 nm TiN with 350 °C in one run. The reason for such modification is explained in subsection 4.2.7.

4.2.5. Photolithography

In this part, the photolithography processes were introduced and explained step by step:
0. Surface treatment;
1. Coating:
1.1 Coating method (spin or spray coating);
1.2 Choice of photoresist (positive or negative; pure or diluted);
1.3 Photoresist recipes;
2. Alignment and exposure;
3. Development (automatic or manual).
The photolithography processes referenced in Appendix A & B are listed in Table 4.2.

Table 4.2: Photolithography processes during the entire fabrication

Mask	COMURK	Cavity	Metal-1	Metal-2	Contact	DRIE
Appendix A.step number	1-4	/	10-14	21-25	31-34	40-42
Appendix B.step number	1-4	9-12	23-26	34-37	44-47	53-55

Step 0: Surface treatment

Before the coating process, HMDS (hexamethyldisilizane) pre-treatment was applied for improving the photoresist adhesion to wafer substrates (to make the wafer surface more hydrophobic). The HMDS treatment was done automatically during the spin coating process in the EVG120 Coater/Developer. And an initial high temperature bake and dehydration process was performed before the vapor of HMDS.

For the spray coating process, the HMDS treatment was done manually in the HMDS manual platform, as shown in Figure 4.5. The wafer should be kept for at least 15 min in the chamber before continuing with spray coating process.

Step 1.1: Spin or spray coating

Photolithography uses light (e.g. UV light) to transfer certain patterns from a mask to a light-sensitive chemical photoresist on the wafer surface. The photoresist is coated on the wafer by either spin coating or spray coating method, as presented in Figure 4.6 [46].

The spin coating process was carried out in the EVG120 Coater/Developer system. The wafer was fixed with a vacuum chuck and was rotated at high speed (i.e. 4000 rpm). The

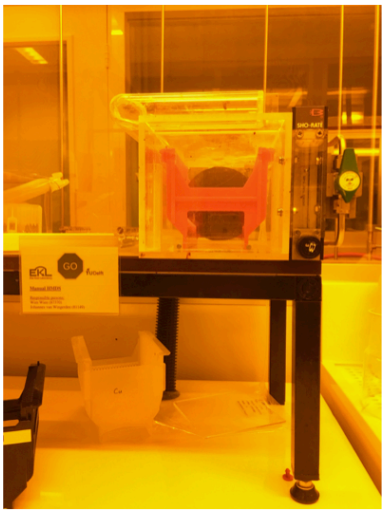

Figure 4.5: Manual HMDS platform.

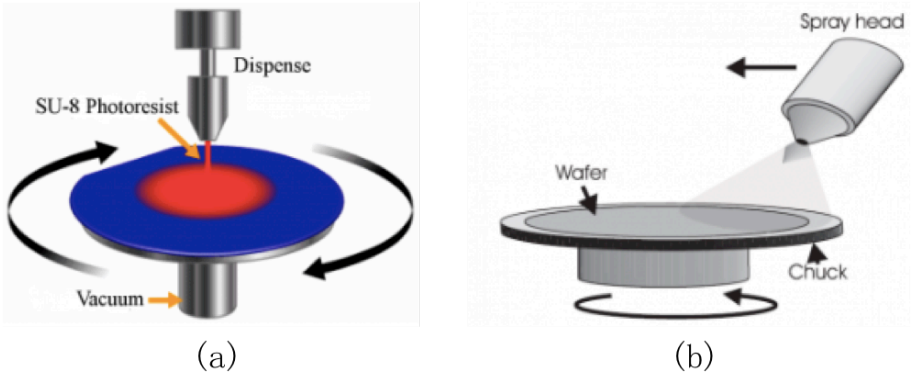

Figure 4.6: Coating methods. (a) Spin coating; (b) Spray coating. [46]

photoresist was dispensed on the center of the wafer and would spread over the entire wafer by the centrifugal forces and the solution's surface tension, resulted in a thin and uniform film left on the wafer surface.

The spray coating process was carried out in the EVG101 Spray Coater system. The wafer was fixed with the vacuum chuck and rotated at low speed (i.e. 80 rpm). The photoresist droplets were sprayed out by a spray nozzle with micrometer-sized dimensions. A swivel arm rotated the spray nozzle across the wafer to form one photoresist layer. Usually, multiple layers are sprayed onto the wafer surface to increase the photoresist uniformity.

The thickness and uniformity of the spray coated photoresist can not be well-controlled when compared to the spin coated photoresist. However, unlike spin coating, spray coating method can be used for non-flat wafers. A diluted photoresist with low viscosity is preferred in this case. The applied diluted negative photoresist in the spray coater contains $35g$ AZ Nlof 2070 photoresist, $70g$ PGMEA and $140g$ MEK.

- For fabrication on wafers **without KOH-etched cavities**, the coating processes were done with the **spin coating method** in EVG120 Coater/Developer.

- For fabrication on wafers **with KOH-etched cavities**, the coating processes were done with the **spray coating method** in EVG101 Spray coater after the creation of cavities.

Step 1.2: Positive or negative photoresist

The applied photoresist can be positive or negative. Figure 4.7 shows the basic performance of positive or negative photoresist after the subsequent exposure and development process. When exposed to UV light, the exposed area of positive photoresist is removed by the developer solution. In contrast, the unexposed area of negative photoresist is removed by the developer solution, which is because the exposed negative photoresist becomes the cross-linked polymer and is more difficult to dissolve in the developer.

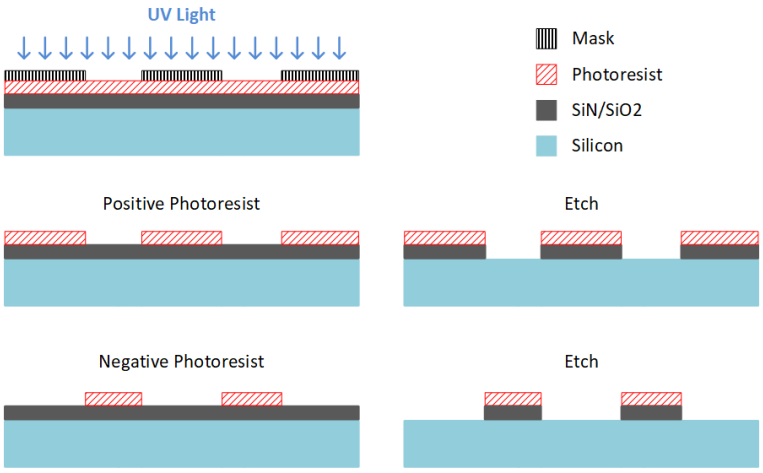

Figure 4.7: Photolithography

The selections of positive or negative photoresist for each mask are specified here:

- “COMURK”: Positive (Default)
- “Cavity”: Positive (Mask with large patterns)
- “Metal-1”: Negative (Mask with small patterns)
- “Metal-2”: Negative (Mask with small patterns)
- “Contact”: Positive (Mask with small patterns)
- “DRIE”: Positive (Mask with large patterns)

When deciding the proper type of photoresist for coating wafers with KOH-etched cavities, close attentions should be paid on small patterns on the mask “Metal-1”, “Metal-2” and “Contact”.

For photolithography processes with masks “Metal-1” and “Metal-2”, photoresist should have a good coverage over “patterning sites” (the electrode sites, contact pads, metal lines and μLED bond pads) after the development process. For photolithography process with the mask“Contact”, photoresist should be removed from “patterning sites” (electrode sites and contact pads). Table 4.3 lists the selection of different photoresist types and the areas need to be exposed.

Table 4.3: Exposed areas on different photoresists

Photoresist	Mask “Metal-1” & “Metal-2”	Mask “Contact”
Positive	Areas exclude patterning sites	Patterning sites
Negative	Patterning sites	Areas exclude patterning sites

In the KOH-etched cavities, the resolutions of small patterns were limited by the reflection of UV lights on cavity's sloped walls. If photoresist areas excluding "patterning sites" were exposed to UV light (Figure 4.8), the small amount of UV light reflections on cavity walls had a chance to expose the small "patterning sites" on cavity bases (red circles in Figure 4.8). This could result in photoresist's coverage problems on "patterning sites", possibly leading to metal line breaks or incomplete μLED bond pads after the subsequent etching processes. While in the other situation, if the "patterning sites" were exposed to UV light, the small amount of light reflections only exposed the unrelated areas and would not influence the small pattern structures. That's why negative photoresist was selected for masks "Metal-1" and "Metal-2" and positive photoresist was selected for mask "Contact" (refer to Table 4.3).

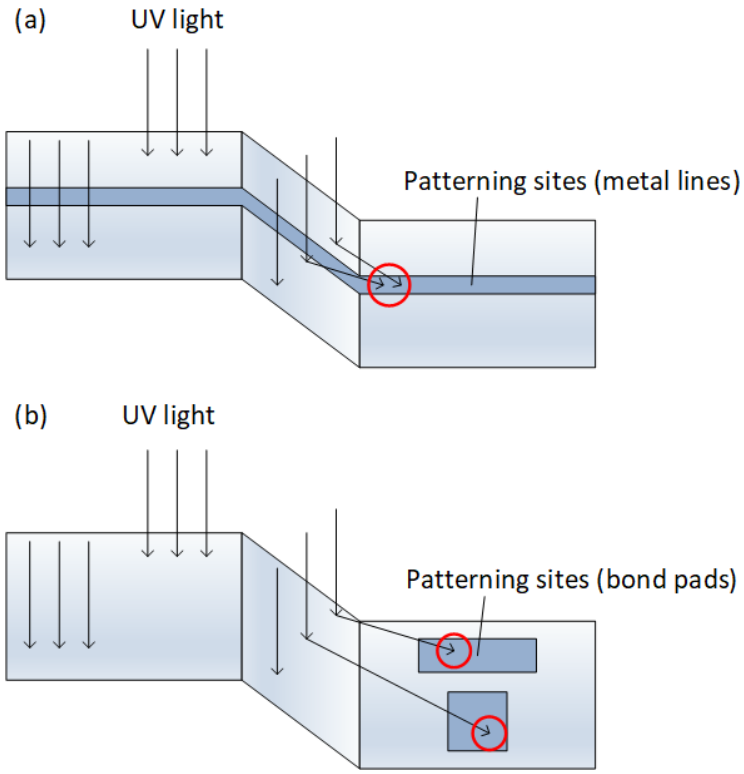

Figure 4.8: Schematics of the UV light reflection. (a) Metal lines being exposed to reflected UV light; (b) Bond pads being exposed to reflected UV light

For other masks, the photolithography processes were carried out on plain wafer surfaces and the aforementioned problems would not occur. Positive photoresist were applied.

Step 1.3: Photoresist recipes

The applied photoresist coating recipes are listed in Table 4.4. "Nlof" represents the negative photoresist.

Step 2: Alignment and exposure

After coating of photoresist and a soft bake process, the alignment and exposure were carried out on wafer substrates to transfer the mask patterns on the coated photoresist. The EVG420 Contact Aligner system (Figure 4.9(b)) was used. The expose time was calculated by the following formulation:

$$Exposuretime[s] = \frac{Exposuredose[mJ/cm^2]}{Intensity[mWatt/cm^2]} \tag{4.1}$$

Table 4.4: Photoresist recipes

Mask	Appendix A	Appendix B
COMURK	Co-3012-zerolayer	Co-3012-zerolayer
Cavity	/	Co-3012-3.1 µm
Metal-1	Nlof-1.5μm-noEBR	(1) Manual HMDS; (2) Diluted AZ Nlof 2070: - HP 1000mbar 2μl 8 layers; - Bake 115 °C for 1 min; - HP 1000mbar 2μl 8 layers; - Bake 115 °C for 5 min.
Metal-2	Nlof-1.5μm-noEBR	(1) Manual HMDS; (2) Diluted AZ Nlof 2070: - HP 1000mbar 2μl 8 layers; - Bake 115 °C for 1 min; - HP 1000mbar 2μl 8 layers; - Bake 115 °C for 5 min.
Contact	Co-3012-2.1μm	(1) Manual HMDS; (2) Diluted Positive PR: - HP 1000mbar 2μl 8 layers; - Bake 115 °C for 1 min; - HP 1000mbar 2μl 8 layers; - Bake 115 °C for 5 min.
DRIE	Co-Syr-9260-12μm-noEBR	AZ 9260 Positive PR: 12μm. Manual Spinner-1 in Polymer Lab

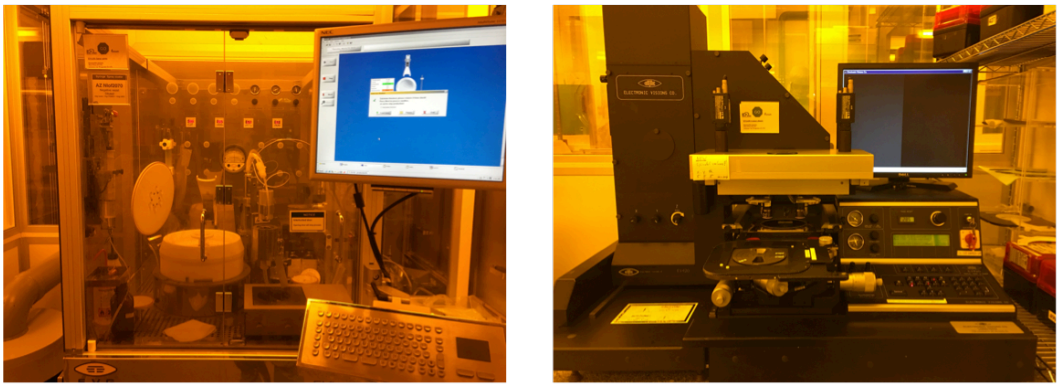

(a) EVG101 Spray Coater (b) EVG420 Contact Aligner

Figure 4.9: Machines in CR100. (a) EVG101 Spray coater; (b) EVG420 Contact aligner

The exposure of UV light changes the photoresist's chemical properties. The exposure dose varies for photoresist of different types (positive or negative), coating methods (spin or spray), photoresist conditions (diluted or not) and thicknesses. And it is also influenced by the substrate material below the photoresist layer. For SiN layer, 110% of specified exposure dose is recommended in the machine manual, which is probably due to the absorption of UV light by the underneath SiN layer. The TiN layer also absorbs some UV light during the exposure process. Hence the total exposure time was increased.

For the alignment and exposure processes on wafers with KOH-etched cavities, the exposure times were increased. For masks "Metal-1", "Metal-2" and "Contact", the recommended exposure dose was 100 mJ/cm^2 and the detected UV light intensity was 14 $mWatt/cm^2$, which

resulted in exposure time of 7 *s*. This exposure time was not sufficient for the later process and was modified to 20 *s* after trials and adjustments (explained in the Problem statement of this subsection).

Step 3: Manual development

After surface per-treatment, photoresist coating, alignment and exposure processes, the development process was performed to remove the exposed positive photoresist or unexposed negative photoresist to clear the photoresist patterns.

1. For processing wafers without KOH-etched cavities, the development of thin photoresist films was done automatically in the EVG120 Coater/Developer with the standard recipe "Dev-SP". The development of thick (12 μm) photoresist (in the case of mask "DRIE") was done manually in the wet bench "Poly-3" in the polymer lab.
2. For processing wafers with KOH-etched cavities, the development of spray coated photoresist films were performed manually in the wet bench "Poly-3" in the polymer lab.

The development process patterned the photoresist layer by dissolving specific photoresist areas in the developer. For manual development processes, diluted AZ400K: H2O = 1 : 2 developer was used for dissolving the positive photoresist and pure MF322 developer was used for dissolving the negative photoresist. The development time needs to be adjusted for different processes.

Problem statement

The photolithography process for patterning negative photoresist on TiN/Ti layers (with masks "Metal-1" and "Metal-2") on wafers with KOH-etched cavities was the most time-consuming step. During the development process, problems happened:

- If the development time was too short, the lines in cavity bases were not fully developed;
- If the development time was too long, the lines in cavity bases were well developed but the lines on the wafer surface vanished.

These problems were possibly due to:

- (1) Low quality of the spray coated photoresist and its bad adhesion with the wafer surface;
- (2) The spray coated photoresist was not uniform;
- (3) Exposure time too short for patterns in the cavity bases;
- (4) Development time was not optimal.

(1) For the first possible cause, different spray coating recipes have been tested. In the initial recipe, 8 layers were sprayed on the wafer in one run and two runs were performed in total, resulting in a total 16 sprayed photoresist layers. A baking process was performed on the hotplate after each run. The trials were to decrease the number of spray coating layers in each run and increase the number of total runs. There were no big differences among photoresist recipes of 8×2 layers, 6×2+4 layers and 4×4 layers after the manual development.

(2) The thickness of spray coated photoresist was not uniform. The average thickness of selected spray coating recipe is around 6 μm, while the thickness at the upper edge of the cavity is around one-third of the average thickness and the thickness at the bottom edge of the cavity is around three times the average thickness. A schematic is presented in Figure 4.10 to illustrate this uniformity problem. The thickness difference of photoresist led to unequal development time. Photoresist residues were observed at the bottom edge of the cavity when the remaining parts were completely developed.

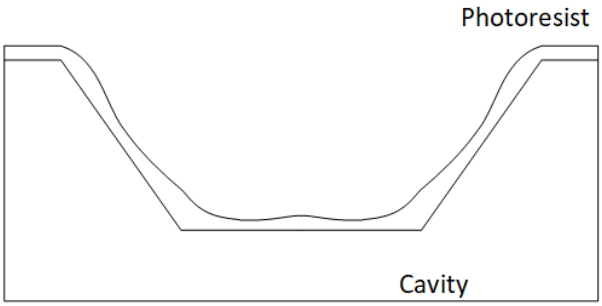

Figure 4.10: Spray coated photoresist uniformity.

(3) As stated before, the initial exposure time was 7 s. Such exposure time was not enough due to (1) an extra gap between the light source and the cavity base; (2) the absorption of UV light by the underneath TiN layer. Different exposure times (10, 15, 20 and 30 seconds) were tested on test wafers to make calibrations (with the same cross-link bake and development time). As we increased the exposure time, an unintentional exposure of the adjacent "dark" areas was observed during development process due to the excessive exposure. As presented in Figure 4.11, the space between two electrodes was exposed when the exposure time was increased to 30 seconds. The optimal exposure time was 20 seconds, resulting in good patterns in the cavity base without much unwanted exposures on the surface area.

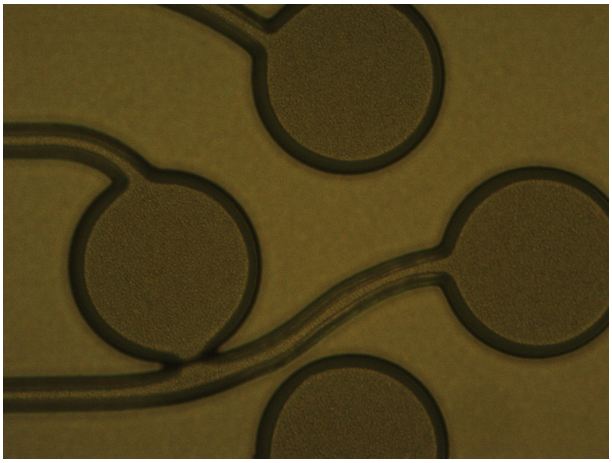

Figure 4.11: Unintentional exposure between two electrodes due to the excessive exposure time.

(4) The development was done manually in pure MF-322 developer and it was advised to inspect the development status in half way and to finely tune the rest development time based on the inspection results.

The spray coating recipes, the exposure time, the cross-link bake time and the development time have been adjusted to reach a well-patterned photoresist layer. The entire processes are listed below:

- Manual HMDS at least 15 min;
- Spray coat diluted negative photoresist in EVG101 Spray coater (recipes in Table 4.4);
- Alignment and exposure (~ 20 s) with Mask "Metal-1/2" in EVG420 Contact Aligner;
- Manual cross-link bake on hot plate 115 $^{\circ}C$ for 2 min 15 s;
- Manual development in Poly-3 wet bench with MF-322 developer for 2-3 min;
- Inspection of line-width and overlay.

4.2.6. Tepla oxygen plasma etcher for photoresist removal

The photoresist was removed in Tepla oxygen plasma etcher after the photolithography process and the subsequent etching process.

In Figure 4.12, a comparison between (a) the TiN surface color directly after metal deposition and (b) the TiN surface color after Tepla negative photoresist removal process is presented. This color change was possibly caused by the acceleration of oxidation process on TiN surface in the oxygen plasma environment during photoresist removal. The gradual oxidation process also happens when TiN/Ti is exposed to the air and the electrode surface area is composed of both titanium oxide and titanium nitride. The influence of this oxidation procedure on the TiN microelectrode impedance level is not well studied.

One possible solution to avoid this accelerated oxidation process in Tepla is to use NMP (1-Methyl-2-pyrrolidon) for removing the negative photoresist.

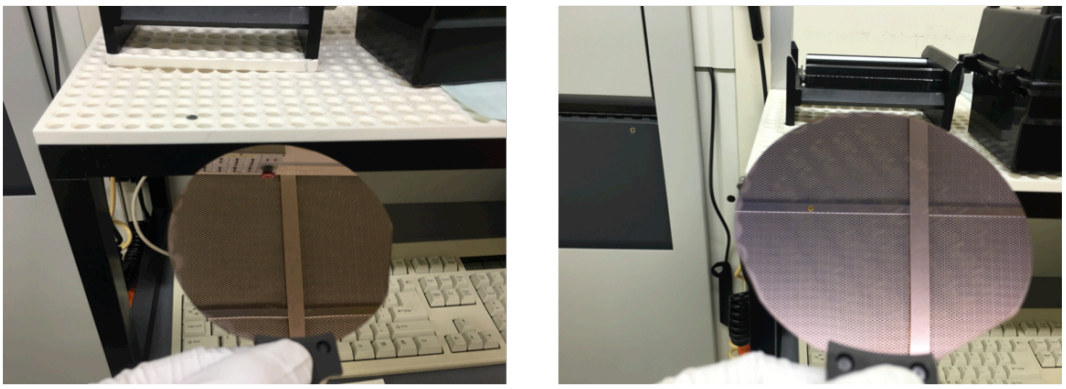

Figure 4.12: TiN surface conditions. (a) surface color after metal deposition; (b) surface color after Tepla oxygen plasma photoresist removal

4.2.7. SEM of TiN/Ti patterns

After the TiN/Ti patterning, the photoresist removal and the wafer cleaning processes, scanning electron microscope (SEM) was used to inspect the TiN/Ti patterns in cavity structures. This was performed to guarantee the metal line's completeness, especially at the top and the bottom edges of KOH-etched cavities. SEM results are presented in Figure 4.13. The lines were intact and the patterns were of good precision.

4.2.8. Contact pads opening

After depositions and patternings of two TiN/Ti layers for microelectrodes and μLED bond pads and depositions of PECVD SiO_2 layers for separating metal layers from the outside environment, a contact pads opening process was carried out to open all microelectrode sites, μLED bond pads and contact pads. The process was done through a wet etching process in the BHF (1:7) solution.

The photolithography process results of contact pads are presented in Figure 4.14. A test wafer was used to test the etch rate of SiO_2 in the BHF (1:7) bath.

Problem statement

As depicted in Figure 4.15, defects existed on the contact pads areas on one processing wafer. This was caused by I mistakenly skipping the wafer moistening step (in "H2O/TRITON X-100" for 1 minute) before wet etching in BHF solution, which led to uneven etching of small structures.

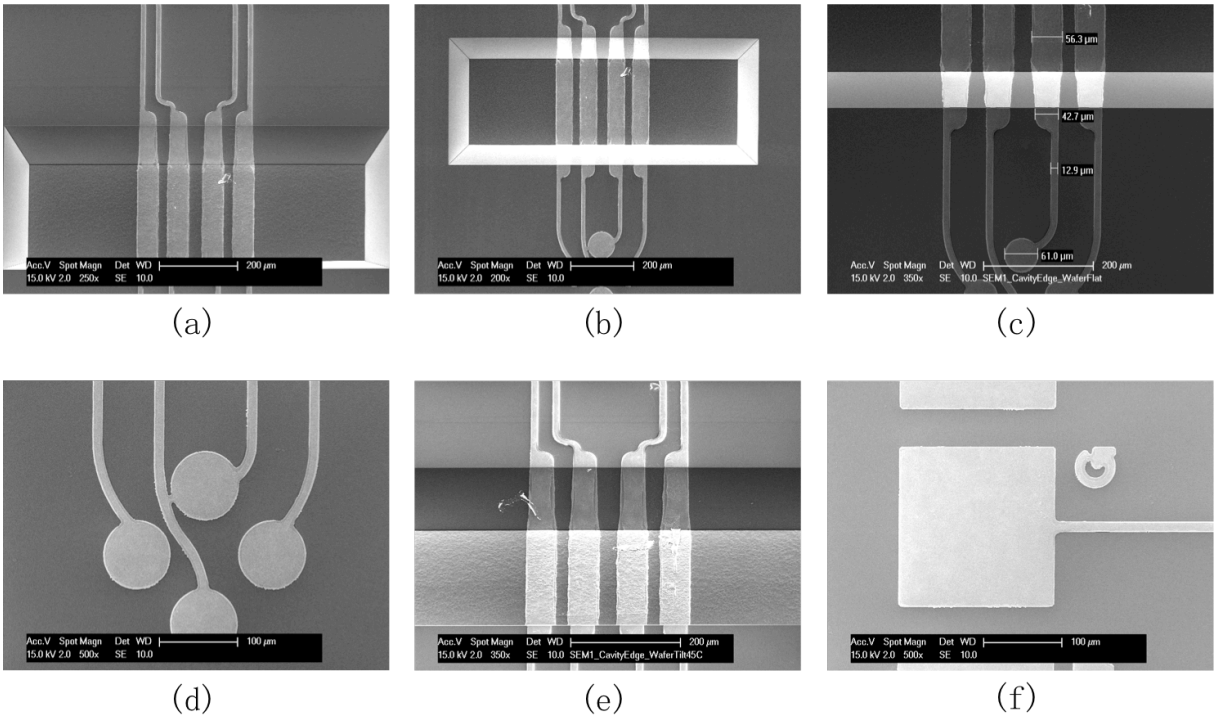

Figure 4.13: SEM

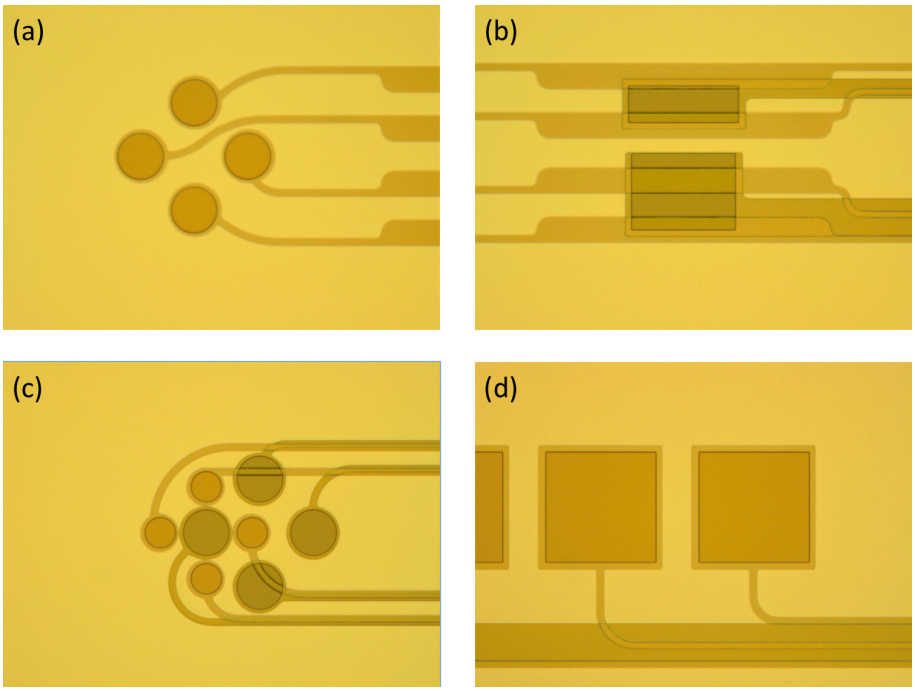

Figure 4.14: Patterning of contact pads after development. (a) Electrodes; (b) μLED bond pads; (c) Electrodes; (d) Wire bond pads.

Another problem is shown in Figure 4.16. The oxide thicknesses above two metal layers were different (around 3 μm SiO_2 on microelectrodes and 2 μm SiO_2 on μLED bond pads). To completely remove the SiO_2 on both metal layers, a total etching time around 15 minutes was required. And TiN was supposed to serve as the etching stop layer to protect the Ti from BHF etchant (Ti can be dissolved in BHF).

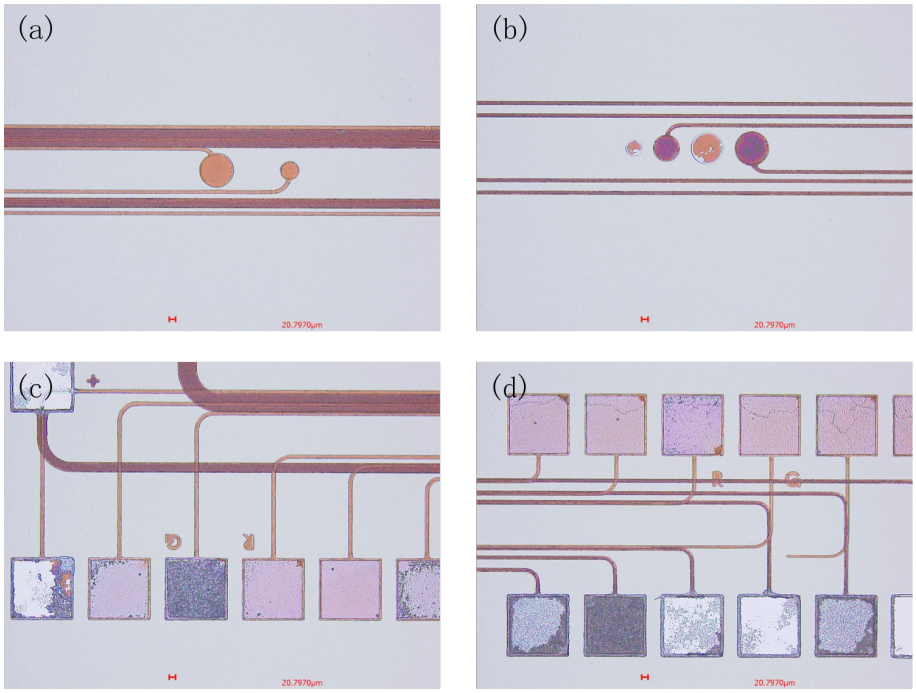

Figure 4.15: BHF wet etching SiO_2 without moistening the test wafer in “H2O/TRITON X-100” bath

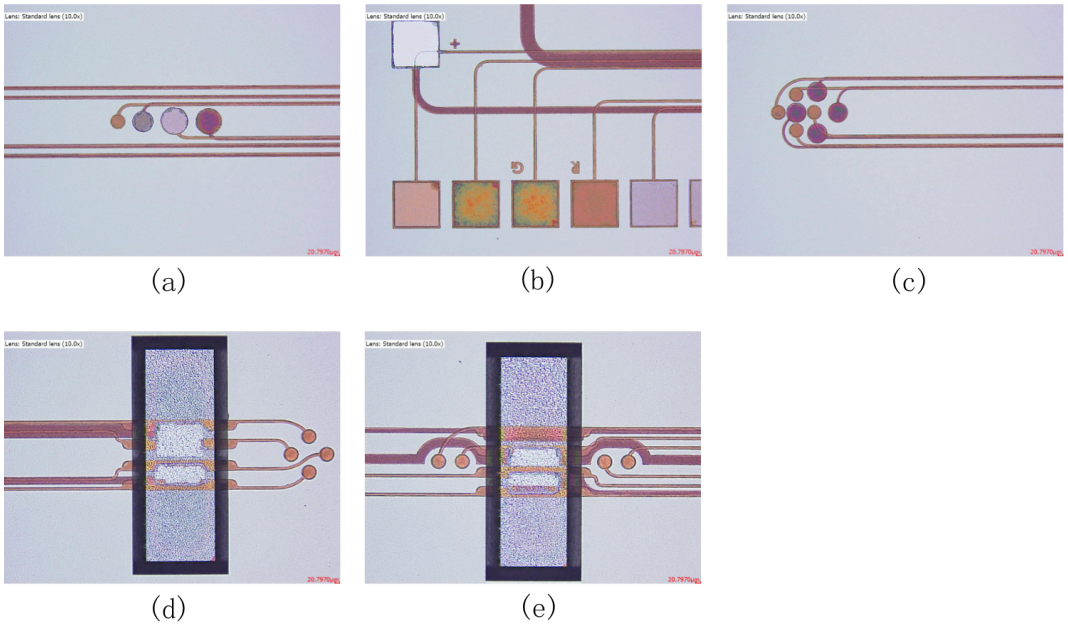

Figure 4.16: Vanish of TiN/Ti in BHF bath during contact pads opening

However, the secondly deposited TiN/Ti layers disappeared after the 15 minutes BHF etching process (white areas in Figure 4.16). The possible reason was because the deposited TiN was too thin (50 μm) and BHF solution dissolved titanium surface through pinholes in the thin TiN layer. Therefore, we modified the metal deposition recipe and increased the thickness of TiN layer to 350 μm.

4.2.9. Deep reactive ion etching (DRIE) from wafer backsides

After opening all contact pads with wet etching in BHF bath, a 500 nm PECVD SiO_2 layer and a 2.4 μm thick Aluminum (Al) layer were deposited on the wafer front side. The SiO_2 layer protected the contact pads from the Al deposition and the Al layer served as mechanical support layer during the backside DRIE process. The photolithography was processed on the backside of the wafer. The photoresist was 12 μm and was thick enough to serve as the soft mask for the entire DRIE process. The DRIE etch rate is influenced by the etch window dimensions and a test wafer was used to test the etch rate. Total etch cycles in DRIE was set to be 400 and was enough to etch through the 300 μm thick silicon wafer.

4.2.10. SiO_2 removal

After the DRIE process for creating the optrode structure, SiO_2 remained in open areas and needs to be removed. As depicted in Figure 4.17, wet etching in BHF solution is fast but leads to undercuts, while dry etching in plasma etcher creates vertical walls and doesn't influence the front side structures but is very slow - the etch rate is dependent on the least dimension of the etch window. Wet etching method was selected and resulted in an undercut around 1-2 μm, which would not influence the front side structures.

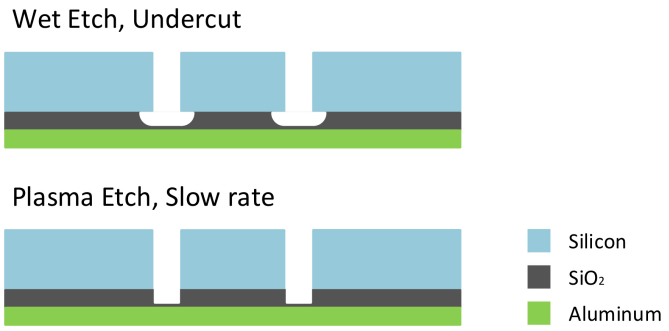

Figure 4.17: Comparison between wet and dry etching for removing the SiO_2 after DRIE process

4.2.11. Al removal after DRIE process

Al layer was etched in the PES bath after wet etching of SiO_2 residues. The PES 77-19-04 bath can hardly etch SiO_2 and TiN layers. However, the TiN/Ti surface was influenced during this wet etching process, as presented in Figure 4.18. Before DRIE step, a SiO_2 layer (initial recipe: 200 nm thickness) and an Al layer (2.4 μm) were deposited onto the front side of the silicon wafer. The SiO_2 layer functioned as the protection layer to separate Al from the contact pads, as stated before. However, this 200 nm PECVD SiO_2 was not able to fully cover the side walls in the contact pads area and the PES solution could possibly leak into exposed TiN/Ti areas. The thickness of deposited SiO_2 was then modified to be 500 nm.

Another solution was to use a carrier wafer as the mechanical support during the DRIE process instead of depositing a layer of Al.

4.2.12. Optrodes under the microscope

Several inspections were done under the microscope after the microfabrication processes of wafers without KOH-etched cavities, as presented from Figure 4.19 to 4.21. The results were good and as expected. The dimensions of metal patterns were in good precision as well.

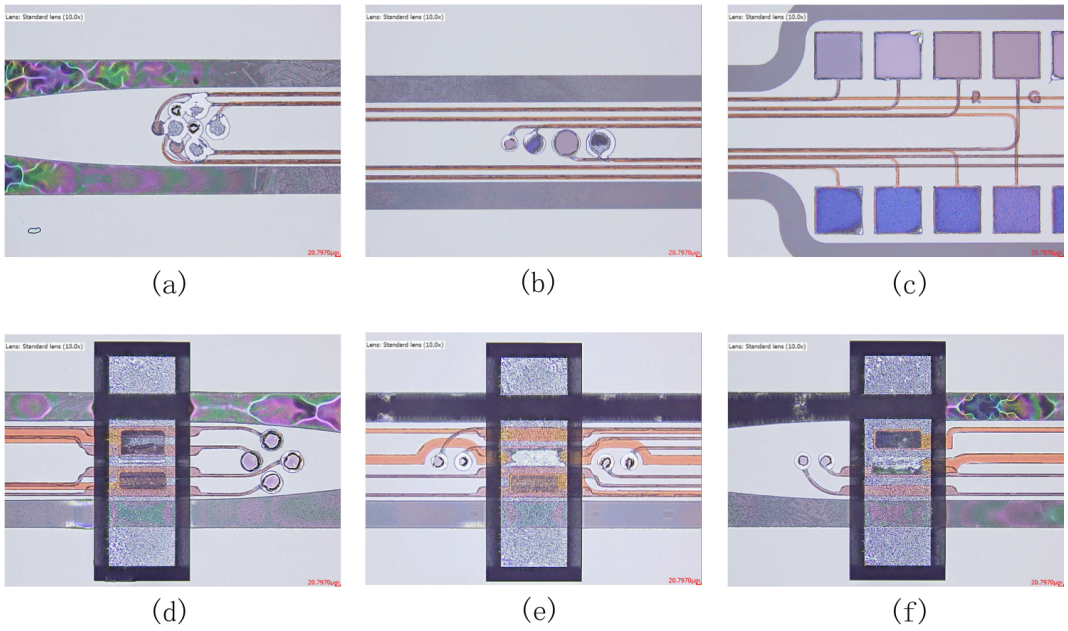

Figure 4.18: Vanish of TiN/Ti in PES bath during Al removal

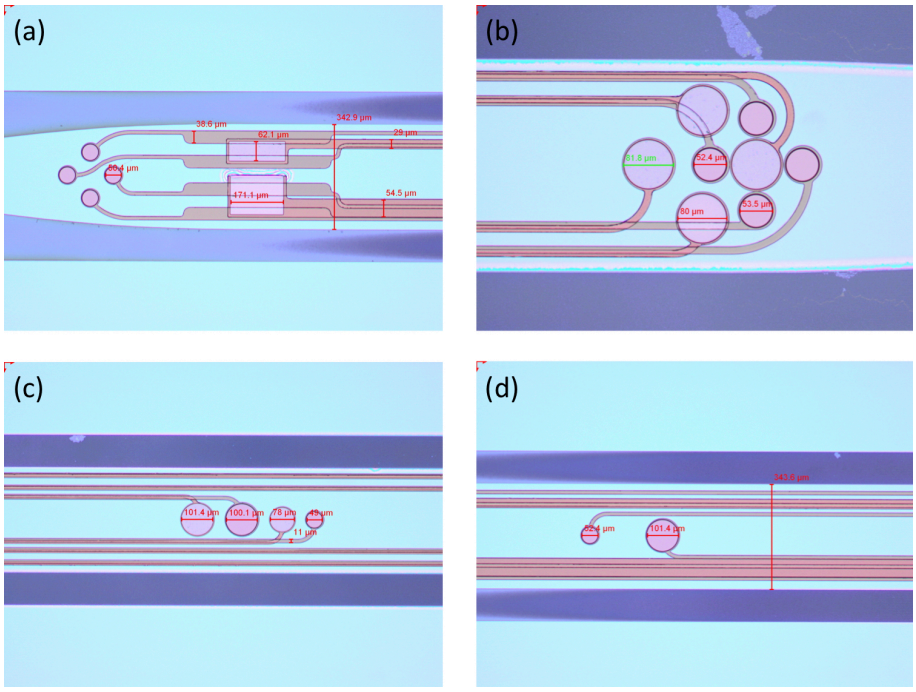

Figure 4.19: Electrodes. (a) 50 μm; (b) 50 & 75 μm; (c) 50 & 75 & 100 μm; (d) 50 & 100 μm

For wafers with KOH-etched cavities, the last processing wafer was broken when performing the cleaning procedure after removing the 12 μm photoresist and no pictures were taken.

4.3. Troubleshooting and Chapter conclusion

In this chapter, the fabrication processes and reasons for selecting specific recipes were explained. Optrode substrates with or without KOH-etched cavities were created. A summary

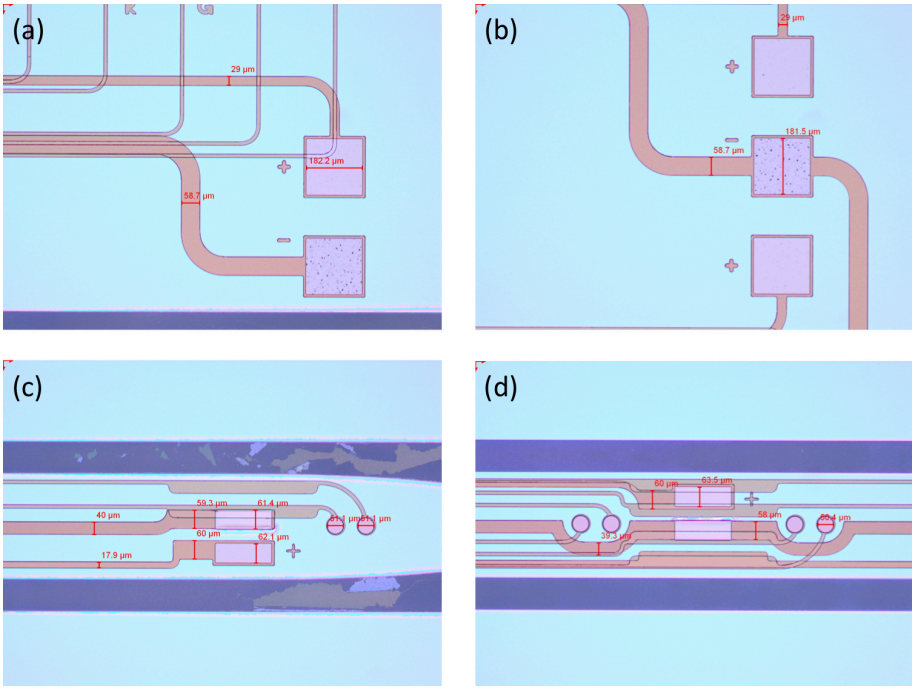

Figure 4.20: Contact Pads. (a) & (b) wire bond pads; (c) & (d) μLED bond pads

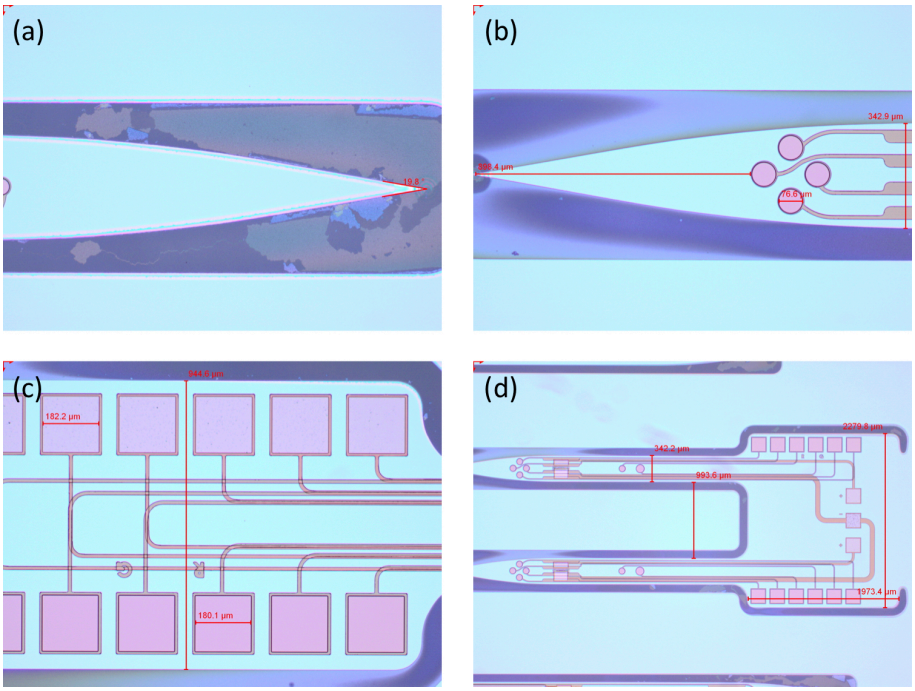

Figure 4.21: Dimensions of the optrode Structure. (a) & (b) tip angle and tip length; (c) optrode head; (d) complete view of the optrode.

of the problems during the fabrication process, possible causes and solutions is presented in Table 4.5.

Table 4.5: Troubleshooting for the Optrode Fabrication Process in Clean Room

Steps	Problems	Possible reasons	Solutions
Drytek dry etching SiN	The etch of SiN in wafer central areas was incomplete.	Helium flow too high for 300μm wafer; unstability of the Drytek machine.	(1) Adjust the Helium flow; (2) Repeat the recipe until the patterns are clear.
Omega dry etching TiN/Ti	The etch of metals was incomplete.	Wrong recipe was used.	Use TiN etching recipes in Omega, and terminate end point detection in the recipe
Photolithography with negative PR	(1) The patterns on the surface disappeared when development time lasted too long; (2) The PR patterns in cavities were not completely developed before the patterns on the surface were lost.	(a) Spray coated photoresist's poor adhesion with the wafer surface due to improper recipes; (b) Exposure time too short; (c) Cross link bake time too short.	Change the spray coating recipe (the number of layers deposited each time and the overall number of layers) Try different exposure times (dividing the test wafer into 4 areas with different exposure time) Increase cross link bake time, but the removal of PR would be more difficult.
Tepla removal of negative PR	Color change of TiN surface	Oxidation of the metal surface	Use NMP (1-Methyl-2-pyrrolidon) for photoresist removal
Alcatel dry etch of SiO2	(Before modifying the flowchart) In the last step of the processes, the secondly deposited TiN/Ti layer is etched away.	The overall thicknesses of SiO2 above two TiN/Ti layers are different; This thickness difference led to an over etch of the second metal layer.	Change the process in the previous steps - open the contact pads completely using wet etching methods.
BHF wet etching SiO2	TiN should act as the stop layer but it was etched away.	TiN was too thin (50μm); BHF solution etched Ti.	Modify the recipe of metal layers deposition: 350nm TiN & 50nmTi
Rapier wafer load	Wafers were not detected in the machine.	300μm wafer was too thin to detect by the optical sensors in the Rapier machine.	Change the slot and reload the wafers; Or use carrier wafers.
Rapier deep reactive ion etching	Si was not etched completely at the edge of the wafer	Wafer underwent several times of recycling during the previous steps	Extra dry etch cycles
Al wet etch	There was 200nm SiO2 layer between the TiN/Ti and Al, but TiN/Ti disappeared after Al removal	200nm PECVD SiO2 had a bad coverage of side walls, the PES solution went to the TiN/Ti through uncovered areas; TiN was too thin; pinholes in PECVD SiO2	Increase the thickness of SiO2 to 500nm; Increase the thickness of TiN to 350; Or avoid the Al deposition step.

5

System Integration

In chapter 5, we described the process steps used to fabricate the optrode substrates using MEMS technology on silicon wafers. The next step followed by the microfabrication process was to make the system integration, which was done by bonding and isolating μLEDs onto the optrode substrate and bonding the optrodes onto the front PCB. These steps were done in the MEMS lab with the "Pick and place" machine and the "Wire bonding" machine, as presented in Figure 5.1. In this chapter, μLEDs were bonded with silver expoxy and isolated with PDMS, and the optrode was wire bonded onto the PCB control panel.

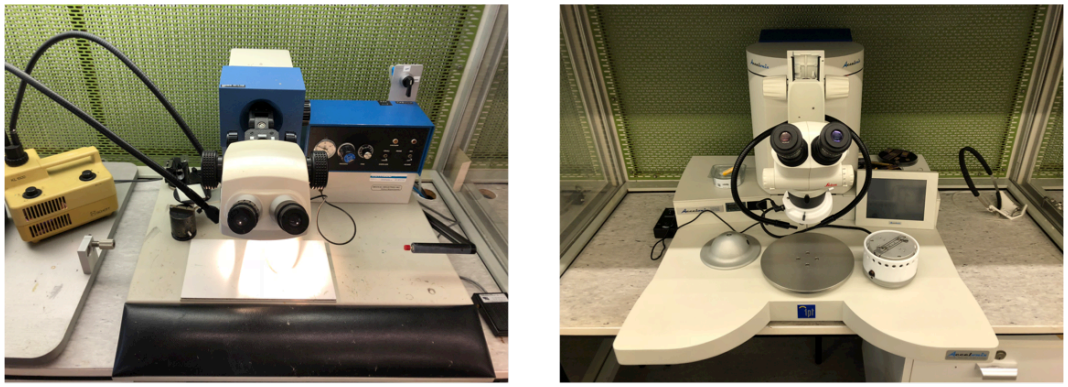

(a) (b)

Figure 5.1: Bonding machines in MEMS Lab. (a) Pick and place machine; (b) Wire bonding machine.

5.1. Die attach μLED with silver epoxy

For the preparation, some optrode substrates (10 samples from plain wafers and 10 samples from wafers with cavities) were detached from processed wafers and were fixed on a plain board by the kapton tape (the optrode itself was too small for the vacuum chuck), as presented in Figure 5.2 (a). There were three issues about the μLED bonding steps due to the equipment limitations:

(1) The silver epoxy was injected out from a nozzle with a diameter around 250 μm. The dimension of injected silver epoxy was much larger than the bonding pads (60×180 μm^2 and 125×170 μm^2).

(2) The upper surface of the μLED is 110×190 μm^2. And the smallest vacuum nozzle for picking up is around 150 μm in diameter, which makes the picking up of μLEDs very difficult to handle.

(3) The cathode and anode on the bottom of μLED need to match with the bond pads on the optrode substrate. Manual handling of such small devices was very difficult and a placement deviation could easily happen.

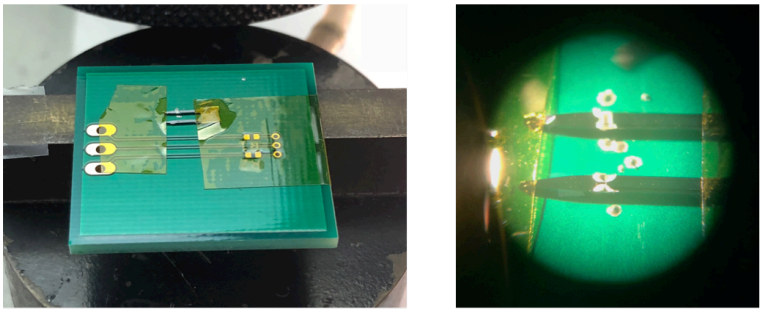

(a) (b)

Figure 5.2: Die attach μLEDs with silver epoxy. (a) Fixation of optrode substrate by kapton tape on plain board; (b) Die attached μLEDs

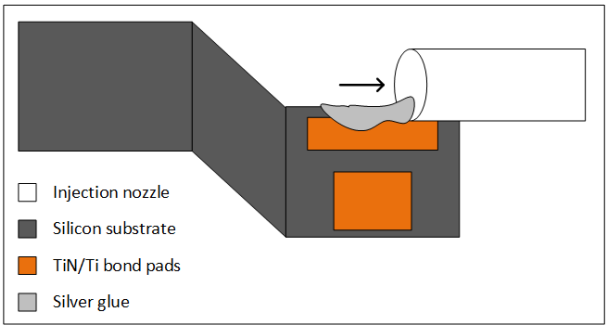

Figure 5.3: Schematics of injecting silver epoxy on μLED bond pads

To solve the first issue, the epoxy injection nozzle was pressed against the edge of the optrode shaft to dip a certain amount of silver epoxy onto pad's edges, as depicted in Figure 5.3. In Figure 5.2 (b), some silver epoxy spots can be seen on the plain board near the probe shafts. Small spots of silver epoxy on outer edges of both pads were enough and two silver epoxy spots should be kept with a certain distance to avoid overlapping when pressing the μLED on top. The second and third issues were inevitable as long as we die attach μLEDs manually and only few samples were made and functioned well (results in chapter 6).

The following steps were taken during the die attaching process:

- Turn on the "Pick and place" machine, take the silver epoxy out from the fridge and keep it in room temperature for a while;
- Attach optrode substrate onto a plain board with kapton tape and attach the board onto the vacuum chuck;
- Dip the silver epoxy onto the bond pads of the optrode substrate;
- Inspect the μLED of its cathode and anode orientation under the microscope;
- Pick the μLED up and place it carefully onto the optrode substrate;
- Cure the silver epoxy in the oven at 90 $^{\circ}C$ for 3-4 hours.

5.2. Bond optrodes with PCBs

After die attaching μLEDs on the optrode substrates, the optrodes were bonded to the front PCB.

5.2.1. Front PCB design and fabrication

The PCB schematics is presented in Figure 5.4. The design of 2-layer PCB was done in the software Eagle and the fabrication was done at PCBWay.com. The board has a gold finish on both sides.

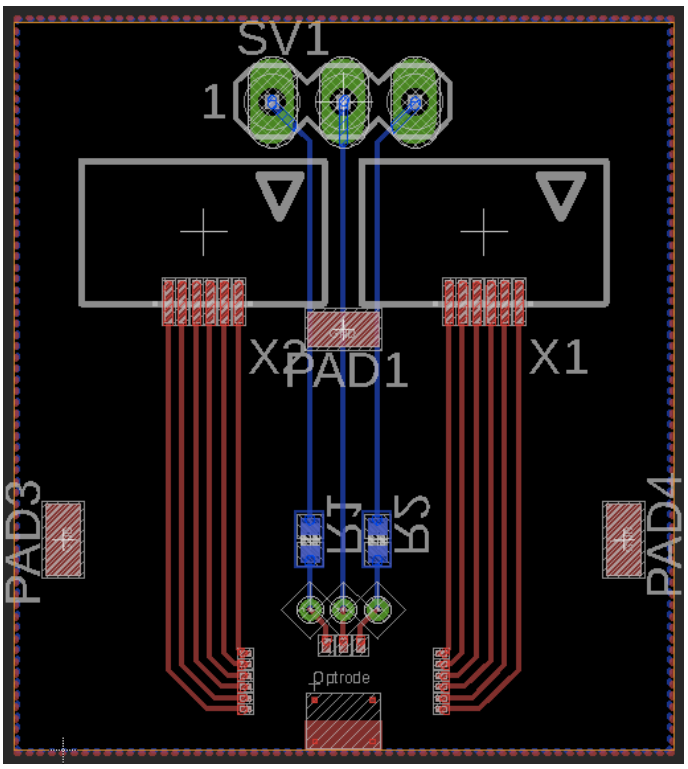

Figure 5.4: PCB schematics

Two FFC (Flexible Flat Cable) connectors were attached to the PCB top layer using both conductive and non-conductive epoxy with the “Pick and place” machine (Figure 5.5). Then the PCB was cured at 110 $^{\circ}C$ for 2 hours. Two load resistors were soldered to the PCB bottom layer afterwards (explained in section 6.1.1). Pin headers soldering was done after the device integration.

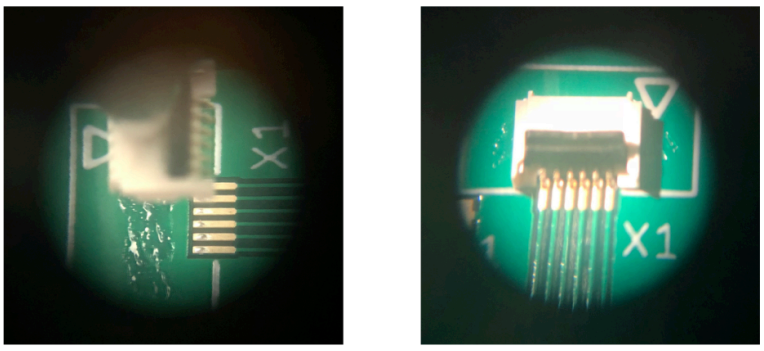

(a) (b)

Figure 5.5: Pick and place FFC connectors with conductive and non-conductive epoxies. (a) Pick of the connector; (b) Placement of the connector

5.2.2. Attach optrodes to the PCB

Non-conductive epoxy was used to attach optrodes to the PCB using the “Pick and place” machine. And the device was cured at 90 $^{\circ}C$ for 3 hours.

5.2.3. Wire-bonding optrodes to the PCBs

The wire bonding process includes the formation of (1) the first bond (on the optrode chip), the wire loop, and the second bond (on the front PCB). The bond pad on the optrode chip was made of TiN and the bond pad on the PCB was made of Gold (Au). The bonding wire we used was made of Aluminum (Al). The applied parameters are shown in Table 5.1. The results are depicted in Figure 5.6.

Table 5.1: Wire bond parameters

Wedge Bonder	Bond 1	Bond 2
US P[mW]	350	400
Time [ms]	400	450
Force [mN]	300	400

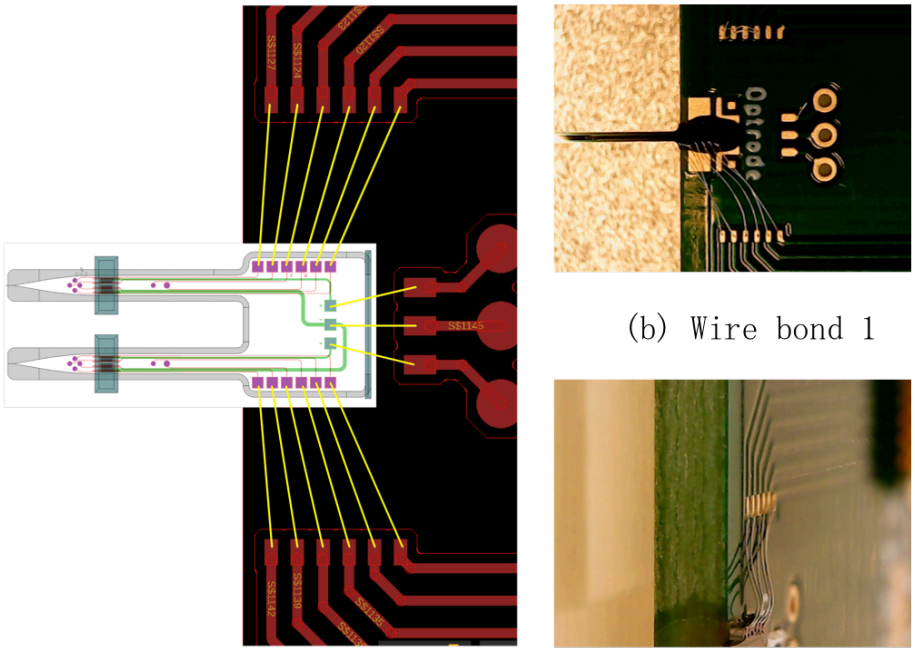

Figure 5.6: Wire bond of optrodes. (a) Guidance for wire bonding between the optrode and the PCB; (b) & (c) examples of wire bonding.

5.3. PDMS Electrical Isolation

In order to minimize body’s reaction towards the optrode, the brain tissue shall be protected against non-biocompatible materials found in both the μLEDs and the wire-bonds. For this purpose, a PDMS (Polydimethylsiloxane) film was manually coated on the μLEDs and the wire-bonds.

PDMS was selected because it's biocompatible, chemically inert and transparent. Its electrical conductivity is $4\times10^{13}\ \Omega m$ (Polymer Data Handbook), which provides the electrical isolation between μLEDs and the brain tissue to avoid the uncontrollable electrical stimulation due to leakage currents coming from the μLED operations.

PDMS was coated onto μLEDs manually. As explained before, one big problem during isolation process is that the isolation material can possibly cover the electrode recording sites, especially during a manual process.

PDMS was prepared in the following procedure in CR100:

- Use a small can to mix Elastomer and Curing agent with weight proportion of 10:1 (first pour elastomer and then curing agent);
- Put the small can in the mixer in polymer-lab, weighing the small can with the proper container in the mixer and adjust the weight scale. Set program 1 and start mixing;
- Cure the small can in the oven at 90 $^{\circ}C$ for 1 hour.

The first trial of the isolation process was to use the kapton tape to protect the electrode recording sites and then dispense PDMS on the μLEDs. The coverage of PDMS was not in good quality due to the viscosity of PDMS on the kapton tape. The electrode sites were not influenced, yet the isolation quality of μLED was not good.

Another unimplemented thought was to cover the electrode sites with photoresist and then dispense PDMS on the μLED sites. Then, the photoresist is removed with acetone after the PDMS curing at 90 $^{\circ}C$. However, the PDMS can also flow on the photoresist the same as on the kapton tape, and PDMS residues could still remain above the electrode recording sites after photoresist removal.

As long as the isolation process is done manually, the quality of isolation layers (such as roughness, thickness, coverage of μLEDs) is not in consistency and can not be well-controlled. The isolation process needs to be improved and some feasible advice is provided in chapter 8.

5.4. Conclusion

In this chapter, samples were made through the integration of μLEDs, optrode substrates and PCBs. Silver epoxy die attach, non-conductive epoxy attachment, wire bonding with Al wires, and PDMS isolation processes were performed.

6

Experiments and Results

In this chapter, the electrical performance of the micromachined optrodes is reported. The set of experiments that were initially intended to be performed are listed in Table 6.1.

Table 6.1: Experiment plans

Test	Description
1. μLEDs	(a) PWM control;
	(b) μLED in-vitro isolation;
	(c) Radiant flux of PDMS-coated μLED;
	(d) Temperature sensing of the μLED site with different duty cycle and pulse frequency.
2. Microelectrodes	(a) Electrochemical impedance spectroscopy;
	(b) Noise analysis on the recorded signals.
	(c) Crosstalk between the μLED driving current and the neural signal recording.

However, due to time constraints, only three experiments were carried out: 1(a) PWM control tests on μLEDs, 1(b) μLEDs isolation test, and 2(a) Microelectrodes impedance test. The remaining tests can be performed after the μLEDs are bonded and isolated with precision.

6.1. Tests of the μLEDs

6.1.1. Experimental Setups

In chapter 3, the pulse-width modulation (PWM) method was selected to control the μLED. To save the time for building a custom control board, the Arduino Mega 2560 board was used to deliver the PWM signals. The Mega 2560 has an on-board microcontroller and has 12 pins supporting PWM outputs (pin 2 to pin 13). Both the duty cycle and the PWM frequency need to be concerned to ensure an effective optical stimulation by the μLED during optogenetics experiments. The duty cycle regulates the output radiant flux from the μLED. During the optical stimulation, neurons or opsins shall not sense the flickering of μLEDs, and PWM frequency above 10 kHz is beyond their response rates, as stated before.

Maximum forward current

The output voltage V_{cc} by Arduino Mega 2560 board is +5 V, while the maximum forward voltage of Cree DA2432 μLED is 3.4 V. Two methods could be applied to protect the μLED from this exceeded voltage V_{cc}. The first method is to set the PWM duty cycle to be lower than 68 % (3.4 V / 5 V), so that the actual maximum voltage drop across the μLED is limited to 3.4 V. The second method is to add a load resistor. Considering the DA2432 model has a typical

forward current of 20 mA at 3.1 V, a 85 Ω SMD resistor was connected to the μLED to limit the maximum voltage drop across the μLED to be 3.1 V. The forward current then reaches a maximum value of 20 mA with the 100% duty cycle of PWM signals, which generates radiant flux of around 30 mW, according to the Cree DA2432 datasheet.

PWM frequency

The PWM signal is generated by built-in timers (5 Timers for the PWM control) on the Arduino board. All 12 pins have a default PWM frequency (pin 2, 3, 5-12: 490 Hz; pin 4, 13: 980 Hz).

The timer clock frequency is calculated through: System clock frequency / Prescaler / PWM mode (number of states).

- The system clock frequency is 16 MHz (crystal oscillator).
- The initial and default prescaler factor is 64, set by the system, and can be changed to 1, 8, 64, 256 or 1024 during custom control. For timer 1-4, the prescaler factors 1, 8, 64, 256 and 1024 result in PWM frequency of 31.3 kHz, 3.9 kHz, 490 Hz (default), 122 Hz and 31 Hz, respectively.
- The PWM has two different modes: fast and phase correct PWM modes. The timer for fast PWM mode counts from 0 to 255 (256 different states), whereas the timer in phase-correct mode counts from 0 to 255 and then back down to 0 (510 different states).

Timer 1-4, for example, have a frequency of 490.20 Hz (16 MHz/64/510) and Timer 0 has a frequency of 976.56 Hz (16 MHz/64/256). The code for controlling Arduino Mega 2560 board to provide optimal PWM frequency, duty cycle and pulse frequency is provided in Appendix C.

6.1.2. Control test

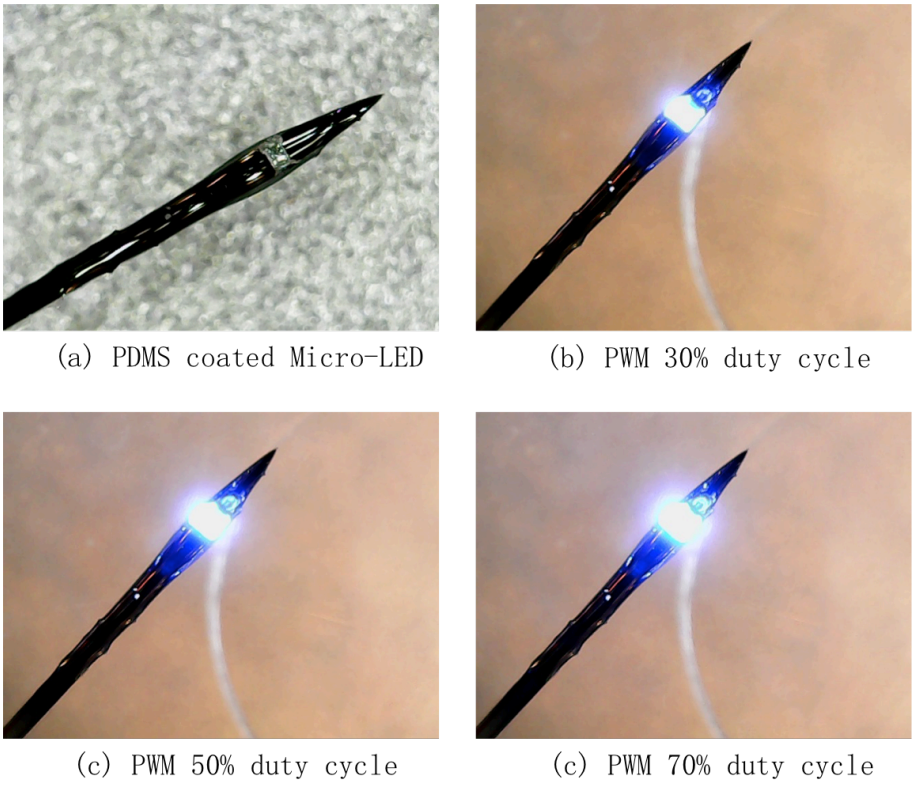

(a) PDMS coated Micro-LED (b) PWM 30% duty cycle

(c) PWM 50% duty cycle (c) PWM 70% duty cycle

Figure 6.1: PWM control over μLEDs.

After programming the Arduino board with Arduino IDE software, μLEDs were connected.

Different duty circles (10%, 30%, 50%, 70% and 90%) were tested and the results are presented in Figure 6.1. Although no instrumentation system (i.e. optical power meter) was used to detect the light power intensity produced by the μLED, one can notice from the picture that the light intensity increases as the duty cycle increases.

6.1.3. Isolation test

A PDMS film was manually coated on the optrode for the isolation experiment. The test was done by inserting the optrode into a PBS solution, as shown in Figure 6.2. The μLED functioned well and there were no bubbles formed at the interface between the μLED and the PBS solution. Although no specific instrumentation was added to the isolation test, this was an indication that there was no significant current leakage coming from the PDMS-coated μLED.

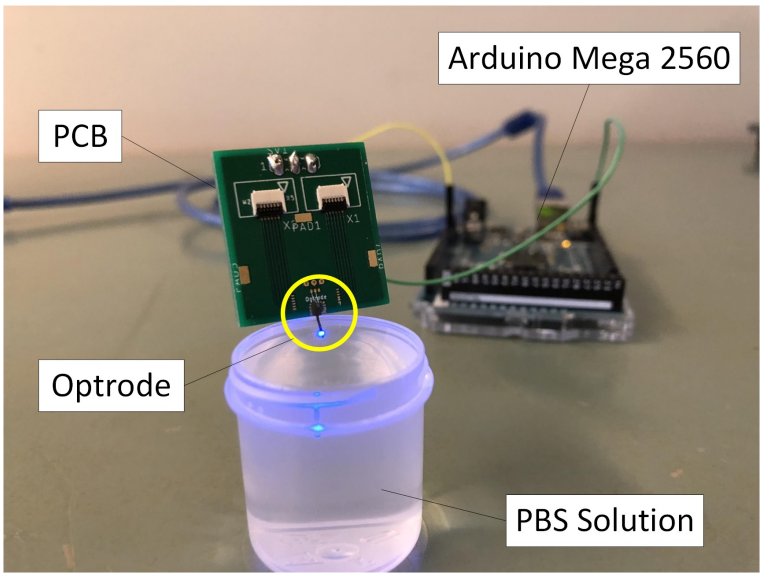

Figure 6.2: In vitro isolation test of the optrode.

6.2. Tests of the Microelectrodes

For testing the microelectrodes, an EIS (electrochemical impedance spectroscopy) measurement was carried out using PBS (phosphate buffered saline) solution. To run this measurement, the Metrohm Autolab system was used.

6.2.1. 3D printed accessories

Some 3D printed accessories were created to assist the experiments, as depicted in Figure 6.3. The 3D designs were created with SolidWorks and the fabrication was done by Shapeways. The material used was fine detail plastic.

The PCB base was not flat because of soldered components on both sides. The assembly in Figure 6.3 (a) was designed with a flat base to facilitate the system integration process in chapter 5.

For the microelectrodes in-vitro test, the optrode shaft should be immersed into the PBS solution. The assembly in Figure 6.3 (b) was designed to fix the PCB on the PBS container.

The assembly in Figure 6.3 (c) & (d) was intended to be the head-stage during the animal experiments.

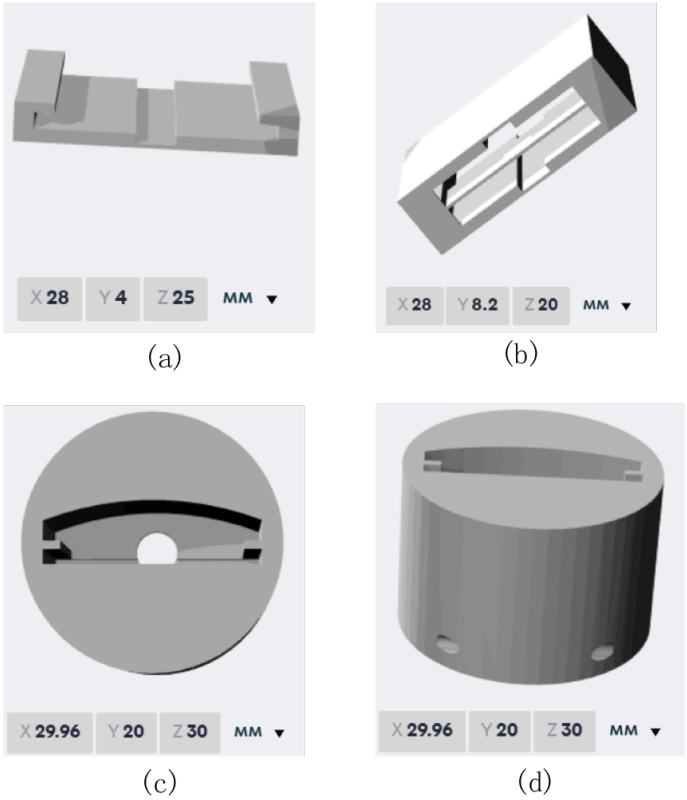

Figure 6.3: 3D printed accessories by Solidworks. (a) 3D part for PCB fixation during system integration; (b) 3D part for fixation of the optrodes during EIS measurement; (c) & (d) Head-stage to be placed on the animal head.

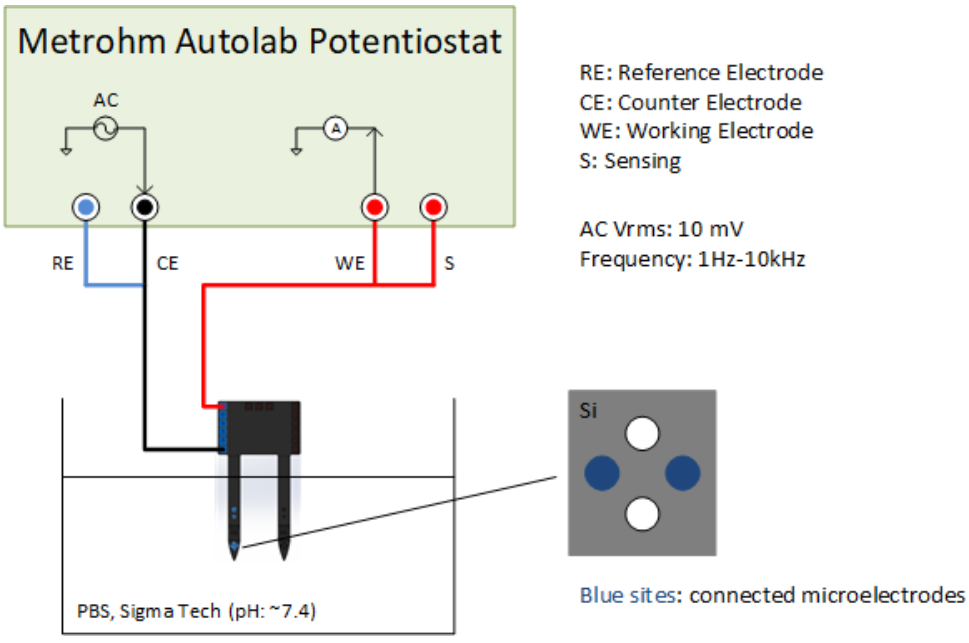

Figure 6.4: Schematics of EIS experimental setup with Metrohm Autolab

6.2.2. Autolab setup for EIS measurement

Figure 6.4 shows the experimental setup in the Autolab system. A two-cell configuration was set by connecting the RE probe with the CE probe (Black and blue probe in Figure 6.5)

and connecting the working electrode (WE) probe with the sensing probe (S) (Red probes in Figure 6.5). By applying an AC signal from the counter electrode to the working electrode (both in the PBS solution), one could measure the current flow from the sensing probe and get the impedance results. Since the counter electrode has a very low impedance level when compared to the working electrode, the counter electrode impedance can be neglected during the EIS measurement. However, the platinum counter electrode (CE) and the Ag/AgCl reference electrode (RE) were not available in the lab. Therefore, two same microelectrodes were connected to the RE/CE pair and the WE/S pair respectively. The measured impedance value between RE and S was composed of (a) two same impedance value at the electrode-electrolyte interfaces and (b) the solution's resistance. The phase angle was determined by two capacitor charging processes at the electrode-electrolyte interfaces. The simplified equivalent circuit model is presented in Figure 6.6, where $R_{electrode}$ is the resistance of TiN/Ti, R_{ct} is the charge transfer resistance, C_{dl} is the double layer capacitance and $R_{solution}$ is the resistance of the PBS solution.

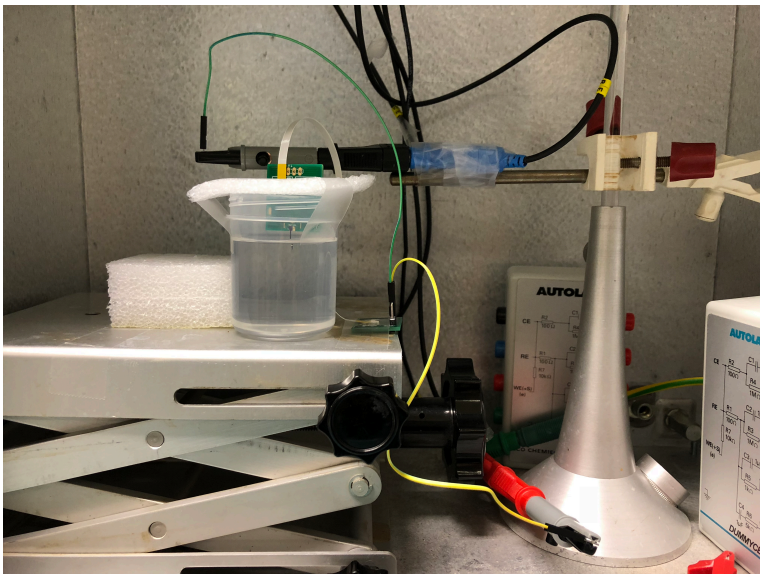

Figure 6.5: Experiment setup in Autolab.

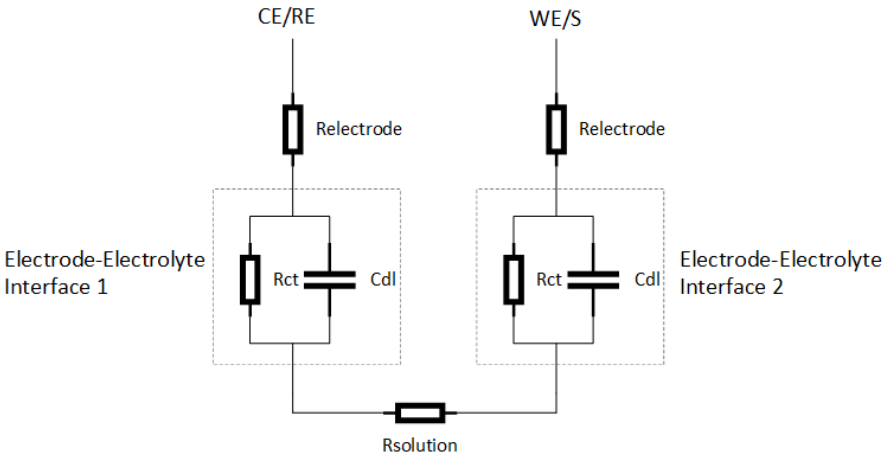

Figure 6.6: Equivalent circuit model of the Electrode-electrolyte interface during EIS measurement.

6.2.3. In-vitro Impedance measurement

For comparison of the electrode impedance from different works, the impedance value at the frequency of 1 kHz is commonly used. It was reported that the impedance of a flat and round TiN microelectrode at 1 kHz with diameter larger than 30 μm is below 100 $k\Omega$ and is approximately 250 to 400 $k\Omega$ for smaller diameters, as stated in Chapter 3 [39]. Though the actual impedance value is dependent on the fabrication process, these reported values give an indication of the impedance range for TiN microelectrodes.

The experiment setup in Autolab is given in Figure 6.5. The setup was kept in a faraday cage to get rid of the Electromagnetic interference (EMI). The PBS was prepared by a research technician in the Faculty of Applied Sciences in TU Delft. The applied AC frequency ranged from 1 Hz to 10 kHz and the applied voltage was 10 mV.

The impedance tests were done on three samples. Sample's descriptions are presented in Table 6.2 and impedance results of two microelectrodes at 1 kHz are presented in Table 6.3. Figure 6.7 shows the numbering of the tested microelectrodes. Bode-Impedance and Phase-angle plots and Nyquist plots of Sample 1 and Sample 2 are presented in Figure 6.8 and Figure 6.9.

Table 6.2: Descriptions of three tested samples.

	Design description	Tested microelectrodes dimensions (μm)	Material
Sample 1	Chronic implant in cerebral cortex	75	TiN/Ti
Sample 2	Acute implant in hippocampus or thalamux	50	TiN/Ti
Sample 3	Comparison of different size microelectrodes	75	TiN/Ti

Table 6.3: Impedance results of electrodes pairs at 1 kHz (in $k\Omega$)

	1st pair	2nd pair	3rd pair
Sample 1 (75 μm)	62.2	123.5	76.1
Sample 2 (50 μm)	1199.2	1298.9	1421.0
Sample 3 (75 μm)	849.8	/	/

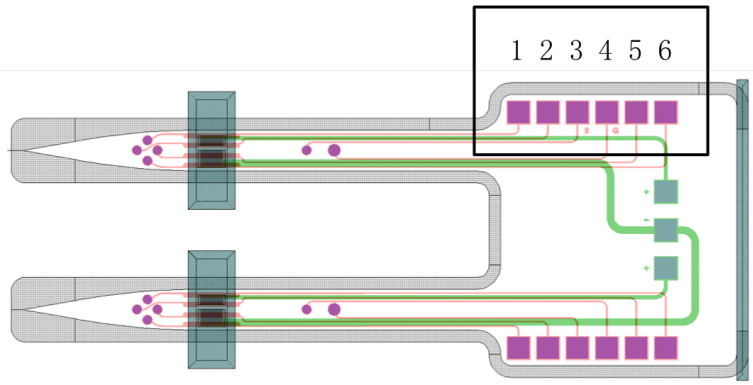

Figure 6.7: Numbering of tested microelectrodes pairs

6.2.4. Results analysis

Impedance

The experiment setup measured two microelectrodes with the same size and material. The tested impedance level from Sample 1 was several tens of kilo-ohms, where as the impedance

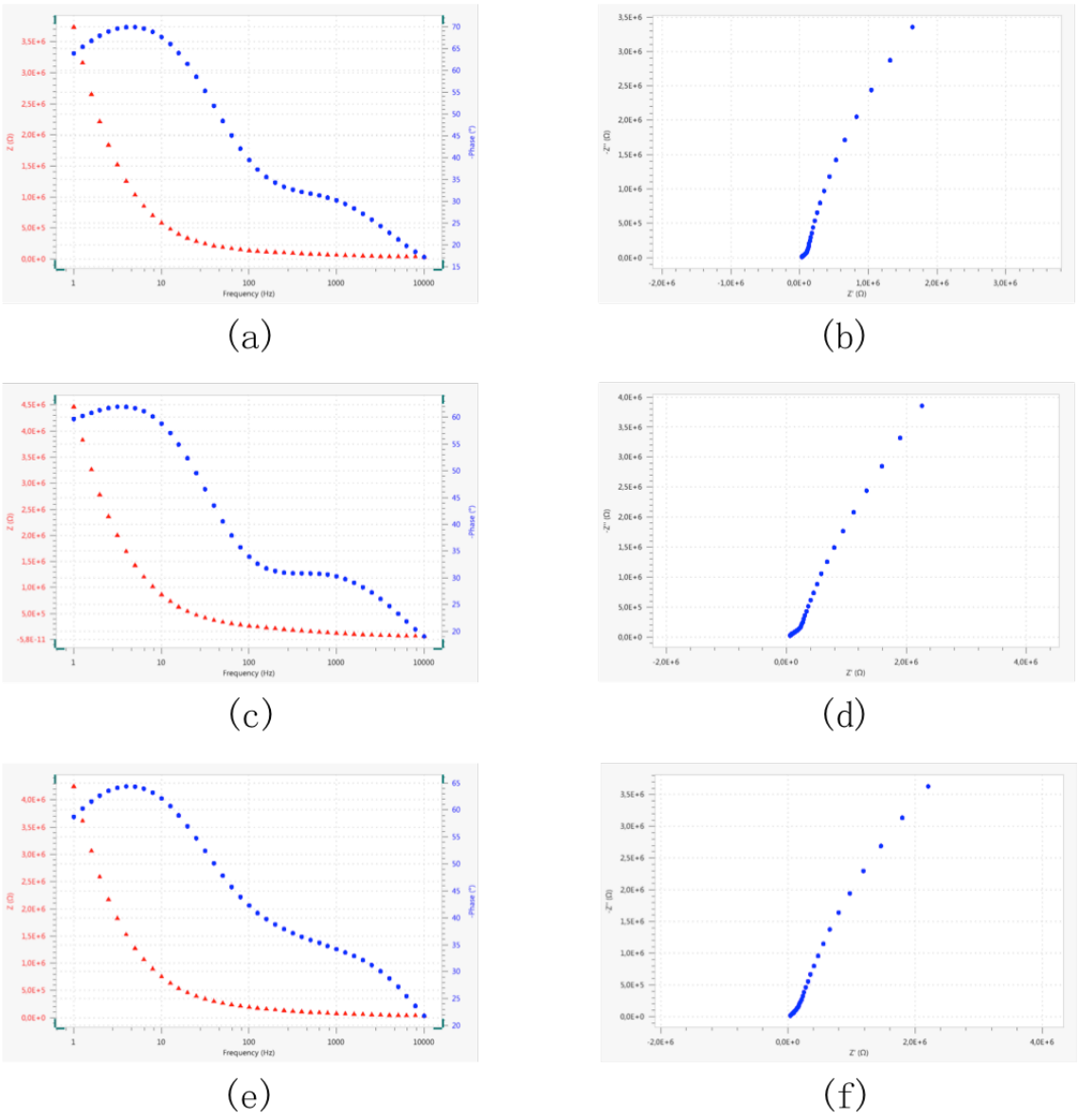

Figure 6.8: Bode-Impedance and Phase-angle plots vs. Frequency (Hz) and Nyquist plots (**Sample 1**). (a) & (b): Electrodes 2 and 3; (c) & (d): Electrodes 2 and 5; (a) & (b): Electrodes 5 and 6.

level from Sample 2 and 3 was several hundreds of kilo-ohms. The huge impedance differences between electrodes with the same size (Sample 1 and Sample 3: 75 μm) and between electrodes with different but close sizes (Sample 1: 75 μm and Sample 2: 50 μm) were not expected.

Phase angle

In the simplified equivalent circuit model in Figure 6.6, the two double layer capacitors C_{dl} are supposed to dominate the impedance level at low frequencies and the resistors dominate the impedance level at high frequencies. At low frequency regions, Warburg impedance with a phase shift of 45 ° needs to be taken into consideration.

Hence, the phase angle at high frequencies were expected to approach 0 °. For Sample 1 (75 μm microelectrodes), the measured phase angle values at 10^4 Hz were in the range of -17 to -21 °, which complied with the trend. And the phase angle values of Sample 1 at low frequencies were in the range of -58 to -63 °. The phase angle reached a maximum value of

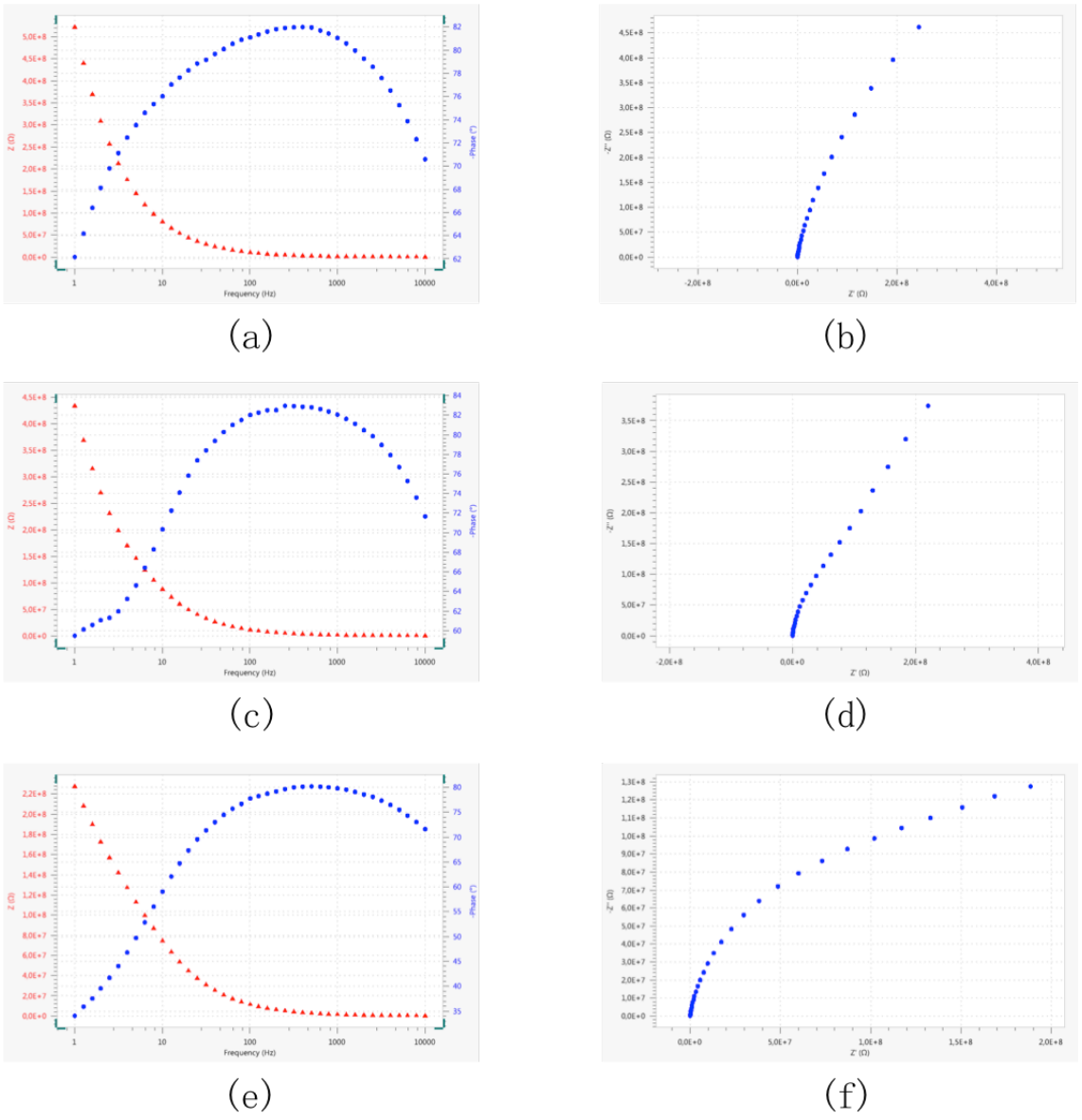

Figure 6.9: Bode-Impedance and Phase-angle plots vs. Frequency (Hz) and Nyquist plots (**Sample 2**). (a) & (b): Electrodes 1 and 2; (c) & (d): Electrodes 1 and 3; (a) & (b): Electrodes 2 and 3.

-70 ° at a frequency of around 3 Hz. The phase angle curves of Sample 1 (Figure 6.8) were in line with expectations.

However, for Sample 2 (50 μm microelectrodes), the measured phase angle values at high frequency (10 kHz) were in the range of -70 to -71 °. One can see from Figure 6.9 that the trend of the phase angle curves was right, but the appearance of the expected 0 ° at high frequencies was delayed when compared to Sample 1. A drop in the double layer capacitance value could possibly cause this. And this capacitance drop could also lead to an increase in the impedance level.

The analysis of the Bode plots explained the impedance results presented in Table 6.3. The unexpected large impedance values of Sample 2 and Sample 3 might due to a change of the microelectrode material surface conditions. The reasons could be as follows:

1. The TiN coatings were not intact and the underneath Ti was exposed to the PBS solution, possible reasons:
    - TiN was removed by etchants during wet etching processes;

- Damages on TiN surface when the optrodes were detached from the wafer;
- Corrosion or degradation on TiN surface.

2. Impurities of the TiN layer changed the surface roughness, possible reasons:

- Oxidation of TiN layer and formation of TiO2.

During the EIS measurement, only three different samples were measured. Although these samples were microfabricated using the same process flow, some process variations are expected (i.e. different TiN thickness, over- and under-etching from sample to sample, material roughness and so forth).

Statistically speaking, to achieve more reliable results and converge to a normal distribution and find out its mean, according to the central limit theorem, the number of samples should be at least 30.

6.3. Conclusion

In this chapter, experiments were carried out to characterize the performance of μLEDs and microelectrodes. The PWM method was used to regulate the μLED's light intensity and the pulse frequency. The PWM frequency (> 10 kHz) was adjusted by changing the built-in timers in the Arduino Mega 2560 board. The μLED functioned well in the PBS solution with a PDMS coating. Three optrode samples were tested on the microelectrode impedance performance. The first sample with 75 μm TiN microelectrodes have a reasonable impedance level below 60 $k\Omega$. However, the other two samples with 50 μm TiN microelectrodes and 75 μm TiN microelectrodes resulted in very high impedance level (up to 700 $k\Omega$). Several possible reasons were proposed.

7

Conclusions and Recommendations

In this final chapter, a brief summary is first delivered to give a reminding of the work flow during the entire thesis project. The conclusion is made afterwards to list the key aspects of the project as well as the limitations of the work, followed with some recommendations on the future work.

7.1. Summary

Chapter 1: This chapter included the research backgrounds in the Department of Human Genetics in LUMC. During the internship period, I studied their experimental setups (microelectrodes, laser light source and the neural signal processing system) and had a basic understanding of each function unit's performance and limitations. The idea to build a miniaturized optrode with combined optical stimulation and electrophysiological recording units started from there.

Chapter 2: After establishing the project goal, I started with the literature review to learn the underlying mechanisms and to see how other researchers progressed in this field. The fundamentals of the emerging optogenetic techniques and the basic criteria for fabricating microelectrodes were explained separately in the first two sections. Then the research focus was moved to the combination of the two functional units. By making a summary table of representative works, the limitations of recent works were observed. There seemed to be no existing work that fulfill all the following requirements: well-functioned microelectrodes with low impedance level, integrated light source with sufficient light delivery to microelectrodes regions, miniaturized probe dimensions for a safe and long-term animal experiments, and a precise control over the fabrication process to ensure the consistent quality of the device. The project goal was to fulfill all the aforementioned requirements with the design and fabrication of optrode prototypes.

Chapter 3: The design was carried out in this chapter. Various factors were taken into considerations and their mutual influences were considered as well (i.e. light source selection, optrode shaft geometry, microelectrode size and material, placement of μLEDs, integration of the device). The design specifications met the basic requirements: TiN material for making low impedance microelectrodes, integration of μLEDs to provide sufficient light intensity, shaft width < 350 μm for tolerable tissue damage, and the MEMS microfabrication process to precisely control the optrode quality and allow batch productions. Some special designs were included to further improve the optrode's performance. The mask layouts were produced with L-Edit software based on all determined design specifications and the fabrication technique.

Chapter 4: In this chapter, the MEMS microfabrication process and the microscopic results were presented. All the recipes applied during the fabrication process have been verified. And a troubleshooting table was concluded for the potential future improvement by other researchers.

Chapter 5: After the fabrication of the optrode body, the μLED was integrated on the shaft with silver epoxy die attach method and coated with PDMS to prevent the current leakage to surrounding tissues during in-vivo experiments. And the optrode was attached to a PCB for testing (i.e. electrode impedance, light intensity and pulse frequency). In this chapter, all the integration steps were performed manually, so that the qualities of either die attaching or isolating the μLED were not in consistency and precision. However, the manual process verified the feasibility of the whole design. And one can expect that with the automatic integration processes, much better device performances could be reached.

Chapter 6: In this chapter, experiments were performed to characterize the μLED performance and the TiN microelectrode impedance level. Arduino Mega 2560 board was used to control the μLED light intensity and pulse frequency with the PWM control method. The PDMS-coated μLED functioned well in the PBS solution. For the impedance tests, Autolab electrochemical impedance spectroscopy setup was used and the impedance value of 75 μm TiN microelectrodes was below 60 $k\Omega$, which was optimal for electrophysiological recordings.

7.2. Conclusion

In this section, the achieved goals and the insufficiency are presented.

7.2.1. Achieved goals

1. Combined optical stimulation (μLEDs) and electrical recording (TiN microelectrodes) in one single device;
2. Custom designed optrodes for various research applications: (1) target different brain layers including cerebral cortex, hippocampus and thalamus, and (2) target different sites within the same brain layer;
3. Decreased the overall optrode dimensions (shaft width<350 μm) and minimized the μLED-induced tissue damage by placing the μLED in cavity structures;
4. Developed and verified the microfabrication process and recipes for producing the main part of the optrode;
5. Precisely controlled the μLED functioning with the PWM method.

7.2.2. Insufficiency

(1) Bonding and isolation process of μLEDs:

The bonding and isolation of μLEDs were done manually, which result in some drawbacks: (a) Difficult to control the amount of silver epoxy attached onto the μLED bond pads; (b) Difficult to pick and place the μLED exactly in the cavity; (c) Impossible to control PDMS coating conditions (thickness, coverage of required spaces, uniformity).

Possible solution is to perform an automatic silver epoxy die-attach process first. And then pattern the PDMS onto a bare Silicon wafer and perform wafer level bonding between the wafer with PDMS and the wafer with μLEDs to transfer the patterned PDMS.

(2) Experiments on the radiant flux of PDMS-coated μLEDs:

The μLED model DA2432 provides around 30 mW radiant flux with a typical forward current of 20 mA. The PDMS material offers high transmittance to visible light domain. However, the exact radiant flux of PDMS-coated μLEDs has not been tested yet.

(3) TiN surface morphology tests:

The microelectrode impedance value is influenced by the surface morphology of titanium nitride (surface roughness). During and after the fabrication process, the atomic force microscopy (AFM) tool can be applied to study the property change of the TiN surface roughness. The AFM can be done at stages such as: (a) directly after TiN/Ti layer deposition in Sigma,

(b) after negative photoresist removal by Tepla oxygen plasma, (c) after contact opening by Alcatel dry etcher, and (d) after performing in-vitro EIS tests. Through the comparison studies, the surface conditions of titanium nitride shall be clear and can give an insight to the microelectrode impedance performance.

(4) Experimental results on microelectrode impedance:
The electrochemical impedance spectroscopy test is done in a chemical environment (PBS solution). To get a convincing result, a number of samples should be tested in the same experimental setup and the data needs to be analyzed to provide both average and standard deviation values. However, during the integration process, optrodes are wire bonded to PCBs to allow a connection between the microelectrodes and the Autolab system, which is time consuming and it is not possible to produce mass samples.

(5) Reference and ground microelectrodes:
The reference and ground microelectrodes should be (a) placed in electrophysiological "silent" areas and (b) have lower impedance levels. Only the first requirement was achieved in this design. The low impedance level can be achieved by either surface modification on the electrode sites or enlarging the total surface area. The former option requires an extra mask for specifically coating materials onto the reference and ground sites.

(6) Crosstalk between μLED and the recording units:
The crosstalk between functioning μLEDs and recording units needs to be studied to make sure if the switching on or off μLEDs (with a high frequency) would induce unwanted artifacts to the recorded neural signals.

7.3. Recommendations

With the recent development in fabrication technology of polymers (such as parylene, polyimide, PDMS, PEDOT) and nano-materials (such as graphene, carbon nanotube), more possibilities exist for fabricating an optrode with decreased dimensions and increased performance.

7.3.1. Improvement on microelectrodes: PEDOT and nanomaterials

TiN is a biocompatible material for making microelectrodes with low impedance and is easy for fabrication. However, some other materials (such as PEDOT and CNTs) can improve the electrode impedance level further. Poly(3,4ethylenedioxythiophene) PEDOT is a conductive polymer material and can be coated onto electrodes surface through a electrochemical polymerization process. It was recently reported to provide a 94% reduction of the electrochemical impedance at 1 kHz when compared with TiN microelectrodes [47]. Carbon nanotube (CNT) coating also decreases the impedance level. One work by Shoval *et al.* increased the SNR level by three times by using CNT coatings when compared to TiN electrodes [48]. Graphene is the other optimal nanomaterial for making microelectrodes. Though the impedance level of graphene is higher, its transparency property makes it an interesting material when combined with optogenetics.
The improvements on the electrode material lead to changes of the fabrication process, which needs to be taken into considerations.

7.3.2. Improvement on coating/packaging layer of optrodes: Polymers

SiO_2 is used to isolate all conducting wires from the liquid environment in this optrode design. However, PECVD SiO_2 was reported to have an average dissolution rate of around 3.5 nm/day in vivo, as stated before. For a long term animal experiment (i.e. 3 months), such dissolution process would not cause device malfunctions. However, considering a further requirement on device's safety issues, polymers such as polyimide and PDMS are good

candidates because they are chemically inert and remain stable in the body. Both materials can be spin coated onto wafer surface and are cured with a relatively low temperature (< 300 $^{\circ}C$).

7.3.3. Integration of CMOS technology and IC designs

One reason for fabricating optrodes on the rigid silicon substrate was because of the silicon wafer's compatibility with CMOS technology. For the optrodes, more function units can be added. Ronaldo Martins da Ponte is currently developing a novel temperature sensor with CMOS technology and attempts to combine both designs together. Other function units such as simple pre-amplifiers and the MOSFET switch can be integrated as well.

7.3.4. Waveguide optical stimulation with Parylene N and SU-8

Other than on-chip-μLEDs, waveguide can be another option for providing optical stimulation with the advanced technology in polymers fabrication. Parylene N and SU-8 have been reported to serve as good waveguide materials with high transmission property of visible light [49, 50].

The optrodes can be applied to study neural circuits and their correlations with progressing neurological diseases in animal brains with improved temporal and spatial resolutions. Its development provides the possibility for a future miniaturized bioelectronic medicine devices to be implanted in human nervous system to perform certain treatments.

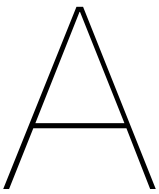

Flowchart: Processing on Plain Wafers

1. COATING AND BAKING (Process wafers and Test wafers)
    - Use the EVG 120 Coater/developer to coat the wafers with resist, and follow the instructions specified for this equipment.
    - The process consists of a treatment with HMDS (hexamethyldisilazane) vapor with nitrogen as a carrier gas, spin coating with Shipley SPR3012 positive photoresist, and a soft bake at 95degC for 1.5 minute.
    - Always check the temperature of the hotplate and the relative humidity (48 ± 2 %) in the room first.
    - Use coating Co – 3012 - zerolayer (resist thickness: 1.400 µm).
2. ALIGNMENT AND EXPOSURE
    - Tool: PAS5500/80 waferstepper
    - Location: Class 100 Litho room
    - Mask ID: COMURK
    - Exposure job: litho/zefwam
    - Layer ID: 1
    - Focus: 0
    - Energy: 140 mJ/cm2
    - Settings: no additional user settings are required.
    - Notes: The chuck-side of the wafers should be free of photoresist and other polymers.
3. DEVELOPMENT
    - Use the developer station of the EVG120 system to develop the wafers. The process consists of a post-exposure bake at 115 °C for 90 seconds, developing with Shipley MF322 with a single puddle process, and a hard bake at 100 °C for 90 seconds.
    - Always follow the instructions for this equipment.
    - Use program, ”Dev - SP”.
4. INSPECTION: LINEWIDTH AND OVERLAY
    - Visually inspect the wafers through a microscope, and check the linewidth. No resist residues are allowed.
5. PLASMA ETCHING OF ALIGNMENT MARKS
    - Use the Trikon Ωmega 201 plasma etcher.
    - Follow the operating instructions from the manual when using this machine.

- The process conditions of the etch program may not be changed!
- Use sequence urk_npd for 120nm and set the platen temperature to 20 °C.

6. CLEANING PROCEDURE
   - Plasma strip
     - Use the Tepla plasma system to remove the photoresist in an oxygen plasma.
     - Follow the instructions specified for the Tepla stripper, and use the quartz carrier.
     - Use Program 1: detects end point plus 2min overetch.
   - Standard Si Cleaning
     - Cleaning: 10 minutes in fuming nitric acid (Merck: HNO3 (100%), selectipur; ambient temperature).
     - QDR: Rinse in the Quick Dump Rinser with the standard program until the resistivity is 5 MΩ.
     - Cleaning: 10 minutes in concentrated nitric acid (Merck: HNO3 (65%); temp. 110°C).
     - QDR: Rinse in the Quick Dump Rinser with the standard program until the resistivity is 5 MΩ.
     - Drying: Use the Semitool ”Rinser/dryer” with the standard program, and the white carrier with a red dot.
7. PECVD DEPOSITION: 1000nm SiO2
   - Use the Novellus Concept One PECVD reactor.
   - Follow the operating instructions from the manual when using this machine.
   - It is not allowed to change the process conditions and time from the deposition recipe!
   - Add bare silicon wafer (T1) as dummy wafer to measure thickness later. (optional)
   - Use XXXSIOSTD to deposit a 1000 nm thick SiO2 layer. Time: ~ 16s. Check the log book.
   - Note: The deposition time is subject to minor changes, in order to obtain the correct film thickness.
8. MEASUREMENT: Silicon Oxide Thickness
   - Use the Leitz MPV-SP measurement system for layer thickness measurements.
   - Follow the operating instructions from the manual when using this equipment.
   - Measure Test wafer T1.
9. METALLIZATION: 50nm Ti & 350nm TiN in one run
   - Tool: TRIKON Sigma Sputtering
   - Location: CR100
   - Manual: <location>
   - Recipe name: Check the recipes in the machine.
10. COATING AND BAKING
    - Use the EVG 120 Coater/developer to coat the wafers with resist, and follow the instructions specified for this equipment.
    - Always check the temperature of the hotplate and the relative humidity (48 ± 2 %) in the room first.
    - Use coating Nlof-1.5um-noEBR (negative photoresist, 1.5um)
11. ALIGNMENT AND EXPOSURE - EVG420 CONTACT ALIGNER.
    - PRESET #1

- Mask Box: 490
- Mask: METAL-1
- Expose Dose: ~12s (Check manual), Hard Contact
- Check the contact aligner mode to be sure it is in Preset 1 and proximity off!! Exposure time needs to be calculated by equation: exposure dose/exposure energy, check manual and calculate the exposure time.

12. X-LINK BAKE (automatic)
    - Use the developer station of the EVG120 system to cross-link the exposed AZ Nlof 2000 resist. The process consists of:
    - A cross-link bake 115 °C for 90 seconds
    - Always follow the instructions for this equipment.
    - Use program ”Only – X-link bake (Si)”.
13. DEVELOPMENT
    - Use the developer station of the EVG120 system to develop the wafers.
    - Always follow the instructions for this equipment.
    - Use program, ”Dev - SP - no PEB”.
14. INSPECTION: Linewidth and overlay
    - Visually inspect the wafers through a microscope, and check the line width and overlay. No “resist” residues are allowed.
15. PLASMA ETCHING: 50nm Ti & 350nm TiN
    - Use the Trikon Ωmega 201 plasma etcher.
    - Follow the operating instructions from the manual when using this machine.
    - It is not allowed to change the process conditions and times from the etch recipe!
    - Recipe: Recipe that etches 500nm TiN could work. Or ask Alexander to edit a new recipe.
    - INSPECTION: No residues or undercut are allowed. (pay attention to the sloppy sidewall)
16. LAYER STRIPPING PHOTORESIST
    - Use the Tepla Plasma 300 system to remove the photoresist in an oxygen plasma.
    - Follow the instructions specified for the Tepla stripper, and use the quartz carrier.
    - Use Program 4.
17. CLEANING: HNO3 99% METAL
    - Clean: 10 minutes in fuming nitric acid at ambient temperature. This will dissolve organic materials. Use wet bench ”HNO3 99% (metal)” and the carrier with a red and yellow dot.
    - Rinse: Rinse in the Quick Dump Rinser with the standard program until the resistivity is 5 MΩ.
    - Dry: Use the Semitool ”rinser/dryer” with the standard program, and the white carrier with a black dot.
    - Note: Do not perform a ”HNO3 69,5% 110C (Si)” cleaning step!
18. PECVD DEPOSITION: 1000nm SiO2
    - Use the Novellus Concept One PECVD reactor.
    - Follow the operating instructions from the manual when using this machine.
    - It is not allowed to change the process conditions and time from the deposition recipe!

- Add silicon wafer (T1) as dummy wafer to measure thickness later. (optional)
- Use XXXSIOSTD to deposit a 1000 nm thick SiO2 layer. Time: ~ 16s. Check the log book.
- Note: The deposition time is subject to minor changes, in order to obtain the correct film thickness.

19. MEASUREMENT: Silicon Oxide Thickness
    - Use the Leitz MPV-SP measurement system for layer thickness measurements.
    - Follow the operating instructions from the manual when using this equipment.
    - Measure Test wafer T1. (Overall ~ 2000nm)
20. METALLIZATION: 50nm Ti & 350nm TiN in one run
    - Tool: TRIKON Sigma Sputtering
    - Location: CR100
    - Manual: <location>
    - Recipe name: Check the recipes in the machine.
21. COATING AND BAKING
    - Use the EVG 120 Coater/developer to coat the wafers with resist, and follow the instructions specified for this equipment.
    - Always check the temperature of the hotplate and the relative humidity (48 ± 2 %) in the room first.
    - Use coating Nlof-1.5um-noEBR (negative photoresist, 1.5um)
22. ALIGNMENT AND EXPOSURE - EVG420 CONTACT ALIGNER.
    - PRESET #1
    - Mask Box: 490
    - Mask: METAL-2
    - Expose Time: ~ 12s (Check manual), Hard Contact
    - Check the contact aligner mode to be sure it is in Preset 1 and proximity off!! Exposure time needs to be calculated by equation: exposure dose/exposure energy, check manual and calculate the exposure time.
23. X-LINK BAKE (automatic)
    - Use the developer station of the EVG120 system to cross-link the exposed AZ Nlof 2000 resist. The process consists of:
    - A cross-link bake 115 °C for 90 seconds
    - Always follow the instructions for this equipment.
    - Use program ”Only – X-link bake (Si?)”.
24. DEVELOPMENT
    - Use the developer station of the EVG120 system to develop the wafers.
    - Always follow the instructions for this equipment.
    - Use program, ”Dev - SP - no PEB”.
25. INSPECTION: Linewidth and overlay
    - Visually inspect the wafers through a microscope, and check the line width and overlay. No “resist” residues are allowed.
26. PLASMA ETCHING: 50nm Ti & 350nm TiN
    - Use the Trikon Ωmega 201 plasma etcher.
    - Follow the operating instructions from the manual when using this machine.
    - It is not allowed to change the process conditions and times from the etch recipe!

- Recipe: Recipe that etches 500nm TiN could work. Or ask Alexander to edit a new recipe.
- INSPECTION: No residues or undercut are allowed. (pay attention to the sloppy sidewall)

27. LAYER STRIPPING PHOTORESIST
    - Use the Tepla Plasma 300 system to remove the photoresist in an oxygen plasma.
    - Follow the instructions specified for the Tepla stripper, and use the quartz carrier.
    - Use Program 4.
28. CLEANING: HNO3 99% METAL
    - Clean: 10 minutes in fuming nitric acid at ambient temperature. This will dissolve organic materials. Use wet bench ”HNO3 99% (metal)” and the carrier with a red and yellow dot.
    - Rinse: Rinse in the Quick Dump Rinser with the standard program until the resistivity is 5 MΩ.
    - Dry: Use the Semitool ”rinser/dryer” with the standard program, and the white carrier with a black dot.
    - Note: Do not perform a ”HNO3 69,5% 110C (Si)” cleaning step!
29. PECVD DEPOSITION: 2000nm SiO2
    - Use the Novellus Concept One PECVD reactor.
    - Follow the operating instructions from the manual when using this machine.
    - It is not allowed to change the process conditions and time from the deposition recipe!
    - Add silicon wafer (T1) as dummy wafer to measure thickness later. (optional)
    - Use XXXSIOSTD to deposit a 2000 nm thick SiO2 layer. Time: ~ 32s. Check the log book.
    - Note: The deposition time is subject to minor changes, in order to obtain the correct film thickness.
30. MEASUREMENT: Silicon Oxide Thickness
    - Use the Leitz MPV-SP measurement system for layer thickness measurements.
    - Follow the operating instructions from the manual when using this equipment.
    - Measure Test wafer T1 (Overall ~ 4000nm).
31. COATING AND BAKING (Incl. test wafer T1)
    - Use the EVG 120 Coater/developer to coat the wafers with resist, and follow the instructions specified for this equipment.
    - The process consists of a treatment with HMDS (hexamethyldisilazane) vapor with nitrogen as a carrier gas, spin coating with Shipley SPR3012 positive photoresist, and a soft bake at 95 degC for 1.5 minute.
    - Always check the temperature of the hotplate and the relative humidity (48 ± 2 %) in the room first.
    - Use coating Co-3012-2.1um.
32. ALIGNMENT AND EXPOSURE - EVG420 CONTACT ALIGNER.
    - PRESET #1
    - Mask Box: 490
    - Mask: Openings
    - Expose Dose: ~ 12s (Check manual), Hard Contact

- Check the contact aligner mode to be sure it is in Preset 1 and proximity off!! Exposure time needs to be calculated by equation: exposure dose/exposure energy, check manual and calculate the exposure time.

33. DEVELOPMENT
    - Use the developer station of the EVG120 system to develop the wafers.
    - Always follow the instructions for this equipment.
    - Use program, ”Dev - SP”.
34. INSPECTION: Linewidth and overlay
    - Visually inspect the wafers through a microscope, and check the line width and overlay. No “resist” residues are allowed. Dektak measure the depth of photoresist pattern.
35. WET ETCHING: BHF (1:7) METAL
    - Moisten: Rinse for 1 minute in wet bench ”H2O/TRITON X-100” and use the carrier with the blue dot. The bath contains 1 ml Triton X-100 per 5000 ml demi water.
    - ETCHING: Use wet bench ”SiO2-ets (1:7)” at ambient temperature, and the carrier with the blue dot. The bath contains a buffered HF solution (Merck LSI selectipur, SiO2 1:7)
    - Etch time: needs to be tested first. Use test wafer T1 to test the etch rate, etch 10min and use Dektak to measure the etch depth. Loss of photoresist should also be considered.
    - QDR: Rinse in the Quick Dump Rinser with the standard program until the resistivety is 5 MΩ.
    - Drying: Use the Semitool ”rinser/dryer” with the standard program, and the orange carrier with a red dot.
    - Inspection: Visually through a microscope. All the windows must be open and the hydrophobic test may be applied.
36. LAYER STRIPPING PHOTORESIST
    - Use the Tepla Plasma 300 system to remove the photoresist in an oxygen plasma.
    - Follow the instructions specified for the Tepla stripper, and use the quartz carrier.
    - Use Program 1.
37. CLEANING: HNO3 99% METAL
    - Clean: 10 minutes in fuming nitric acid at ambient temperature. This will dissolve organic materials. Use wet bench ”HNO3 99% (metal)” and the carrier with a red and yellow dot.
    - Rinse: Rinse in the Quick Dump Rinser with the standard program until the resistivity is 5 MΩ.
    - Dry: Use the Semitool ”rinser/dryer” with the standard program, and the white carrier with a black dot.
    - Note: Do not perform a ”HNO3 69,5% 110C (Si)” cleaning step!
38. PECVD DEPOSITION: 500nm SiO2
    - Use the Novellus Concept One PECVD reactor.
    - Follow the operating instructions from the manual when using this machine.
    - It is not allowed to change the process conditions and time from the deposition recipe!
    - Add bare silicon wafer (T2) as dummy wafer to measure thickness later. (optional)
    - Use XXXSIOSTD to deposit a 500 nm thick SiO2 layer. Time: ~ 8s. Check the log book.

- Note: The deposition time is subject to minor changes, in order to obtain the correct film thickness.

39. METALLIZATION: 2400nm Al (1% Si)
    - Tool: TRIKON Sigma Sputtering
    - Location: CR100
    - Manual: <location>
    - Recipe name: Check the recipes in the machine.
    - Add silicon wafer (T2, T3). (Optional, from step 39-43, T2 for test run in step 44, T3 for DRIE etch rate test)
40. COATING AND BAKING
    - Use the EVG 120 Coater/developer to coat the wafers with resist, and follow the instructions specified for this equipment.
    - Always check the temperature of the hotplate and the relative humidity (48 ± 2 %) in the room first.
    - Use coating Co-Syr-9260-12um-no EBR (positive photoresist, 12um)
    - Wait ~ 30min before Exposure
41. ALIGNMENT AND EXPOSURE - EVG420 CONTACT ALIGNER.
    - PRESET #3 (Follow the instruction in manual)
    - Mask Box: 490
    - Mask: Backside_DRIE
    - Expose Dose: ~ 90s (Check manual)
    - Check the contact aligner mode to be sure it is in Preset 3 and proximity off!! Exposure time needs to be calculated by equation: exposure dose/exposure energy, check manual and calculate the exposure time.
    - Wait ~ 30min before Development
42. MANUAL DEVELOPMENT
    - Use the developer area polymer lab
    - Developing with the Diluted AZ400K: H2O = 1 : 2 XXX developer for 2-3 min.
    - Do not use to much developer and rinsing fluid (mostly water) during the developing..
    - Note: Dispose the developer into the right container if it is not water based.
    - Note: When finished always turn of the DI-water.
43. DRIE PLASMA ETCHING SILICON
    - Use the STPS RAPIER plasma etcher.
    - Follow the operating instructions from the manual when using this machine.
    - It is not allowed to change the process conditions and times from the etch recipe!
    - Recipe name: EKL Smooth @ 20C (In WAFERVIEW)
    - Total etch cycles: ~ 400 CYCLES (could do a test run first)
    - The 300um plain wafer might not be detected by the sensor in Rapier machine. Thus loading the wafer several times until it being sensed (change the slot during each load).
44. WET ETCHING SILICON OXIDE (METAL) (ALCATEL DRY ETCH TAKES LONGER TIME)
    - Use test wafer T2 to calibrate etch rate. Calculate etch time, over etch is allowed.
    - Triton (Al. etch) for 1 min
    - Etch in BHF (1:7) Metal

- Rinse: in the Quick Dump Rinser with the standard program.
- Dry: Use the Semitool ”rinser/dryer” with the standard program, and the orange carrier with a red dot.

45. ALUMINUM REMOVAL
    - Moisten: Rinse for 1 minute in wet bench ”H2O/Triton X-100 tbv Al. Ets”. Use the carrier with the yellow dot. The bath contains 1 ml Triton X-100 per 5000 ml deionized water.
    - Etching: Use wet bench ”Al. ets 35°C”, and the carrier with the yellow dot.
    - 1 liter buffered aluminum etch fluid contains: 770 ml concentrated phosphorus acid (H3PO4 85%), 19 ml concentrated nitric acid (HNO3 65%), 140 ml concentrated acetic acid (CH3COOH 100%) and 71 ml deionized water.
    - Etch time: Use test wafer T2 or T3 to calibrate the aluminum etch rate, over etch is allowed.
    - QDR: Rinse in the Quick Dump Rinser with the standard program until the resistivity is 5 MΩ.
    - Drying: Use the Semitool ”rinser/dryer” with the standard program, and the orange carrier with a black dot.
46. LAYER STRIPPING PHOTORESIST
    - Use the Tepla Plasma 300 system to remove the photoresist in an oxygen plasma.
    - Follow the instructions specified for the Tepla stripper, and use the quartz carrier.
    - Use Program 4.
47. CLEANING: HNO3 99% METAL
    - Clean: 10 minutes in fuming nitric acid at ambient temperature. This will dissolve organic materials. Use wet bench ”HNO3 99% (metal)” and the carrier with a red and yellow dot.
    - Rinse: Rinse in the Quick Dump Rinser with the standard program until the resistivity is 5 MΩ.
    - Dry: Use the Semitool ”rinser/dryer” with the standard program, and the white carrier with a black dot.
    - Note: Do not perform a ”HNO3 69,5% 110C (Si)” cleaning step!
48. ALCATEL PLASMA ETCHING WITHOUT MASK
    - Etch ~ 500nm Silicon Oxide, over etch is allowed.
    - All contact pads need to be open completely.

B

Flowchart: Processing on Wafers with KOH-etched Cavities

1. COATING AND BAKING (Process wafers and Test wafers)
    - Use the EVG 120 Coater/developer to coat the wafers with resist, and follow the instructions specified for this equipment.
    - The process consists of a treatment with HMDS (hexamethyldisilazane) vapor with nitrogen as a carrier gas, spin coating with Shipley SPR3012 positive photoresist, and a soft bake at 95degC for 1.5 minute.
    - Always check the temperature of the hotplate and the relative humidity (48 ± 2 %) in the room first.
    - Use coating Co – 3012 - zerolayer (resist thickness: 1.400 μm).
2. ALIGNMENT AND EXPOSURE
    - Tool: PAS5500/80 waferstepper
    - Location: Class 100 Litho room
    - Mask ID: COMURK
    - Exposure job: litho/zefwam
    - Layer ID: 1
    - Focus: 0
    - Energy: 140 mJ/cm2
    - Settings: no additional user settings are required.
    - Notes: The chuck-side of the wafers should be free of photoresist and other polymers.
3. DEVELOPMENT
    - Use the developer station of the EVG120 system to develop the wafers. The process consists of a post-exposure bake at 115 °C for 90 seconds, developing with Shipley MF322 with a single puddle process, and a hard bake at 100 °C for 90 seconds.
    - Always follow the instructions for this equipment.
    - Use program, ”Dev - SP”.
4. INSPECTION: LINEWIDTH AND OVERLAY
    - Visually inspect the wafers through a microscope, and check the linewidth. No resist residues are allowed.

5. PLASMA ETCHING OF ALIGNMENT MARKS
   - Use the Trikon Ωmega 201 plasma etcher.
   - Follow the operating instructions from the manual when using this machine.
   - The process conditions of the etch program may not be changed!
   - Use sequence urk_npd for 120nm and set the platen temperature to 20 °C.
6. CLEANING PROCEDURE
   - Plasma strip
     - Use the Tepla plasma system to remove the photoresist in an oxygen plasma.
     - Follow the instructions specified for the Tepla stripper, and use the quartz carrier.
     - Use Program 1: detects end point plus 2min overetch.
   - Standard Si Cleaning
     - Cleaning: 10 minutes in fuming nitric acid (Merck: HNO3 (100%), selectipur; ambient temperature).
     - QDR: Rinse in the Quick Dump Rinser with the standard program until the resistivity is 5 MΩ.
     - Cleaning: 10 minutes in concentrated nitric acid (Merck: HNO3 (65%); temp. 110°C).
     - QDR: Rinse in the Quick Dump Rinser with the standard program until the resistivity is 5 MΩ.
     - Drying: Use the Semitool ”Rinser/dryer” with the standard program, and the white carrier with a red dot.
7. **LPCVD DEPOSITION: 500 nm low-stress SiN**
   - In Furnace E2
   - 4INCHST, Edit deposition time (check the logbook).
8. **MEASUREMENT: Silicon Nitride Thickness**
   - Leitz MPV-SP measurement system.
9. **COATING AND BAKING**
   - Use the EVG 120 Coater/developer to coat the wafers with resist, and follow the instructions specified for this equipment.
   - The process consists of a treatment with HMDS (hexamethyldisilazane) vapor with nitrogen as a carrier gas, spin coating with Shipley SPR3012 positive photoresist, and a soft bake at 95degC for 1.5 minute.
   - Always check the temperature of the hotplate and the relative humidity (48 ± 2 %) in the room first.
   - Use coating 1 - Co – 3012 - 3.1 µm.
10. **EVG420 CONTACT ALIGNER**
    - Mask Box: 490, PRESET #1, Mask: Front_Cavity.
    - Expose Time: ~ 12s (Check manual), Hard Contact.
11. **DEVELOPMENT**
    - EVG120, ”Dev - SP”.
12. **INSPECTION: LINEWIDTH AND OVERLAY**

- Visually inspect the wafers through a microscope, and check the line width and overlay. No “resist” residues are allowed.

13. **PLASMA ETCHING: 500 nm SILICON NITRIDE**
    - Drytek Triode 384T, STDSIN, Edit Helium flow and Etch time.
14. **CLEANING PROCEDURE**
    - Remove Photoresist in Tepla, Program 1.
    - Stardard Si cleaning line.
15. **KOH ETCHING: 100 μm, in SAL LAB**
    - KOH 33% 85 deg C, (test wafer) for KOH etch rate.
    - Rinse and dry.
16. **CLEANING PROCEDURE**
    - **Si+ cleaning**
    - Stardard Si cleaning line.
17. **DEPTH MEASUREMENT**
    - Dektak profilometer measure cavity depth.
18. **WET ETCHING SiN**
    - 85% Phosphoric acid 157 deg C, etch until no SiN residues exist.
19. **CLEANING PROCEDURE**
    - Stardard Si cleaning line.
20. PECVD DEPOSITION: 1000nm SiO2
    - Use the Novellus Concept One PECVD reactor.
    - Follow the operating instructions from the manual when using this machine.
    - It is not allowed to change the process conditions and time from the deposition recipe!
    - Add bare silicon wafer (T1) as dummy wafer to measure thickness later. (optional)
    - Use XXXSIOSTD to deposit a 1000 nm thick SiO2 layer. Time: ~ 16s. Check the log book.
    - Note: The deposition time is subject to minor changes, in order to obtain the correct film thickness.
21. MEASUREMENT: Silicon Oxide Thickness
    - Use the Leitz MPV-SP measurement system for layer thickness measurements.
    - Follow the operating instructions from the manual when using this equipment.
    - Measure Test wafer T1.
22. METALLIZATION: 50nm Ti & 350nm TiN in one run
    - Tool: TRIKON Sigma Sputtering
    - Location: CR100
    - Manual: <location>
    - Recipe name: Check the recipes in the machine.
23. **COATING AND BAKING**

- Manual HMDS 15min.
- EVG110 Spray coater.
- **Diluted AZ Nlof 2070** photoresist.
- Recipe:
  - HP 1000mbar 2ul 8 layers
  - Bake 115 deg C 1 min
  - HP 1000mbar 2ul 8 layers
  - Bake 115 deg C for 5 min.

24. **EVG420 CONTACT ALIGNER.**
    - Mask Box: 490, PRESET #1, Mask: METAL-1.
    - Expose Time: ~ 20s (Check manual), Hard Contact.
25. **X-LINK BAKE**
    - Use the Hotplate in EVG110 Spray coater.
    - 115 deg C for 2 min 15 sec.
26. **MANUAL DEVELOPMENT**
    - Use the wet bench Poly-3 in Polymer lab.
    - MF322 developer 2-3 min. Inspect the wafers in halfway (around 2 min) to check the linewidth on wafer surface and in KOH-etched cavities. No photoresist residues are allowed at the bottom edges of the cavities. After inspection, adjust the remained development time.
    - Rinse and dry.
27. INSPECTION: Linewidth and overlay
    - Visually inspect the wafers through a microscope, and check the line width and overlay. No “resist” residues are allowed.
28. PLASMA ETCHING: 50nm Ti & 350nm TiN
    - Use the Trikon Ωmega 201 plasma etcher.
    - Follow the operating instructions from the manual when using this machine.
    - It is not allowed to change the process conditions and times from the etch recipe!
    - Recipe: Recipe that etches 500nm TiN could work. Or ask Alexander to edit a new recipe.
    - INSPECTION: No residues or undercut are allowed. (pay attention to the sloppy sidewall)
29. LAYER STRIPPING PHOTORESIST
    - Use the Tepla Plasma 300 system to remove the photoresist in an oxygen plasma.
    - Follow the instructions specified for the Tepla stripper, and use the quartz carrier.
    - Use Program 4.
30. CLEANING: HNO3 99% METAL
    - Clean: 10 minutes in fuming nitric acid at ambient temperature. This will dissolve organic materials. Use wet bench ”HNO3 99% (metal)” and the carrier with a red and yellow dot.
    - Rinse: Rinse in the Quick Dump Rinser with the standard program until the resistivity is 5 MΩ.

- Dry: Use the Semitool ”rinser/dryer” with the standard program, and the white carrier with a black dot.
- Note: Do not perform a ”HNO3 69,5% 110C (Si)” cleaning step!

31. PECVD DEPOSITION: 1000nm SiO2

    - Use the Novellus Concept One PECVD reactor.
    - Follow the operating instructions from the manual when using this machine.
    - It is not allowed to change the process conditions and time from the deposition recipe!
    - Add silicon wafer (T1) as dummy wafer to measure thickness later. (optional)
    - Use XXXSIOSTD to deposit a 1000 nm thick SiO2 layer. Time: ~ 16s. Check the log book.
    - Note: The deposition time is subject to minor changes, in order to obtain the correct film thickness.

32. MEASUREMENT: Silicon Oxide Thickness

    - Use the Leitz MPV-SP measurement system for layer thickness measurements.
    - Follow the operating instructions from the manual when using this equipment.
    - Measure Test wafer T1. (Overall ~ 2000nm)

33. METALLIZATION: 50nm Ti & 350nm TiN in one run

    - Tool: TRIKON Sigma Sputtering
    - Location: CR100
    - Manual: <location>
    - Recipe name: Check the recipes in the machine.

34. **COATING AND BAKING**

    - Manual HMDS 15min.
    - EVG110 Spray coater.
    - **Diluted AZ Nlof 2070** photoresist.
    - Recipe:
        - HP 1000mbar 2ul 8 layers
        - Bake 115 deg C 1 min
        - HP 1000mbar 2ul 8 layers
        - Bake 115 deg C for 5 min.

35. **EVG420 CONTACT ALIGNER.**

    - Mask Box: 490, PRESET #1, Mask: METAL-2.
    - Expose Time: ~ 20s (Check manual), Hard Contact.

36. **X-LINK BAKE**

    - Use the Hotplate in EVG110 Spray coater.
    - 115 deg C for 2 min 15 sec.

37. **MANUAL DEVELOPMENT**

    - Use the wet bench Poly-3 in Polymer lab.

- MF322 developer 2-3 min. Inspect the wafers in halfway (around 2 min) to check the linewidth on wafer surface and in KOH-etched cavities. No photoresist residues are allowed at the bottom edges of the cavities. After inspection, adjust the remained development time.
- Rinse and dry.

38. INSPECTION: Linewidth and overlay

- Visually inspect the wafers through a microscope, and check the line width and overlay. No “resist” residues are allowed.

39. PLASMA ETCHING: 50nm Ti & 350nm TiN

- Use the Trikon Ωmega 201 plasma etcher.
- Follow the operating instructions from the manual when using this machine.
- It is not allowed to change the process conditions and times from the etch recipe!
- Recipe: Recipe that etches 500nm TiN could work. Or ask Alexander to edit a new recipe.
- INSPECTION: No residues or undercut are allowed. (pay attention to the sloppy sidewall)

40. LAYER STRIPPING PHOTORESIST

- Use the Tepla Plasma 300 system to remove the photoresist in an oxygen plasma.
- Follow the instructions specified for the Tepla stripper, and use the quartz carrier.
- Use Program 4.

41. CLEANING: HNO3 99% METAL

- Clean: 10 minutes in fuming nitric acid at ambient temperature. This will dissolve organic materials. Use wet bench ”HNO3 99% (metal)” and the carrier with a red and yellow dot.
- Rinse: Rinse in the Quick Dump Rinser with the standard program until the resistivity is 5 MΩ.
- Dry: Use the Semitool ”rinser/dryer” with the standard program, and the white carrier with a black dot.
- Note: Do not perform a ”HNO3 69,5% 110C (Si)” cleaning step!

42. PECVD DEPOSITION: 2000nm SiO2

- Use the Novellus Concept One PECVD reactor.
- Follow the operating instructions from the manual when using this machine.
- It is not allowed to change the process conditions and time from the deposition recipe!
- Add silicon wafer (T1) as dummy wafer to measure thickness later. (optional)
- Use XXXSIOSTD to deposit a 2000 nm thick SiO2 layer. Time: ~ 32s. Check the log book.
- Note: The deposition time is subject to minor changes, in order to obtain the correct film thickness.

43. MEASUREMENT: Silicon Oxide Thickness

- Use the Leitz MPV-SP measurement system for layer thickness measurements.
- Follow the operating instructions from the manual when using this equipment.
- Measure Test wafer T1 (Overall ~ 4000nm).

44. **COATING AND BAKING**

- Manual HMDS 15min.
- EVG110 Spray coater.
- Diluted **Positive** photoresist.
- Recipe:
  - HP 1000mbar 2ul 8 layers
  - Bake 115 deg C 1 min
  - HP 1000mbar 2ul 8 layers
  - Bake 115 deg C for 5 min.

45. **EVG420 CONTACT ALIGNER**

- Mask Box: 490, PRESET #1, Mask: Contact.
- Expose Time: ~ 20s (Check manual), Hard Contact.

46. **MANUAL DEVELOPMENT**

- Use the wet bench Poly-3 in Polymer lab.
- Diluted AZ400K: H2O = 1 : 2 developer for 2-3 min.
- Rinse and dry.

47. INSPECTION: Linewidth and overlay

- Visually inspect the wafers through a microscope, and check the line width and overlay. No “resist” residues are allowed. Dektak measure the depth of photoresist pattern.

48. WET ETCHING: BHF (1:7) METAL

- Moisten: Rinse for 1 minute in wet bench ”H2O/TRITON X-100” and use the carrier with the blue dot. The bath contains 1 ml Triton X-100 per 5000 ml demi water.
- ETCHING: Use wet bench ”SiO2-ets (1:7)” at ambient temperature, and the carrier with the blue dot. The bath contains a buffered HF solution (Merck LSI selectipur, SiO2 1:7)
- Etch time: needs to be tested first. Use test wafer T1 to test the etch rate, etch 10min and use Dektak to measure the etch depth. Loss of photoresist should also be considered.
- QDR: Rinse in the Quick Dump Rinser with the standard program until the resistivety is 5 MΩ.
- Drying: Use the Semitool ”rinser/dryer” with the standard program, and the orange carrier with a red dot.
- Inspection: Visually through a microscope. All the windows must be open and the hydrophobic test may be applied.

49. LAYER STRIPPING PHOTORESIST

- Use the Tepla Plasma 300 system to remove the photoresist in an oxygen plasma.
- Follow the instructions specified for the Tepla stripper, and use the quartz carrier.
- Use Program 1.

50. CLEANING: HNO3 99% METAL

- Clean: 10 minutes in fuming nitric acid at ambient temperature. This will dissolve organic materials. Use wet bench ”HNO3 99% (metal)” and the carrier with a red and yellow dot.

- Rinse: Rinse in the Quick Dump Rinser with the standard program until the resistivity is 5 MΩ.
- Dry: Use the Semitool ”rinser/dryer” with the standard program, and the white carrier with a black dot.
- Note: Do not perform a ”HNO3 69,5% 110C (Si)” cleaning step!

51. PECVD DEPOSITION: 500nm SiO2

- Use the Novellus Concept One PECVD reactor.
- Follow the operating instructions from the manual when using this machine.
- It is not allowed to change the process conditions and time from the deposition recipe!
- Add bare silicon wafer (T2) as dummy wafer to measure thickness later. (optional)
- Use XXXSIOSTD to deposit a 500 nm thick SiO2 layer. Time: ~ 8s. Check the log book.
- Note: The deposition time is subject to minor changes, in order to obtain the correct film thickness.

52. METALLIZATION: 2400nm Al (1% Si)

- Tool: TRIKON Sigma Sputtering
- Location: CR100
- Manual: <location>
- Recipe name: Check the recipes in the machine.
- Add silicon wafer (T2, T3). (Optional, from step 39-43, T2 for test run in step 44, T3 for DRIE etch rate test)

53. **COATING AND BAKING**

- Manual spinner in Polymer lab. (Spray coater costs too much time)
- Coat AZ 9260, Edit spinning rpm to coat a ~ 12um photoresist.
- Soft bake at 115 deg C, check the manual.

54. ALIGNMENT AND EXPOSURE - EVG420 CONTACT ALIGNER.

- PRESET #3 (Follow the instruction in manual)
- Mask Box: 490
- Mask: Backside_DRIE
- Expose Dose: ~ 90s (Check manual)
- Check the contact aligner mode to be sure it is in Preset 3 and proximity off!! Exposure time needs to be calculated by equation: exposure dose/exposure energy, check manual and calculate the exposure time.

55. MANUAL DEVELOPMENT

- Use the developer area polymer lab
- Developing with the Diluted AZ400K: H2O = 1 : 2 XXX developer for 2-3 min.
- Do not use to much developer and rinsing fluid (mostly water) during the developing..
- Note: Dispose the developer into the right container if it is not water based.
- Note: When finished always turn of the DI-water.

56. DRIE PLASMA ETCHING SILICON

- Use Dektak measuring photoresist thickness (optional).
- Use the STPS RAPIER plasma etcher.
- Follow the operating instructions from the manual when using this machine.
- It is not allowed to change the process conditions and times from the etch recipe!
- Recipe name: EKL Smooth @ 20C (In WAFERVIEW)
- Total etch cycles: ~ 400 CYCLES (could do a test run first)
- The 300um plain wafer might not be detected by the sensor in Rapier machine. Thus loading the wafer several times until it being sensed (change the slot during each load).

57. KEYENCE DEPTH MEASUREMENT

- Use Keyence to measure DRIE-cavity depth. The value should > 300 μm (300 μm & photoresist thickness).

58. WET ETCHING SILICON OXIDE (METAL) (ALCATEL DRY ETCH TAKES LONGER TIME)

- Use test wafer T2 to calibrate etch rate. Calculate etch time, over etch is allowed.
- Triton (Al. etch) for 1 min
- Etch in BHF (1:7) Metal
- Rinse: in the Quick Dump Rinser with the standard program.
- Dry: Use the Semitool ”rinser/dryer” with the standard program, and the orange carrier with a red dot.

59. ALUMINUM REMOVAL

- Moisten: Rinse for 1 minute in wet bench ”H2O/Triton X-100 tbv Al. Ets”. Use the carrier with the yellow dot. The bath contains 1 ml Triton X-100 per 5000 ml deionized water.
- Etching: Use wet bench ”Al. ets 35°C”, and the carrier with the yellow dot.
- 1 liter buffered aluminum etch fluid contains: 770 ml concentrated phosphorus acid (H3PO4 85%), 19 ml concentrated nitric acid (HNO3 65%), 140 ml concentrated acetic acid (CH3COOH 100%) and 71 ml deionized water.
- Etch time: Use test wafer T2 or T3 to calibrate the aluminum etch rate, over etch is allowed.
- QDR: Rinse in the Quick Dump Rinser with the standard program until the resistivity is 5 MΩ.
- Drying: Use the Semitool ”rinser/dryer” with the standard program, and the orange carrier with a black dot.

60. LAYER STRIPPING PHOTORESIST

- Use the Tepla Plasma 300 system to remove the photoresist in an oxygen plasma.
- Follow the instructions specified for the Tepla stripper, and use the quartz carrier.
- Use Program 4.

61. CLEANING: HNO3 99% METAL

- Clean: 10 minutes in fuming nitric acid at ambient temperature. This will dissolve organic materials. Use wet bench ”HNO3 99% (metal)” and the carrier with a red and yellow dot.
- Rinse: Rinse in the Quick Dump Rinser with the standard program until the resistivity is 5 MΩ.

- Dry: Use the Semitool ”rinser/dryer” with the standard program, and the white carrier with a black dot.
- Note: Do not perform a ”HNO3 69,5% 110C (Si)” cleaning step!

62. ALCATEL PLASMA ETCHING WITHOUT MASK

- Etch ~ 500nm Silicon Oxide, over etch is allowed.
- All contact pads need to be open completely, two TiN/Ti layers should have the same color.

C

Arduino IDE Code

```
//Duty cycle test
//PWM output pin no. is 13

const int PWM_PIN = 13;

void setup() {
  pinMode(PWM_PIN, OUTPUT);
}

void loop() {
  // put your main code here, to run repeatedly:
  // LED in 30% duty cycle & 1kHz
  // LED 'on' 0.5s & 'off' 1s.
  for (int i=0; i<=5000; i++){
    digitalWrite(PWM_PIN, HIGH);
    delayMicroseconds(30);
    digitalWrite(PWM_PIN, LOW);
    delayMicroseconds(100 - 30);
  }
  delay(1000);
}
```

List of Figures

List of Tables

Bibliography

[1] Thijs Houben, Inge CM Loonen, Serapio M Baca, Maarten Schenke, Johanna H Meijer, Michel D Ferrari, Gisela M Terwindt, Rob A Voskuyl, Andrew Charles, Arn MJM van den Maagdenberg, et al. Optogenetic induction of cortical spreading depression in anesthetized and freely behaving mice. *Journal of Cerebral Blood Flow & Metabolism*, 37(5): 1641–1655, 2017.

[2] Lief Fenno, Ofer Yizhar, and Karl Deisseroth. The development and application of optogenetics. *Annual review of neuroscience*, 34, 2011.

[3] Melissa R Warden, Jessica A Cardin, and Karl Deisseroth. Optical neural interfaces. *Annual review of biomedical engineering*, 16:103–129, 2014.

[4] Kay M Tye and Karl Deisseroth. Optogenetic investigation of neural circuits underlying brain disease in animal models. *Nature Reviews Neuroscience*, 13(4):251, 2012.

[5] Matthew E Carter and Luis de Lecea. Optogenetic investigation of neural circuits in vivo. *Trends in molecular medicine*, 17(4):197–206, 2011.

[6] Samarendra K Mohanty and Vasudevan Lakshminarayananan. Optical techniques in optogenetics. *Journal of modern optics*, 62(12):949–970, 2015.

[7] Suzie Dufour and Yves De Koninck. Optrodes for combined optogenetics and electrophysiology in live animals. *Neurophotonics*, 2(3):031205–031205, 2015.

[8] Niten Olofsson, Iakovos Lazaridis, Konstantinos Meletis, Marie Carlén, Ulf Tingström, Håkan Karlsson, and Cobolt SE. Lasers, optics enhance optogenetics studies.

[9] Jacob G Bernstein, Xue Han, Michael A Henninger, Emily Y Ko, Xiaofeng Qian, Giovanni Talei Franzesi, Jackie P McConnell, Patrick Stern, Robert Desimone, and Edward S Boyden. Prosthetic systems for therapeutic optical activation and silencing of genetically-targeted neurons. In *Proceedings of SPIE–the International Society for Optical Engineering*, volume 6854, page 68540H. NIH Public Access, 2008.

[10] F Nassirinia. Wireless power transfer and optogenetic stimulation of freely moving rodents. 2016.

[11] Bahareh Ghane-Motlagh and Mohamad Sawan. Design and implementation challenges of microelectrode arrays: a review. *Materials Sciences and Applications*, 4(08):483, 2013.

[12] You-Yin Chen, Hsin-Yi Lai, Sheng-Huang Lin, Chien-Wen Cho, Wen-Hung Chao, Chia-Hsin Liao, Siny Tsang, Yi-Fan Chen, and Si-Yue Lin. Design and fabrication of a polyimide-based microelectrode array: application in neural recording and repeatable electrolytic lesion in rat brain. *Journal of neuroscience methods*, 182(1):6–16, 2009.

[13] LA Geddes and R Roeder. Criteria for the selection of materials for implanted electrodes. *Annals of biomedical engineering*, 31(7):879–890, 2003.

[14] Wendy Franks, Iwan Schenker, Patrik Schmutz, and Andreas Hierlemann. Impedance characterization and modeling of electrodes for biomedical applications. *IEEE Transactions on Biomedical Engineering*, 52(7):1295–1302, 2005.

[15] Anil Koklu, Ahmet C Sabuncu, and Ali Beskok. Rough gold electrodes for decreasing impedance at the electrolyte/electrode interface. *Electrochimica acta*, 205:215–225, 2016.

[16] Subramaniam Venkatraman, Jeffrey Hendricks, Zachary A King, Andrew J Sereno, Sarah Richardson-Burns, David Martin, and Jose M Carmena. In vitro and in vivo evaluation of pedot microelectrodes for neural stimulation and recording. *IEEE Transactions on Neural Systems and Rehabilitation Engineering*, 19(3):307–316, 2011.

[17] Hubin Zhao, Danil Sokolov, and Patrick Degenaar. An implantable optrode with self-diagnostic function in 0.35 μm cmos for optical neural stimulation. In *Biomedical Circuits and Systems Conference (BioCAS), 2014 IEEE*, pages 244–247. IEEE, 2014.

[18] Suzie Dufour, Guillaume Lavertu, Sophie Dufour-Beauséjour, Alexandre Juneau-Fecteau, Nicole Calakos, Martin Deschênes, Réal Vallée, and Yves De Koninck. A multimodal micro-optrode combining field and single unit recording, multispectral detection and photolabeling capabilities. *PloS one*, 8(2):e57703, 2013.

[19] Jing Wang, Fabien Wagner, David A Borton, Jiayi Zhang, Ilker Ozden, Rebecca D Burwell, Arto V Nurmikko, Rick van Wagenen, Ilka Diester, and Karl Deisseroth. Integrated device for combined optical neuromodulation and electrical recording for chronic in vivo applications. *Journal of neural engineering*, 9(1):016001, 2011.

[20] Eran Stark, Tibor Koos, and György Buzsáki. Diode probes for spatiotemporal optical control of multiple neurons in freely moving animals. *Journal of neurophysiology*, 108 (1):349–363, 2012.

[21] Hung Cao, Ling Gu, SK Mohanty, and J-C Chiao. An integrated μled optrode for optogenetic stimulation and electrical recording. *Ieee Transactions on Biomedical Engineering*, 60(1):225–229, 2013.

[22] Niall McAlinden, David Massoubre, Elliot Richardson, Erdan Gu, Shuzo Sakata, Martin D Dawson, and Keith Mathieson. Thermal and optical characterization of micro-led probes for in vivo optogenetic neural stimulation. *Optics letters*, 38(6):992–994, 2013.

[23] Joel Voldman, Martha L Gray, and Martin A Schmidt. Microfabrication in biology and medicine. *Annual review of biomedical engineering*, 1(1):401–425, 1999.

[24] Polina Anikeeva, Aaron S Andalman, Ilana Witten, Melissa Warden, Inbal Goshen, Logan Grosenick, Lisa A Gunaydin, Loren M Frank, and Karl Deisseroth. Optetrode: a multichannel readout for optogenetic control in freely moving mice. *Nature neuroscience*, 15 (1):163–170, 2012.

[25] B Fan and W Li. Miniaturized optogenetic neural implants: a review. *Lab on a Chip*, 15 (19):3838–3855, 2015.

[26] Tae-il Kim, Jordan G McCall, Yei Hwan Jung, Xian Huang, Edward R Siuda, Yuhang Li, Jizhou Song, Young Min Song, Hsuan An Pao, Rak-Hwan Kim, et al. Injectable, cellular-scale optoelectronics with applications for wireless optogenetics. *Science*, 340 (6129):211–216, 2013.

[27] Led. `https://ledhydroponicsblog.co.uk/index.php/growing-info/led/`.

[28] Per Andersen and Edvard I Moser. Brain temperature and hippocampal function. *Hippocampus*, 5(6):491–498, 1995.

[29] Mark A Rossi, Vinson Go, Tracy Murphy, Quanhai Fu, James Morizio, and Henry H Yin. A wirelessly controlled implantable led system for deep brain optogenetic stimulation. *Frontiers in integrative neuroscience*, 9, 2015.

[30] Pulse width modulation (pwm) vs. analog dimming of leds. `http://www.aimtec.com/site/Aimtec/files/documents/ApplicationNotes/a031e%20pwm%20vs%20analog%20dimming%20of%20leds.pdf`. Revision: 2011-04-04.

[31] Fu-Yu Beverly Chen, David M Budgett, Yuhui Sun, Simon Malpas, Daniel McCormick, and Peter S Freestone. Pulse-width modulation of optogenetic photo-stimulation intensity for application to full-implantable light sources. *IEEE transactions on biomedical circuits and systems*, 11(1):28–34, 2017.

[32] Khalil Najafi and Jamille F Hetke. Strength characterization of silicon microprobes in neurophysiological tissues. *IEEE Transactions on Biomedical Engineering*, 37(5):474–481, 1990.

[33] David J Edell, VV Toi, Vincent M Mcneil, and LD Clark. Factors influencing the biocompatibility of insertable silicon microshafts in cerebral cortex. *IEEE Transactions on Biomedical Engineering*, 39(6):635–643, 1992.

[34] Raeyoung Kim, Sunghoon Joo, Hyunjun Jung, Nari Hong, and Yoonkey Nam. Recent trends in microelectrode array technology for in vitro neural interface platform. *Biomedical Engineering Letters*, 4(2):129–141, 2014.

[35] Marie Engelene J Obien, Kosmas Deligkaris, Torsten Bullmann, Douglas J Bakkum, and Urs Frey. Revealing neuronal function through microelectrode array recordings. *Frontiers in neuroscience*, 8, 2014.

[36] Luis A Camuñas-Mesa and Rodrigo Quian Quiroga. A detailed and fast model of extracellular recordings. *Neural computation*, 25(5):1191–1212, 2013.

[37] John O'Keefe and Michael L Recce. Phase relationship between hippocampal place units and the eeg theta rhythm. *Hippocampus*, 3(3):317–330, 1993.

[38] Susumu Takahashi, Yuichiro Anzai, and Yoshio Sakurai. A new approach to spike sorting for multi-neuronal activities recorded with a tetrode—how ica can be practical. *Neuroscience research*, 46(3):265–272, 2003.

[39] Multi Channel Systems MCS GmbH. Microelectrode array (mea) manual. `https://www.multichannelsystems.com/sites/multichannelsystems.com/files/documents/manuals/MEA_Manual.pdf`. Printed: 2018-07-25.

[40] Properties of silicon and silicon wafers. `http://www.el-cat.com/silicon-properties.htm`.

[41] Gyan Dutt & Ravi Bhatkal. Led die attach selection considerations - alpha assembly solutions. `https://alphaassembly.com/-/media/Files/CooksonElectronics/Whitepapers/LED/LED-Die-Attach-Technologies---Considerations---Whitepaper.pdf`.

[42] Javier DeFelipe. The evolution of the brain, the human nature of cortical circuits, and intellectual creativity. *Frontiers in neuroanatomy*, 5:29, 2011.

[43] S Mizuno, A Verma, H Tran, P Lee, and B Nguyen. Dielectric constant and stability of fluorine doped pecvd silicon oxide thin films. *Thin Solid Films*, 283(1-2):30–36, 1996.

[44] Badih El-Kareh. *Fundamentals of semiconductor processing technology*. Springer Science & Business Media, 2012.

[45] Reza Bavadi and Shahoo Valedbagi. Physical properties of titanium nitride thin film prepared by dc magnetron sputtering. *Materials Physics and Mechanics*, 15(2):167–172, 2012.

[46] Photolithography overview participant guide. `http://www.scme-nm.org/index.php?option=com_docman&task=cat_view&gid=86&Itemid=226`. Revision: 2017-03-31.

[47] Affan Affan Kaysa Waafi. Fabrication and characterization of pedot coated microelectrodes array for organ-on-chip application. 2018.

[48] Ulises A Aregueta-Robles, Andrew J Woolley, Laura A Poole-Warren, Nigel H Lovell, and Rylie A Green. Organic electrode coatings for next-generation neural interfaces. *Frontiers in neuroengineering*, 7:15, 2014.

[49] S Yamagiwa, M Ishida, and T Kawano. Flexible optrode array: Parylene-film waveguide arrays with microelectrodes for optogenetics. In *Solid-State Sensors, Actuators and Microsystems (TRANSDUCERS), 2015 Transducers-2015 18th International Conference on*, pages 277–280. IEEE, 2015.

[50] K Kwon and W Li. Integrated multi-led array with three-dimensional polymer waveguide for optogenetics. In *Micro Electro Mechanical Systems (MEMS), 2013 IEEE 26th International Conference on*, pages 1017–1020. IEEE, 2013.